

Leibniz Institute of Virology

**Human cytomegalovirus genetic determinants of viral  
tropism in epithelial cells and human leukocytes**

**Dissertation**

Submitted to the

Department of Chemistry

Faculty of Mathematics, Informatics and Natural Sciences

University of Hamburg

In fulfilment of the requirements for the degree of

Doctor of Natural Sciences (Dr.rer.nat.)

By

**Giorgia Cimato**

Born in Bologna, Italy

Hamburg, July 2024



First reviewer: Prof. Dr. Wolfram Brune

Second reviewer: Prof. Dr. Nicole Fischer

Examination committee: Prof. Dr. Wolfram Brune

Prof. Dr. Michael Kolbe

Prof. Dr. Jens Bosse

Date of disputation: 20.09.2024



This study was conducted between October 2020 and June 2024 at the Leibniz Institute of Virology (LIV) under the supervision of Prof. Dr. Wolfram Brune, PD Dr. Giada Frascaroli, and Dr. Tobias Dallenga.



# I. List of publications, oral and poster presentations

## Publications

Parts of the study presented in this thesis were published in:

Human cytomegalovirus glycoprotein variants governing viral tropism and syncytium formation in epithelial cells and macrophages.

G. Cimato, X. Zhou, W. Brune, G. Frascaroli

Journal of Virology, June 2024

A virus genetic system to analyze the fusogenicity of human cytomegalovirus glycoprotein B variants.

X. Zhou, G. Cimato, Y. Zhou, G. Frascaroli, W. Brune

Viruses, April 2023

## Oral and poster presentations

Parts of this thesis were presented at the following conferences:

<b>LIV Scientific Retreat 2022</b>	May 2022, Hamburg, Germany Poster
<b>15<sup>th</sup> Mini-Herpesvirus Workshop 2022</b>	September 2022, Essen, Germany Oral presentation
<b>32<sup>nd</sup> Annual Meeting of the Society for Virology (GfV) 2023</b>	March 2023, Ulm, Germany Poster
<b>LIV Scientific Retreat 2023</b>	May/June 2023, Hamburg, Germany Poster
<b>33<sup>rd</sup> Annual Meeting of the Society for Virology (GfV) 2024</b>	March 2024, Vienna, Austria Poster
<b>48<sup>th</sup> Annual International Herpesvirus Workshop (IHW) 2024</b>	July 2024, Portland, USA Poster





## II. Table of Contents

1 Zusammenfassung .....	15
2 Abstract .....	17
3 Introduction .....	19
3.1 Human cytomegalovirus.....	19
3.1.1 Human cytomegalovirus genome and virion structure .....	19
3.1.2 Human cytomegalovirus life cycle.....	20
3.1.3 Human cytomegalovirus pathogenesis and seroprevalence .....	22
3.2 Human cytomegalovirus genetic variability.....	23
3.3 Human cytomegalovirus cell tropism.....	25
3.3.1 Role of epithelial cells in cytomegalovirus pathogenesis.....	26
3.3.2 Role of endothelial cells in cytomegalovirus pathogenesis and dissemination .....	26
3.3.3 Role of leukocytes in cytomegalovirus pathogenesis and dissemination.....	27
3.3.3.1 Neutrophils.....	28
3.3.3.2 Monocytes and macrophages .....	29
3.4 Viral glycoproteins mediating virus binding and entry .....	30
3.4.1 Neutralizing antibody response.....	32
3.5 Cell-cell fusion and syncytium formation in viral pathogenesis .....	33
3.5.1 Determinants and mechanisms of syncytium formation .....	34
4 Aims of the study .....	37
5 Results .....	39
5.1 HCMV strain VR1814 shows high infectivity and fusogenicity in several cell types .....	39
5.2 Identification of the genetic differences between VR1814 and FIX.....	41
5.3 Role of VR1814-specific glycoprotein variants in the infectivity on epithelial cells .....	43
5.4 Role of VR1814-specific glycoprotein variants in cell-cell fusion and syncytium formation in epithelial cells .....	47
5.5 Characterization of FIX-derived variants of UL128 and UL130 for the infectivity and cell-cell fusion in epithelial cells .....	51
5.6 Role of VR1814-specific glycoprotein variants in the infectivity on macrophages .....	53
5.7 Role of VR1814-specific glycoprotein variants in cell-cell fusion and syncytium formation in macrophages.....	57
5.8 Role of VR1814-specific glycoprotein variants in determining human primary macrophage tropism of HCMV .....	59
5.9 Strategies for HCMV transfer to neutrophils .....	62
5.10 HCMV viral particles localization in neutrophils .....	64
5.11 Characterization of the interaction of neutrophils and donor cells.....	66
6 Discussion.....	69

6.1 HCMV strain VR1814 shows broad cell tropism and induction of cell-cell fusion .....	69
6.2 VR1814-specific gB and UL128L variants increase the infectivity of FIX in epithelial cells .....	70
6.3 VR1814-specific gB and UL128L variants promote cell-cell fusion and syncytium formation in epithelial cells .....	71
6.4 FIX-derived variants of UL128 and UL130 impair infectivity and cell-cell fusion in epithelial cells .....	72
6.5 Role of VR1814-specific glycoprotein variants in promoting macrophage tropism .....	72
6.6 Interaction of HCMV-infected endothelial cells and neutrophils <i>in vitro</i> .....	74
6.7 Summary .....	76
7 Material .....	77
7.1 Cells.....	77
7.2 Viruses.....	77
7.3 Bacteria .....	78
7.4 Plasmids .....	78
7.5 Primers .....	79
7.5.1 Molecular cloning primers.....	79
7.5.2 BAC mutagenesis primers .....	79
7.5.3 qPCR primers.....	83
7.6 Antibodies.....	83
7.6.1 Primary Antibodies .....	83
7.6.2 Secondary Antibodies.....	83
7.6.3 Nuclear dyes .....	84
7.7 Chemical and reagents .....	84
7.7.1 Antibiotics .....	84
7.7.2 Enzymes .....	84
7.7.3 Molecular mass standard.....	84
7.7.4 Other reagents and chemicals.....	85
7.8 Media and buffers .....	85
7.8.1 Cell culture media and buffers .....	85
7.8.2 Bacteria growth media .....	87
7.8.3 Agarose gel electrophoresis buffers.....	87
7.8.4 SDS polyacrylamide gel electrophoresis (SDS-PAGE) and western blot buffers ..	87
7.8.5 Immunofluorescence buffers .....	89
7.8.6 DNA preparation from bacteria (Mini Prep) buffers .....	89
7.8.7 FACS buffers.....	89
7.9 Kits.....	89

8 Methods .....	91
8.1 Molecular biology methods .....	91
8.1.1 Preparation of <i>E. coli</i> DH10B electrocompetent bacteria .....	91
8.1.2 Preparation of <i>E. coli</i> GS1783 electrocompetent bacteria.....	91
8.1.3 Transformation of bacteria.....	91
8.1.4 Extraction of plasmid DNA and BAC DNA (Mini Prep) .....	92
8.1.5 Extraction of plasmid DNA and BAC DNA (Midi Prep) .....	92
8.1.6 Storage of bacteria .....	92
8.1.7 Polymerase chain reaction (PCR).....	93
8.1.8 Restriction enzyme digestion of DNA.....	93
8.1.9 Agarose gel electrophoresis .....	93
8.1.10 Purification of DNA fragments.....	93
8.1.11 DNA ligation .....	93
8.1.12 Quantitative polymerase chain reaction (qPCR) .....	94
8.1.13 DNA sequencing.....	94
8.1.14 <i>En Passant</i> BAC mutagenesis.....	94
8.1.15 Gibson assembly cloning.....	95
8.2 Cell biology and virology methods.....	95
8.2.1 Cell culture .....	95
8.2.2 Transfection of plasmid DNA .....	96
8.2.3 Transfection of BAC DNA .....	97
8.2.4 Production of lentivirus .....	97
8.2.5 Transduction of cells.....	97
8.2.6 Preparation of HCMV stocks .....	98
8.2.7 Titration of HCMV stocks .....	98
8.2.8 Viral infections .....	98
8.2.9 Viral replication kinetics .....	99
8.2.10 Cell-cell fusion assay .....	99
8.2.11 Syncytium formation inhibition assay .....	99
8.2.12 Cytospin and Giemsa staining .....	100
8.2.13 Uptake of cell-associated HCMV by PMNs .....	100
8.2.14 Fluorescence-activated cell sorting (FACS) .....	100
8.3 Protein biochemistry methods.....	101
8.3.1 Cell lysis for immunoblotting .....	101
8.3.2 Protein concentration measurement .....	101
8.3.3 SDS polyacrylamide gel electrophoresis (SDS-PAGE) and immunoblot.....	101
8.4 Microscopy methods.....	102

8.4.1 Immunofluorescence (IF).....	102
8.4.2 Transmission electron microscopy (TEM).....	103
8.4.3 Correlative light and electron microscopy (CLEM) .....	103
9 References.....	105
10 Appendix .....	121
10.1 Curriculum vitae .....	121
10.2 List of hazardous substances.....	122
11 Acknowledgements .....	125
12 Declaration on oath .....	127

### III. List of abbreviations

<b>AIDS</b>	Acquired immunodeficiency syndrome
<b>APCs</b>	Antigen-presenting cells
<b>APS</b>	Ammonium persulfate
<b>BAC</b>	Bacterial artificial chromosome
<b>CD</b>	Cluster of differentiation
<b>CPE</b>	Cytopathic effects
<b>C-term</b>	Carboxyl-terminus
<b>DB</b>	Dense bodies
<b>dNTPs</b>	Deoxynucleotide
<b>DOC</b>	Deoxycholic acid sodium salt
<b>dpi</b>	Days post-infection
<b>dsDNA</b>	Double-stranded DNA
<b>DSP</b>	Dual split protein
<b>E</b>	Early
<b>EDTA</b>	Ethylenediamine tetraacetic acid
<b>EGFR</b>	Epidermal growth factor receptor
<b>EM</b>	Electron microscopy
<b>ER</b>	Endoplasmic reticulum
<b>EYFP</b>	Enhanced yellow fluorescent protein
<b>FACS</b>	Fluorescence-activated cell sorting
<b>FFWO/FFWI</b>	Fusion from without/within
<b>FIX</b>	Fusion-inducing factor-X
<b>GAPDH</b>	Glycerinaldehyd-3-phosphat-dehydrogenase
<b>GFP</b>	Green fluorescent protein
<b>HCMV</b>	Human cytomegalovirus
<b>HPCs</b>	Hematopoietic progenitor cells
<b>HSGs</b>	Heparin sulphate proteoglycans
<b>HR</b>	Homologous recombination
<b>hpi</b>	Hours post-infection
<b>ICAM-1</b>	Intercellular adhesion molecule 1
<b>IE</b>	Immediate early
<b>IF</b>	Immunofluorescence
<b>IFN</b>	Interferon
<b>IL</b>	Interleukin
<b>IRL/S</b>	Internal repeat long/short

<b>IU</b>	Infectious units
<b>Kan</b>	Kanamycin
<b>L</b>	Late
<b>LeGO</b>	Lentiviral gene ontology
<b>LFA-1</b>	Lymphocyte function-associated antigen 1
<b>MIEP</b>	Major immediate early promoter
<b>MOI</b>	Multiplicity of infection
<b>ncRNAs</b>	Non-coding RNAs
<b>NIEPs</b>	Non-infectious enveloped particles
<b>N-term</b>	Amino-terminus
<b>OR1411</b>	Olfactory receptor family 14 subfamily I member 1
<b>ORF</b>	Open reading frame
<b>PAMPs</b>	Pathogen-associated molecular pattern molecules
<b>PBMC</b>	Peripheral blood mononuclear cells
<b>PCR</b>	Polymerase chain reaction
<b>PDGFR<math>\alpha</math></b>	Platelet-derived growth factor receptor alpha
<b>PM</b>	Point mutation
<b>PMNL</b>	Polymorphonuclear leukocytes
<b>qPCR</b>	Quantitative polymerase chain reaction
<b>Rev</b>	Revertant virus
<b>RLuc</b>	<i>Renilla</i> luciferase
<b>ROIs</b>	Regions of interest
<b>RT</b>	Room temperature
<b>SBF-SEM</b>	Serial block-face scanning electron microscopy
<b>SDS</b>	Sodium dodecyl sulphate
<b>SNPs</b>	Single nucleotide polymorphisms
<b>TEM</b>	Transmission electron microscopy
<b>TEMED</b>	Tetramethylethylenediamine
<b>TRL/TRS</b>	Terminal repeat long/short
<b>UL</b>	Unique long
<b>US</b>	Unique short
<b>vAC</b>	Viral assembly compartment
<b>WB</b>	Western blot
<b>WT</b>	Wild type
<b><math>\Delta</math></b>	Delta
<b><math>\Delta\Delta</math>CT</b>	Double-delta cycle threshold

# 1 Zusammenfassung

Das humane Cytomegalievirus (HCMV) weist *in vitro* und *in vivo* einen breiten Zelltropismus auf. Die Fähigkeit von HCMV verschiedene Zelltypen zu infizieren wird durch spezifische Hüllglykoproteine bestimmt, die die Bindung an zelluläre Rezeptoren und damit den Eintritt des Virus in menschliche Zellen vermitteln. Die Infektion von Epithel-, Endothel- und hämatopoetischen Zellen ermöglicht die virale Übertragung, die systemische Ausbreitung und die Pathogenese im Wirt. Unter den menschlichen Leukozyten sind nur Zellen der myeloiden Linie permissiv für HCMV und spielen eine entscheidende Rolle sowohl bei der lytischen als auch bei der latenten Infektion. Im Gegensatz dazu fungieren lymphatische Zellen, wie z. B. Neutrophile, als Vehikel für die HCMV-Verbreitung *in vivo*, obwohl sie keinen lytischen Replikationszyklus unterstützen. HCMV-Stämme unterscheiden sich in ihrer Fähigkeit, verschiedene Zelltypen zu infizieren und sich in ihnen zu vermehren, doch die genetische Grundlage dieser Unterschiede ist bisher nur unzureichend untersucht. Ziel dieser Studie war es daher, die genetischen Faktoren zu charakterisieren, die für den breiten Zelltropismus eines bestimmten HCMV-Stammes, VR1814, und seine Fähigkeit, Synzytiumbildung in Epithelzellen und Makrophagen zu induzieren, verantwortlich sind. Durch Sequenzvergleiche und gentechnische Veränderung des BAC-Klons FIX von VR1814, der *in vitro* eine stark reduzierte Infektiosität aufwies, identifizierte ich spezifische Varianten von VR1814 in den Hüllglykoproteinen gB, UL128 und UL130 als Hauptdeterminanten für den verstärkten Tropismus in Epithelzellen und Makrophagen. Ich konnte zeigen, dass eine Aminosäuresubstitution in UL130 von FIX die Expression des Pentamers in viralen Partikeln reduziert, was sowohl die Infektiosität als auch die Synzytiumbildung in Epithelzellen beeinträchtigt. Darüber hinaus konnte ich zeigen, dass eine VR1814-spezifische Mutation in US28, die zu einer C-terminalen Verkürzung des Proteins führt, die Expression des IE-Gens in menschlichen Makrophagen fördert, was die HCMV-Infektion und nicht die Latenz in diesem Zelltyp begünstigt. Als weiteres Ziel dieser Studie sollte der HCMV-Transport in neutrophilen Zellen untersucht werden, ein Prozess, der *in vivo* stattfindet und möglicherweise eine entscheidende Rolle für die Verbreitung des Virus im menschlichen Wirt spielt. Da VR1814 die Fähigkeit behält, auf menschliche Leukozyten übertragen zu werden, habe ich ein *In-vitro*-System entwickelt, um den Transfer von zellassoziertem HCMV von infizierten Endothelzellen auf Neutrophile zu untersuchen. Heterogenes virales Material, bestehend aus viralen Partikeln und dichten Körpern, wurde in großen Vesikeln im Zytoplasma der Neutrophilen gefunden, was darauf hindeutet, dass die Virusaufnahme aus infizierten Endothelzellen hauptsächlich durch Endozytose erfolgt. Zusammenfassend lässt sich sagen, dass diese Studie die viralen genetischen Faktoren identifiziert, die den HCMV-Tropismus in Epithelzellen und menschlichen Leukozyten diktiert. Des Weiteren hebt diese Studie die Bedeutung von

Instrumenten hervor, die für die Untersuchung der Mechanismen und der Bedeutung der Zell-Zell-Fusion und des Leukozytentransfers bei der HCMV-Pathogenese und -Verbreitung erforderlich sind.



## 2 Abstract

Human cytomegalovirus (HCMV) exhibits a broad cell tropism *in vitro* and *in vivo*. The ability of HCMV to replicate efficiently in different cell types is governed by specific envelope glycoproteins that mediate the binding to cellular receptors and consequently the virus entry into human cells. The infection of epithelial, endothelial, and hematopoietic cells supports viral transmission, systemic spread, and pathogenesis in the host. Among human leukocytes, only cells of the myeloid lineage are permissive to HCMV and play a crucial role in both lytic and latent infection. By contrast, lymphoid cells, such as neutrophils, act as vehicle for HCMV dissemination *in vivo* although they do not support a lytic replicative cycle. HCMV strains differ in their ability to infect and replicate in various cell types, but the genetic basis of these differences has remained poorly investigated. The aim of this study was to characterize the genetic factors involved in the broad cell tropism of a specific HCMV strain, VR1814, and its ability to induce syncytium formation in epithelial cells and macrophages. By sequence comparison and genetic engineering of VR1814's BAC clone, FIX, that displayed a strongly reduced infectivity *in vitro*, I identified specific variants of VR1814 in the envelope glycoproteins gB, UL128, and UL130 as major determinants of the increased tropism in epithelial cells and macrophages. I could show that an amino acid substitution in UL130 of FIX reduces the pentamer expression in viral particles, affecting both infectivity and syncytium formation in epithelial cells. Additionally, I demonstrated that a VR1814-specific mutation in US28 leading to a C-terminal truncation of the protein promotes IE gene expression in human macrophages, facilitating HCMV infection rather than latency in this cell type. This study also aimed to investigate HCMV trafficking in neutrophils, a process that occurs *in vivo* and may play a crucial role for viral dissemination in the human host. As VR1814 retained the capability to be transferred to human leukocytes, I established an *in vitro* system to study the transfer of cell-associated HCMV from infected endothelial cells to neutrophils. Heterogeneous viral material consisting of viral particles and dense bodies was found in large vesicles in neutrophils cytoplasm, suggesting that virus uptake from infected endothelial cells mainly occurred via endocytosis. In conclusion, this study identifies the viral genetic factors dictating HCMV tropism in epithelial cells and human leukocytes. Furthermore, the study highlights the importance of tools necessary for investigating the mechanisms and relevance of cell-cell fusion and leukocyte transfer in HCMV pathogenesis and dissemination.



## 3 Introduction

### 3.1 Human cytomegalovirus

#### 3.1.1 Human cytomegalovirus genome and virion structure

Human cytomegalovirus (HCMV) is a large, enveloped double-stranded DNA virus, belonging to the *Betaherpesvirinae* subfamily of herpesviruses [1]. Among all human viruses, the genome of HCMV is the largest with a length of over 235 kb, comprising 192 open reading frames (ORFs) with the potential to encode viral proteins [2]. Interestingly, only 26% of canonical genes has been demonstrated to be essential for viral replication *in vitro*, while almost 75% of viral genes encodes proteins involved in virus-host interactions [3–5]. The HCMV genome structure consists of a unique long (UL) and a unique short (US) region, each flanked by two sets of terminal (TRL/TRS) and internal (IRL/IRS) inverted repeats. Graphically, the HCMV genome can be represented as  $ab\text{-UL-}b'a'c'\text{-US-}ca$ , where the primes indicate the inverted repeats of  $a$ ,  $b$ , and  $c$  (Figure 1) [6,7]. The UL region comprises the genetic loci UL1 to UL151, while the US region the loci US1 to US34. Moreover, the ORFs RL1 to RL14 are contained in the TRL domain, the IRS1 gene is present in the IRS region, and the TRS1 locus in the TRS domain. In addition, the HCMV genome comprises polyadenylated non-coding RNAs (RNA2.7, RNA1.2, RNA4.9, and RNA5.0) as well as non-polyadenylated RNAs, such as micro-RNAs [8].



**Figure 1. Schematics of HCMV genome structure.** The HCMV genome contains a unique long (UL) and a unique short (US) region, each flanked by terminal and internal inverted repeats ( $ab/b'a'$  and  $a'c'/ca$ ).

Mature particles of HCMV show a diameter of approximately 200 nm and are formed by an icosahedral nucleocapsid containing the viral linear genome and enclosed within a lipid envelope (Figure 2) [9,10]. The nucleocapsid is surrounded by an amorphous tegument formed by mainly viral phosphoproteins as well as cellular and viral RNAs [10–12]. The outer layer formed by the lipid envelope exposes several viral glycoproteins, which mediate virus attachment to the host cell surface and virus entry. In addition to mature virions, non-infectious viral particles (NIEPs) and dense bodies (DBs) can be released by infected cells [13]. NIEPs

resemble the structure of infectious virions but lack of the viral DNA core, while DBs are aggregates of viral tegument proteins and glycoproteins enclosed in the viral envelope.

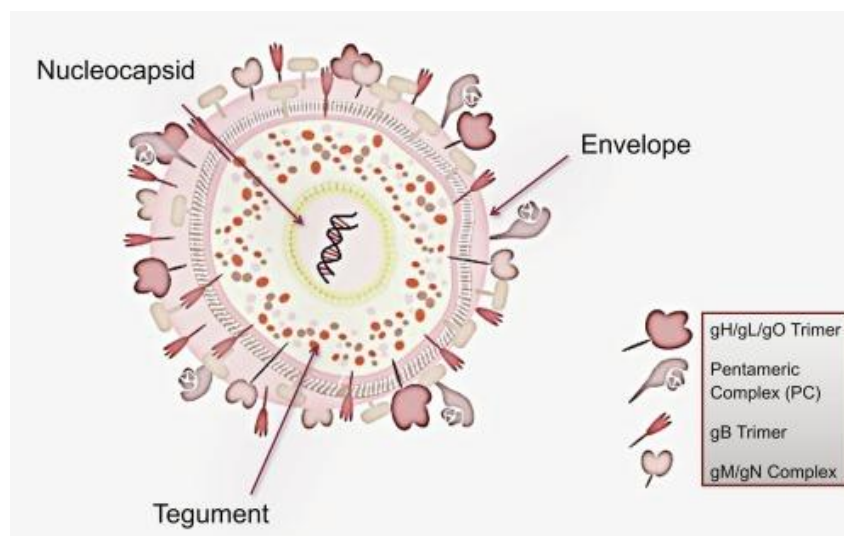


**Figure 2. HCMV virion structure.** Schematic of the HCMV mature virion. The viral DNA is contained in a nucleocapsid, surrounded by a tegument and an outer envelope, where viral glycoproteins are exposed. Picture taken from [14].

### 3.1.2 Human cytomegalovirus life cycle

Several human cells are susceptible to HCMV infection [15]. According to the target cell, the entry process can either occur through direct fusion of the viral envelope with the plasma membrane or via endocytosis-like processes [16–18]. First, the viral adhesion to the host cell is mediated by the binding of viral glycoproteins to specific cell surface receptors (Figure 3) [19–21]. The genome-containing nucleocapsids are then released into the cytoplasm and translocated to the nucleus, where the viral DNA circularizes prior to replication. During this first phase, the tegument proteins drive nuclear translocation and genome delivery, inhibit cell responses to viral infection and transactivate the viral gene expression [22–25]. In permissive cells, which support the viral replicative cycle, the expression of HCMV genes proceeds in a temporal cascade initiated with the expression of immediate-early (IE) genes, followed by early (E) and late (L) genes. The first genes to be expressed in the cells are the IE1 and IE2 at 1-2 hours post-infection (hpi), which encode for transcription factors and promote the expression of early genes, responsible for initiation and process of the viral DNA replication. At 24-48 hpi, the late viral genes are transcribed and encode for structural components of the virus and other proteins involved in virus assembly and egress [26]. After viral replication, the newly synthesized viral DNAs are encapsidated and translocated to the cytoplasm through envelopment and de-envelopment processes at the nuclear membrane [27]. The capsids accumulate in the viral assembly compartment, where final tegumentation and envelopment of viral particles occur. Once virions acquire the envelope, mature viral particles are released

from infected cells by exocytosis at the plasma membrane [28,29]. Overall, HCMV life cycle is rather slow and takes approximately 48-72 hours from virus entry to the release of newly synthesized viral particles in fibroblasts and smooth muscle cells, while in epithelial and endothelial cells the replication cycle is further protracted [30].

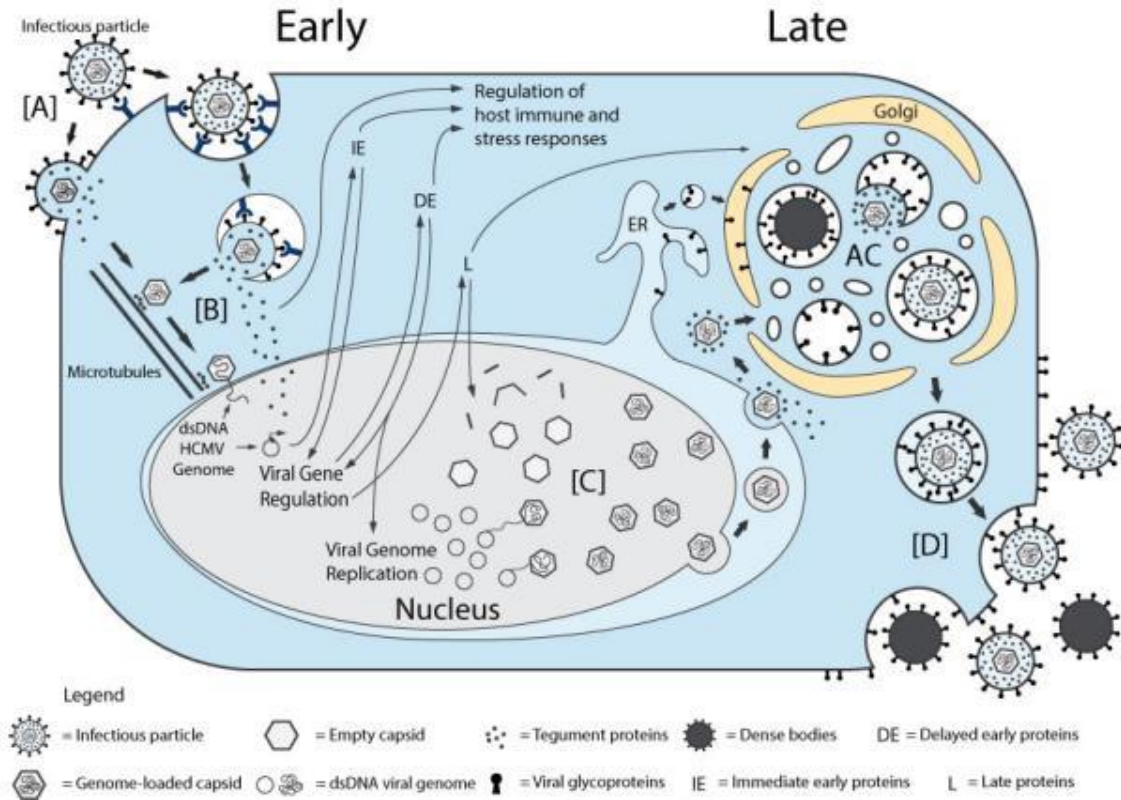


**Figure 3. HCMV lytic replicative cycle.** (A) Infectious viral particles attach to the host cell and enter by direct fusion to the plasma membrane or via endocytosis. (B) Capsids and tegument proteins are first delivered to the cytoplasm and then translocated into the nucleus. (C) There, the viral DNA replication takes place resulting in the synthesis of new viral genomes. Capsids assembly starts in the nucleus, followed by nuclear egress to the cytoplasm. In the viral assembly compartment, capsids associate with tegument proteins and acquire the envelope. (D) Mature viral particles and dense bodies are released by exocytosis at the plasma membrane. Picture taken from [29].

In cells that are susceptible to HCMV but do not support the lytic replicative cycle, such as CD34+ hematopoietic progenitor cells (HPCs) and monocytes, an alternative transcription program is activated after nuclear translocation of the viral DNA (Figure 4). This program leads to a limited set of transcripts, essential for establishment and maintenance of latency in these cells [31–33]. During latency, IE gene expression is suppressed and tightly regulated by the major immediate early promoter (MIEP) [34,35]. A repressive chromatin state occurs at the MIEP and is essential for the maintenance of latent virus in the cells [36]. In presence of this transcriptional repression, the few transcripts that are expressed include vIL-10, UL130, US28, UL144, and the ncRNA2.7 [37–40]. The sustained repression of MIEP and the effective maintenance of latency have been demonstrated to require an intracellular signalling activated

by US28, a viral chemokine receptor homolog [41,42]. Virus reactivation from latency occurs in presence of external stimuli, such as pro-inflammatory cytokines, that trigger cell differentiation of infected monocytes into macrophages and dendritic cells and promote dechromatinization at the MIEP and transient activation of IE gene expression. Virus reactivation in these permissive cells leads to expression of the full cascade of viral genes with final production of new infectious viral particles [43–45].

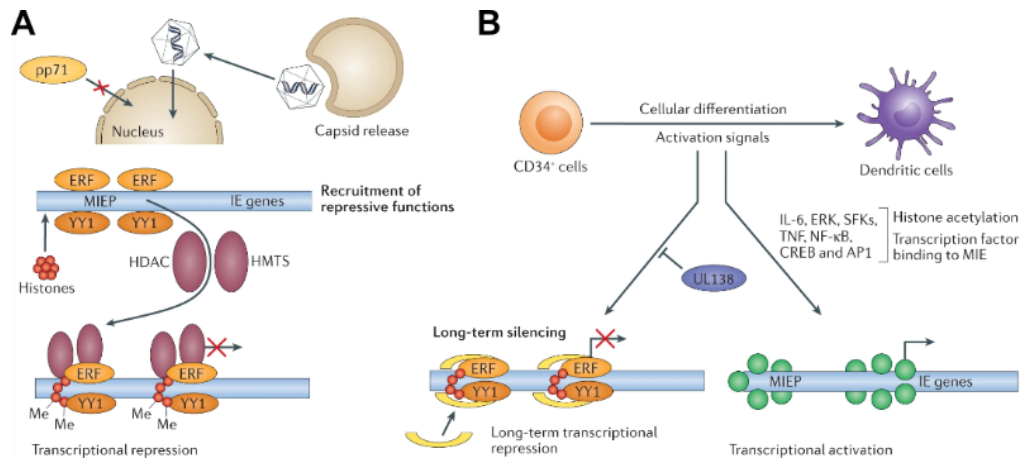


**Figure 4. HCMV latency.** (A) HCMV latency in myeloid cells depends on an effective silencing of the MIEP promoter. (B) After pro-inflammatory stimuli, cell differentiation into permissive macrophages and dendritic cells leads to activation of MIEP and complete viral gene expression. Picture modified from [46].

### 3.1.3 Human cytomegalovirus pathogenesis and seroprevalence

HCMV is a ubiquitous pathogen highly prevalent in the human population. The seroprevalence worldwide ranges from 40% in developed countries to more than 98% in developing countries and is highly dependent on sex and age of the individuals as well as on the socioeconomic status (Figure 5) [47].

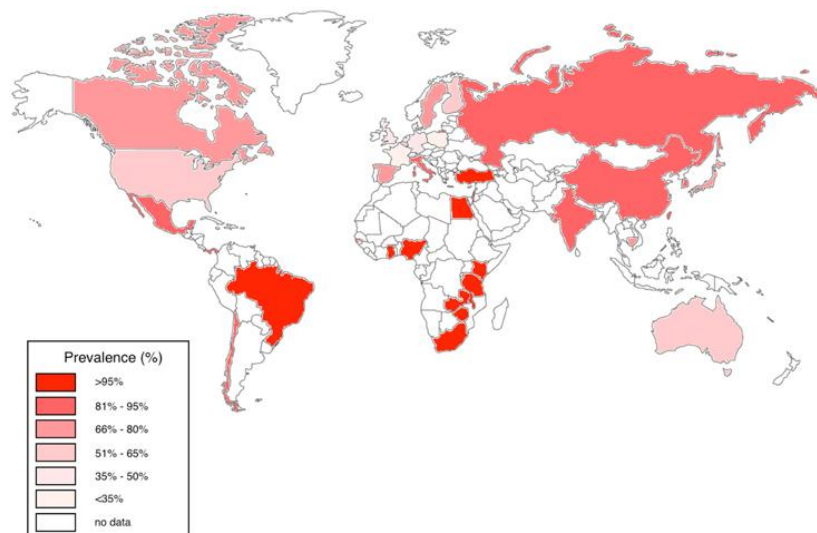


**Figure 5. HCMV seroprevalence rates in adults.** Picture taken from [47].

HCMV transmission among the population occurs either by contact with bodily fluids, such as saliva, tears, urine, and semen, or via solid-organ transplantation and hematopoietic stem cell transfusion [28,47]. In immunocompetent individuals, HCMV infection is usually mild and self-limiting, as the virus induces a strong immune response. However, the host immune system is not able to completely eliminate the virus, which enters latency in hematopoietic cells causing lifelong persistence with periodic reactivations during the lifespan of the host [48]. In immunocompromised patients, HCMV infection leads to high viremia associated with a severe and invasive infection and development of retinitis, pneumonitis, enterocolitis, esophagitis, and hepatitis [49–51]. Thus, HCMV is one of the major complications and causes of morbidity and mortality in immunocompromised individuals, such as AIDS patients and transplant recipients [52]. Furthermore, vertical transmission is known to be crucial in HCMV pathogenesis, as the virus is able to cross the placental barrier and be transmitted from mother to foetus during pregnancy or to neonates through breast milk. HCMV is considered the leading cause of congenital infection and birth defect worldwide [52,53]. Congenital infections may lead to neurological sequelae, sensorineural hearing loss, and mental retardation [54]. It has been demonstrated that primary HCMV infection of seronegative women during the first trimester of pregnancy drastically increases the risk of severe HCMV infection of the foetus [55].

Currently, several antiviral treatments for HCMV infection are available, including ganciclovir, foscarnet, cidofovir, and letermovir. The mechanisms of action of these drugs aim to suppress viral replication by targeting the viral DNA polymerase or interfere with viral genome packaging [56]. However, their use is limited due to high cytotoxicity and side effects reported as well as onset of antiviral resistance. Although experimental vaccines against HCMV are constantly being researched, so far no commercial HCMV vaccines are available on the market [57].

### **3.2 Human cytomegalovirus genetic variability**

HCMV shows a high level of genetic variability *in vivo* due to high frequency of multi-strain co-infections, virus reactivation from latency, and virus recombination [58]. Although several genes are conserved across clinical HCMV strains, some genetic loci are associated to high density of single nucleotide polymorphisms (SNPs) [59]. The majority of these genes encodes for envelope glycoproteins, including gB, gH, and gN, or for proteins involved in immune evasion mechanisms [58]. These highly polymorphic genes may be associated to different viral fitness, pathogenesis, and dissemination *in vivo* [60,61].

The first HCMV genome to be characterized and sequenced was the laboratory-adapted strain AD169, isolated from adenoids of an infected child [62]. Another laboratory-adapted HCMV strain broadly used was Towne, isolated from the urine of a congenitally infected infant. Historically, human fibroblasts have been the preferred cells for HCMV recovery and passaging after isolation to ensure viral replication to high titers and cell-free viral spread.

However, both AD169 and Towne accumulated numerous mutations in their genomes due to the extensive propagation in fibroblasts, and consequently lost the tropism for epithelial cells, endothelial cells, and macrophages [5,63,64]. Sequencing of other HCMV strains, such as Toledo and Merlin, that were propagated for a limited number of passages in fibroblasts, has allowed the identification of an additional 15 kb region, lost in the genome of the initial HCMV strains [65]. Thus, the extensive passaging in fibroblasts of AD169 led to a deletion of a 15 kb region comprising the ORFs UL133 to UL150A, replaced by RL14-1, and a mutation in UL131A [62]. Although Merlin has been passaged only three times in human fibroblasts after isolation from the urine of a congenitally infected infant, the sequencing revealed the acquisitions of two mutations in the genetic loci UL128 and RL13, respectively [65]. The cloning of Merlin into a self-excising bacterial artificial chromosome (BAC) vector allowed the generation of a genetically intact wild type strain [66]. This discovery draws the attention to the selective pressure and adaptive mutations that HCMV undergoes in cell culture and to the importance to preserve the broad cell tropism of HCMV for research purposes. Hence, other clinical HCMV isolates were propagated in endothelial cells after isolation, such as the low-passage strains VHL/E, TR, PH, TB40/E, and VR1814 [15,67–69]. These HCMV strains show less degree of adaptive mutations in their genome and resemble more wild type virus circulating in the human population.

Since these genetic variations occur in non-essential genes for viral replication *in vitro* and are often deleted or mutated in laboratory-adapted HCMV strains, it has been proposed that these variations were a result of selection and adaptation in cell culture. The most affected regions during *in vitro* propagation have been identified in the genes RL13, UL128 locus (UL128L), and UL/b' segment comprising the ORFs UL133 to UL150A [66,70]. Mutations in RL13 and UL128L occur within the very first passages *in vitro* and are generally associated to loss of broad cell tropism but fibroblasts [70]. The genetic loci RL13 encodes for a poorly characterized viral glycoprotein and if mutated leads to increased cell-free virus production in fibroblasts, while the UL128L encodes for three envelope glycoproteins, named UL128, UL130, and UL131A, which associate with the gH/gL complex forming the pentameric complex. The UL128L proteins are the major determinant of virus entry into epithelial, endothelial, and myeloid cells, and mutations in this genetic locus lead to loss of tropism for these cell types. In addition, certain genes in the UL/b' region of HCMV genome can also undergo selective and adaptive mutations. Some of these genes have been demonstrated to be associated with latency, including UL138, required for latency in myeloid progenitor cells, and UL144 [39,71]. Other genes exhibit immune modulatory functions, such as UL141 and UL142 that regulate the expression of cell surface receptors on NK cells [72–74], or play a role in the viral processing during assembly and maturation in endothelial cells, like the genetic loci UL135 and UL136 [75].



### 3.3 Human cytomegalovirus cell tropism

HCMV exhibits a broad cell and tissue tropism *in vivo* as documented by disseminated HCMV infection in immunocompromised patients [15,76]. The main target of HCMV infection *in vivo* are epithelial cells, endothelial cells, and fibroblasts, sites of primary infection (Figure 6) [77]. In the host, the viral spread mainly occurs in a cell-associated manner, requiring direct contact between infected cells and neighbouring uninfected cells [78]. The lytic replicative cycle in endothelial and epithelial cells leads to HCMV spread to immune cells, which play a crucial role in viral systemic spread and lifelong persistence. It has been demonstrated that infected endothelial cells recruit immune cells by secreting chemoattractants, such as IL-8 [79,80], and promote the adhesion of leukocytes to the endothelium by increasing the expression of adhesion molecules, like ICAM-1 and vCAM-1 [81,82]. CD34+ HPCs and monocytes are not permissive to a full replicative cycle and HCMV establishes latency in these cells. Thus, the latent virus can induce myeloid cell activation and migration into tissues, where the cells differentiate into permissive macrophages and dendritic cells leading to viral reactivation [83]. In the tissues, HCMV can be transmitted to other permissive cells leading to secretion in bodily fluids and spread to a new host. Nevertheless, HCMV can also induce monocyte infiltration in the bone marrow, allowing viral spread and persistence in new hematopoietic progenitor and stem cells, which serve as major reservoirs of latent HCMV in the host.

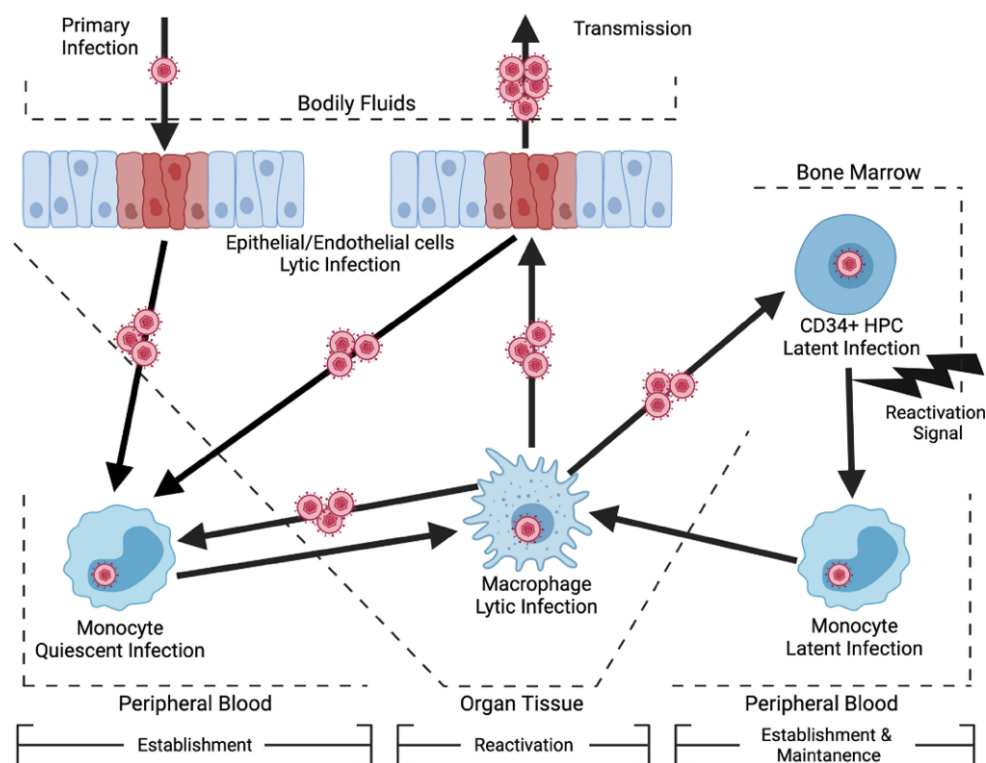


**Figure 6. HCMV dissemination in the host.** The primary target of HCMV infection are epithelial cells, followed by virus transmission to the endothelium. In these cell types the virus replicates and spreads to monocytes in the peripheral blood. Latently infected monocytes can either migrate to the bone marrow and transfer the virus to CD34+ HPCs, the main reservoir

of latent HCMV, or infiltrate in the tissue and differentiate into macrophages and dendritic cells, leading to viral reactivation and release of infectious viral particles. Picture taken from [84].

### **3.3.1 Role of epithelial cells in cytomegalovirus pathogenesis**

Epithelial cells are one of the most abundant cell type throughout the body covering skin, organ surfaces, and blood vessels [85]. The epithelium is highly specialized, and its crucial physiological functions depend on cell morphology and location. Epithelial cells show a structural polarity, with the apical domain towards the organ lumen or the external environment, a basal domain connected to the basal lamina that separates the connective tissues from the epithelium, and lastly a lateral domain that allows cell-cell connection through a variety of junctional complexes.

Epithelial cells have been recognized as an essential target of HCMV infection *in vivo* as their infection allows viral lytic replication with production of an infectious viral progeny that can be released and spread to other susceptible cells in the host. Infected epithelial cells have been detected in several organ tissues of patients with disseminated HCMV infection, including lungs, kidneys, gastrointestinal tract, and secretory glands, suggesting their role in mediating HCMV pathogenesis *in vivo* [76]. The widespread observed *in vivo* has been also reported *in vitro* by HCMV susceptibility of different epithelial cells from various tissues, including retina, liver, and kidney [68,86]. Furthermore, it has been proposed that epithelial cells may play a crucial role in virus inter-host transmission since infected cells have been observed in a diverse set of bodily fluids, such as broncho-alveolar lavage fluid, urine, and saliva, originated by cell detachment from the basal membrane of the corresponding infected tissue [87].

Epithelial cell tropism is retained by clinical HCMV isolates and lost in many laboratory-adapted HCMV strains, as documented by several studies showing adaptive mutations in UL128L during *in vitro* propagation. These mutations cause the loss of pentamer expression in viral particles and reduce the infectivity in epithelial cells. The entry and infection in this cell type require the expression of a functional pentameric complex on the viral envelope, as confirmed by rescuing the mutation in UL131 of AD169 by BAC mutagenesis leads to recovery of the epithelial cell tropism [88].

### **3.3.2 Role of endothelial cells in cytomegalovirus pathogenesis and dissemination**

Endothelial cells are organized in a single cell layer lining the blood vessels and play an essential role in regulating the exchanges between the bloodstream and the underlying tissues. Endothelial cells provide a remarkable variety of supportive functions, as they are able to adjust their number and location according to specific tissue requirements. Thus, the endothelium supports cell migration, angiogenesis, remodelling of blood vessels, as well as tissue growth and repair [89].

HCMV infection of endothelial cells have been demonstrated to promote the systemic spread in the host throughout hematogenous dissemination. HCMV infected endothelial cells have been detected *in vivo* in several organs of patients with AIDS or disseminated HCMV infection, including gastrointestinal tract, liver, kidneys, lungs, and brain [76,82,90]. Circulating cytomegalic endothelial cells have been also found in the bloodstream after cell detachment from the vessel's lumen [91].

The pivotal role of endothelial cells in HCMV pathogenesis and dissemination has been identified in several virally induced changes in the endothelium secretion and morphology, that mimic variations occurring during inflammation. Leukocytes and endothelial cells are the first cells involved in inflammatory responses as the trafficking of neutrophils and monocytes from the bloodstream to the surrounding tissues is tightly regulated by the endothelium. This regulation requires the secretion of cytokines and other chemoattractants to recruit leukocytes to the site of inflammation, and the expression of adhesion molecules on the endothelium to facilitate attachment and transmigration of leukocytes. Similarly, during HCMV infection, infected endothelial cells secrete in the extracellular space cellular chemokines, such as IL-8 and Gro $\alpha$ , to induce chemotaxis as well as adhesion of monocytes and neutrophils to the endothelium [79]. The expression of cell adhesion molecules, like ICAM-1 and vCAM-1, is upregulated in infected endothelial cells and promotes leukocyte adhesion. The interaction between ICAM-1 on the endothelial plasma membrane to its ligand LFA-1 on neutrophils or Mac-1 on monocytes allows direct contact between the two cell populations and the transfer of virus and viral material by microfusion events [92]. Additionally, the vascular permeability is increased during infection facilitating leukocyte migration through the endothelium [81]. The HCMV glycoproteins binding to  $\beta$ 1 and  $\beta$ 3 integrins or to the epidermal growth factor receptor (EGFR) on endothelial cell surface activates an intracellular signalling via phosphatidylinositol 3-kinase (PI3K) and mitogen-activated protein kinase (MAPK) and increases cell proliferation and motility [93]. All these changes allow viral transmission from infected endothelial cells to leukocytes. The endothelial cell tropism and the capability to transfer viral material to leukocytes is retained by clinical HCMV isolates and often lost in HCMV strains extensively propagated in fibroblasts. Thus, it has become evident that the UL128L region is indispensable for endothelial cell tropism and viral replication in this cell type as well as virus transfer to leukocytes [94].

### **3.3.3 Role of leukocytes in cytomegalovirus pathogenesis and dissemination**

Leukocytes represent the first line of immune defence during infection. In response to inflammatory signals, these cells migrate through the endothelium of blood vessels to the site of infection. There, pathogen-associated molecular patterns (PAMPs) activate immune cells resulting in phagocytosis and recruitment of adaptive immunity [95].

Among human leukocytes, neutrophils and monocytes/macrophages play a pivotal role in HCMV dissemination in the host. HCMV in the bloodstream is mainly cell-associated and several research lines have been demonstrated that neutrophils and monocytes are actively recruited in the primary site of infection and acquire the virus [96]. Once infected, these cells facilitate viral spread to new organs and tissues, where the virus is delivered to new permissive cells, promoting further viral infections. Their contribution to HCMV vertical transmission from mother to foetus in immunocompetent pregnant women have been also discussed [97].

HCMV has evolved several mechanisms to manipulate the host immune system for its own benefit. Many immunomodulatory proteins encoded by HCMV that promote viral dissemination are chemokine homologs. Chemokine are small proteins that induce cellular chemotaxis by generating a chemical gradient [98]. Thus, HCMV encodes for chemoattractants in order to recruit immune cells to the infection site and use them as carriers to spread throughout the body. The most characterized CXC chemokine homologs encoded by HCMV are UL146 and UL147, that encode vCXCL-1 and vCXCL-2, respectively [99–101]. The vCXCL-1 is an IL-8 homolog that activates the CXCR2 chemokine receptor, mainly targeting neutrophils and monocytes.

### 3.3.3.1 Neutrophils

Neutrophils or polymorphonuclear (PMN) leukocytes are short-lived and terminally differentiated immune cells that act as professional phagocytes [102]. Their mechanisms of action involved in pathogen killing consist in the production of reactive oxygen species (ROS), degranulation followed by release of a plethora of antimicrobial granule proteins, and production of neutrophil extracellular traps (NETs).

The role of neutrophils in HCMV infection is still not completely clarified. Neutrophils are neither HCMV-susceptible nor support the lytic replicative cycle. However, these cells are the major carrier of infectious virus in the bloodstream and may contribute to viral dissemination *in vivo* [103,104]. It has been demonstrated that neutrophils acquire virus and other viral material when co-cultured with infected endothelial cells *in vitro* [92]. Additionally, HCMV DNA and pp65 antigen were detected in neutrophils of viraemic patients [103–106]. Thus, it has been hypothesized that neutrophils uptake the virus from infected permissive cells by either phagocytosis or direct fusion with infected cells. Even in absence of an active viral replication, it has been demonstrated that HCMV induces several changes in neutrophil physiology, including increased cell survival via anti-apoptotic signals and secretion of pro-inflammatory cytokines that stimulate monocyte chemotaxis and differentiation [107].

### 3.3.3.2 Monocytes and macrophages

Monocytes and macrophages are peripheral blood mononuclear cells (PBMC), derived from the myeloid lineage. As neutrophils, monocytes are short-lived phagocytes that circulate in the bloodstream and are involved in the host immune defence and in the removal of apoptotic cells [108]. Their activation leads to cell proliferation and differentiation into macrophages or dendritic cells. These cells are professional antigen-presenting cells with a longer lifespan than monocytes and can either circulate in the blood or differentiate into tissue-resident cells. Macrophages are a heterogeneous population and can be distinguished in two main groups based on their polarization and function during the inflammatory response. M1 macrophages are classically activated macrophages and their differentiation is induced by interferon  $\gamma$ , IL-1 $\beta$ , or lipopolysaccharides (LPS). M1 macrophages display a pro-inflammatory activity by releasing several pro-inflammatory cytokines and increasing the expression of marker molecules and major histocompatibility complex class II (MCH-II) on the cell surface. On the other hand, M2 macrophages are alternatively activated macrophages induced by the secretion of IL-4, IL-10, and IL-13. This subpopulation exhibits anti-inflammatory functions and is involved in tissue remodelling and repair [109]. Macrophage polarization can also be induced upon viral infection and many viruses, including HCMV, have evolved mechanisms to counteract the antiviral responses elicited by M1 macrophages and use M2 macrophages for efficient viral replication and spread [110].

Both monocytes and macrophages are susceptible to HCMV entry, which occurs via macropinocytosis after binding to EGFR,  $\beta$ 1 and  $\beta$ 3 integrins [111]. These cells play a dichotomic role in HCMV pathogenesis by supporting the viral hematogenous dissemination throughout the body and life-long persistence in the host. Like neutrophils, monocytes do not support a productive HCMV replication, however the virus is able to establish latency in this cell type. As monocytes show a short lifespan *in vivo*, it has been hypothesized that the virus uses these cells for dissemination rather than as reservoir for latency. Additionally, it has been described that the nuclear translocation of HCMV capsids after virus entry takes approximately 72 hours in monocytes, as it is transported via trans-Golgi network to the nucleus through a series of recycled endosomes [112]. Thus, CD34+ HPCs in the bone marrow have been thought to represent the major site of long-term HCMV latency and persistence *in vivo* [113]. HCMV has evolved several strategies to induce monocyte migration to the primary site of infection and cell differentiation into macrophages, which are permissive for viral replication. The virus initially induces pro-survival signals in infected monocytes by prolonged expression of Mcl-1 and promotes cell migration and tissue recruitment via viral homologs of CXCR-2. After 48 hours, a switch occurs by inducing a series of pro-apoptotic signals and promoting a cell differentiation program [114]. In differentiated macrophages, the virus reactivates from

latency, resulting in lytic production of infectious viral particles. Furthermore, HCMV promotes cell differentiation into macrophages with a unique M1/M2 intermediate phenotype. This viral strategy should maintain a balance between pro- and anti-inflammatory signals by generating a long-term perfect macrophage type for viral replication and spread [114].

### 3.4 Viral glycoproteins mediating virus binding and entry

The ability of HCMV to enter and infect several human cells *in vitro* is driven by specific glycoproteins present on the viral envelope [18]. At least 11 different glycoproteins, including gB, gM, gN, gH, gL, gO, and UL128/UL130/UL131A, are expressed on the envelope and act as ligands and mediators for the entry into target cells [10]. It has become more and more evident that the variety of glycoproteins expressed on the viral envelope and their relative abundance are related to the promiscuity of HCMV infection. According to the target cell, HCMV uses multiple strategies of cell attachment and entry.

The initial adsorption of HCMV virions to the host cell is mediated by glycoprotein B (gB) and the gM/gN complex following the binding to heparin sulphate proteoglycans (HSPGs) (Figure 7) [115]. Virus adsorption to target cells is inhibited by using fibroblast growth factor or heparin, as these molecules compete for the binding to HSG. Then, entry and fusion steps are mediated by the core fusion machinery of HCMV, formed by gB and the two complexes of gH/gL [116].

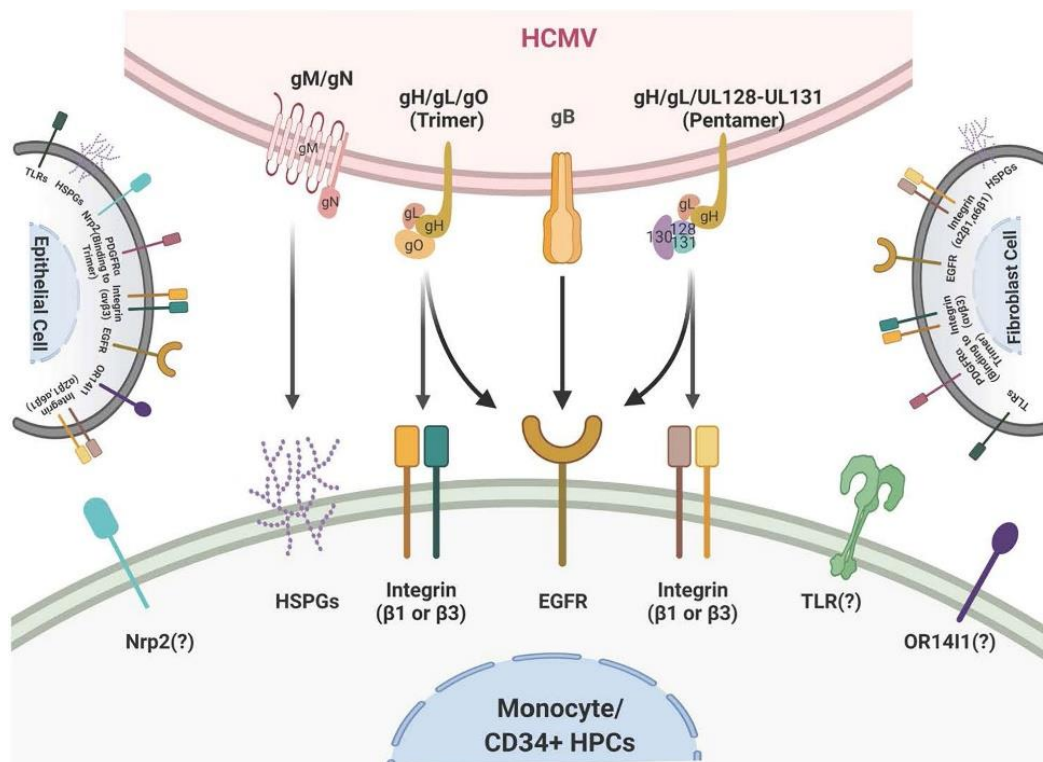


**Figure 7. Viral and cellular receptors involved in HCMV entry.** The viral glycoproteins expressed on the envelope that mediate the entry into target cells are gB, the gM/gN complex, the trimer (gH/gL/gO), and the pentamer (gH/gL/UL128/UL130/UL131A). According to the cell

type, these viral glycoproteins recognize and bind specific cellular receptors on the plasma membrane. Picture taken from [117].

To infect fibroblasts, the trimer formed by the gH/gL/gO complex has been described to directly interact to platelet-derived growth factor receptor alpha (PDGFR $\alpha$ ) on fibroblast surface (Figure 7) [118]. In this complex, gL acts as a chaperone for the fusion receptor gH, while gO mainly contributes to virus entry by binding the cellular receptor PDGFR $\alpha$ . gB can also interact with  $\alpha_v\beta_3$  integrins in mediating fibroblast infection [119]. The virus binding causes a pH-independent fusion of the viral envelope to the plasma membrane, enabling capsid release into the cytoplasm (Figure 8A).

The gH/gL complex may also associate with three proteins encoded by the UL128L, resulting in the pentameric gH/gL/UL128/UL130/UL131A complex. This complex is the major determinant of viral tropism in epithelial, endothelial, and myeloid cells, and mediates the virus transfer from infected cells to leukocytes [88,94]. The pentameric complex has been demonstrated to be highly affected by *in vitro* selection and adaptation. The UL128L rapidly mutates after passaging in human fibroblasts, causing loss of tropism for epithelial, endothelial, and myeloid cells, while driving an efficient cell-free spread [70]. The cellular receptor on epithelial and endothelial cell surface involved in the direct binding to the pentamer has been identified in Neuropilin-2 (Figure 7) [21]. The UL128 and UL131A proteins directly bind the extracellular domains of Neuropilin-2, while the gH/gL complex activates the fusogenic activity of gB [21]. Thus, mutations in the UL128 and UL130 genes result in a drastically reduced binding and entry failure, while mutations in UL130 do not affect the interaction with the receptor. Additionally, the cellular receptor OR1411 has been reported to mediate the entry in epithelial cells by activation of an intracellular signalling leading to endocytosis (Figure 7 and 8B) [120]. The pentamer has been described to indirectly interact with the co-receptor CD147 to mediate virus entry in epithelial and endothelial cells [121]. The virus entry in epithelial and endothelial cells is mediated by endocytosis and low-pH fusion (Figure 8B), whereas macropinocytosis and a pH-independent pathway drive the entry in myeloid cells (Figure 8C) [122,123]. Then, acidification of the vesicles allows the capsid release from the endosomal compartments into the cytoplasm of these cells [21]. It has been reported that fibroblasts express both PDGFR $\alpha$  and Neuropilin-2 receptors on their surface, making this cell type more susceptible to HCMV infection compared to epithelial and endothelial cells, that do not express receptors for the trimer. To confirm this hypothesis, HCMV strains expressing the pentameric complex have been reported to infect PDGFR $\alpha$ -null fibroblasts via interaction to Neuropilin-2 and activation of an alternative pathway for the infection of the cells [21].

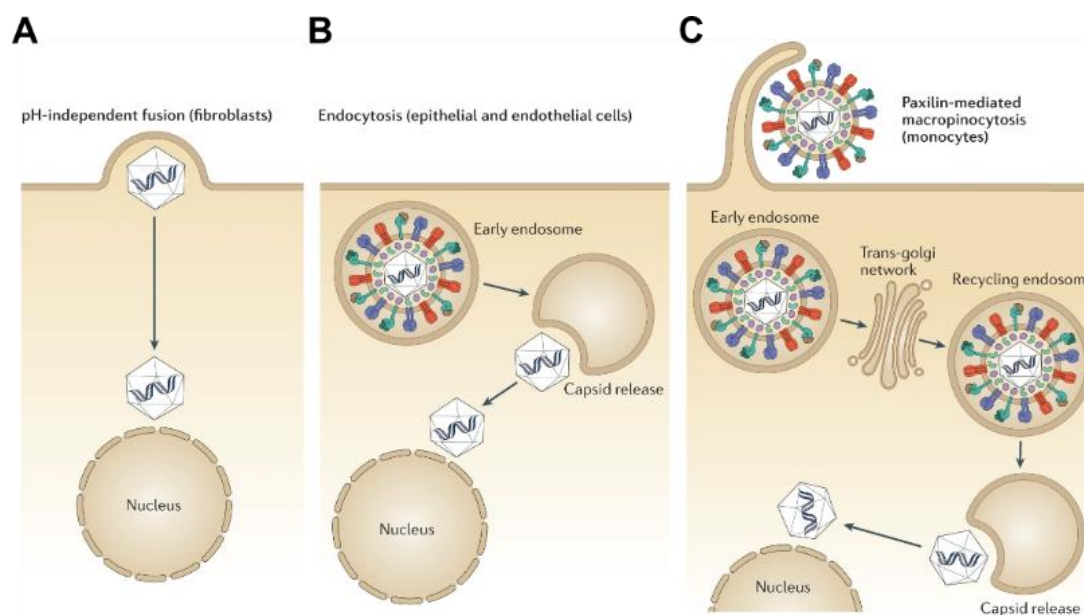


**Figure 8. Mechanisms of HCMV entry.** (A) Virus entry in fibroblasts occurs by direct fusion of the envelope to the plasma membrane. (B) Virus entry into epithelial and endothelial cells is mediated by endocytosis-like processes and low-pH fusion. (C) Virus entry into myeloid cells mainly occurs via macropinocytosis followed by recycling endosomes. Picture modified from [46].

### 3.4.1 Neutralizing antibody response

The identification of HCMV envelope glycoproteins mediating virus binding and entry into target cells has been essential to understand the mechanisms of virus neutralization and to develop new approaches to either inhibit or block the infection *in vivo*. Several studies have demonstrated that the natural human antibody response occurring after primary HCMV infection leads to an efficient virus neutralization. The neutralizing antibodies prevent virus attachment and entry by directly targeting the viral glycoprotein complexes. The most important neutralizing antibodies in HCMV infection have been identified in the glycoproteins gB, trimer, and pentamer, based on their contribution in HCMV cell tropism [124–126].

The neutralizing antibodies show a different level of activity. It has been demonstrated that the neutralizing response depends on the expression levels of gH/gL complexes on viral particles, which is highly variable according to the virus strain and the producer infected cell [127]. Additionally, antibodies to gB or trimer displayed a lower potential of HCMV neutralization, possibly due to the high conservation degree of gO. Several antibodies directed against different binding sites of the pentamer have been identified and showed a strong inhibition potential [128,129]. The neutralization has been reported to be stronger in epithelial and endothelial cell infection than in fibroblasts. These findings suggest the importance to use antibodies direct to the pentameric complex for therapeutic purposes and vaccine design.



Furthermore, a protective role of pentamer neutralizing antibodies in HCMV vertical transmission has been investigated [121,130,131].

Neutralizing antibodies can be divided into two main groups based on their viral target. The first monoclonal antibodies to be characterized bind to the glycoproteins gB, gH, and gM/gN complex. These antibodies show a neutralizing activity in the nanomolar range and prevent HCMV infection in fibroblasts as well as in epithelial and endothelial cells [132]. The second group includes antibodies directed against the pentamer, which are active at picomolar concentrations, but fail in preventing fibroblast infection. The binding sites of these antibodies have been reported to specifically target the UL130/UL131A dimer and, as the UL128L shows a conserved amino acid identity in this region, it has been hypothesized a potentially wide range of activity towards several clinical HCMV isolates [133].

Considering the broad tropism of HCMV and the high genetic variability in circulating HCMV strains, combinations of neutralizing antibodies specific to different viral components have been proposed as valuable asset for HCMV therapy and vaccine development. Currently, several bi-specific antibodies that recognize different epitopes of either pentamer or gB are under investigation in clinical trials [134–136]. The aim of these strategies is to inhibit virus entry in a diverse set of cell types in order to strongly reduce viral transmission in the host.

### **3.5 Cell-cell fusion and syncytium formation in viral pathogenesis**

Cell-cell fusion occurs when two adjacent cells fuse together resulting in the formation of a single multinucleated giant cell, called syncytium [137]. This process has been reported in several physiological as well as pathological conditions, including tumour progression [138]. Additionally, the formation of multinucleated cells has been demonstrated during pathogen infections, such as tuberculosis, schistosomiasis, and viral infections [139–141].

Many enveloped viruses are able to induce cell-cell fusion due to the expression of viral glycoproteins on the cell surface, that mediate not only virus entry into target cells, but also trigger the fusion of infected cells to uninfected neighbouring cells [141]. The presence of proteins with fusogenic activity on the plasma membrane may trigger the fusion of infected cells by binding cell receptors on neighbouring cells, leading to the formation of syncytia. Virus-induced cell-cell fusion and syncytium formation may play a pivotal role in viral dissemination and long-term persistence in the host as these cellular structures may serve to avoid and prevent virus exposure to the host immune defence. Interestingly, infected multinucleated cells have been reported to have an increased survival and motility as well as high capacity of viral production, suggesting their role in promoting immune evasion and viral pathogenesis [142,143]. Thus, within syncytia the virus is protected by T cell control and neutralizing antibodies response and can easily spread in a cell-associated manner. This mechanism has been reported by many respiratory viruses, such as human respiratory syncytial virus, measles

virus, influenza virus, and SARS-coronaviruses, by ensuring an efficient viral transmission from the lungs to other body districts [144]. Additionally, HIV is known to induce syncytium formation in immune cells, such as CD4+ T lymphocytes, macrophages, and dendritic cells, and the presence of multinucleated cells is a hallmark of viral pathogenesis and progression of disease severity [145]. Among herpesviruses, the presence of syncytia in skin lesions has been described in herpes simplex, herpes zoster, and varicella infections [146,147].

Cell-cell fusion and syncytium formation in HCMV infection has been reported both *in vivo* and *in vitro* and seems to be either virus strain-specific and cell type-dependent [148–150]. Although syncytia have been observed in congenital HCMV isolates and clinical HCMV strains, the mechanisms and determinants of their formation have not been completely investigated. The identification of syncytium-forming HCMV variants in congenitally infected infants rises the hypothesis that syncytia may be fundamental in HCMV vertical transmission and may correlated to a more severe viral pathogenesis [149,151].

### 3.5.1 Determinants and mechanisms of syncytium formation

Cell-cell fusion is initiated when specific fusogenic proteins are expressed on the plasma membrane and activated by receptor binding. This binding triggers the fusion receptor to induce conformational changes in the plasma membrane, leading to the formation of a fusion pore first and merging of two adjacent membranes later (Figure 9).

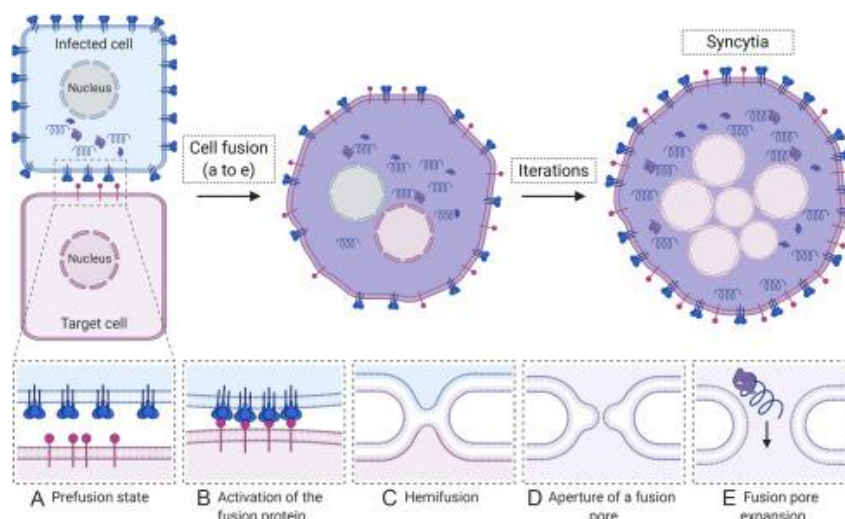


**Figure 9. Cell-cell fusion and syncytium formation.** The expression of viral fusion proteins on the surface of infected cells induces the fusion with uninfected neighbouring cells resulting in the formation of a large multinucleated syncytium. Picture taken from [152].

The fusogenic proteins that drive cell-cell fusion derive from viral glycoproteins present on the envelope and can be expressed on the plasma membrane immediately after virus entry by a vesicle-mediated transfer [153]. This process is known as fusion from without (FFWO). FFWO is generally temperature and pH-dependent and is induced by high concentration of viral

particles, that allows the exposure of high amount of viral glycoproteins immediately after entry. The virus-induced cell-cell fusion can also depend on viral DNA replication and *de novo* synthesis of viral glycoproteins. In this scenario, the newly synthesized fusogenic proteins are accumulated in the cytoplasm and transferred to the plasma membrane prior the embedding into new viral particles. This mechanism of fusion is called fusion from within (FFWI) and is thought to mainly occur *in vivo* supporting viral transmission in the host [153].

Based on this knowledge, it has become clear that an essential requirement of cell-cell fusion is the expression of several viral glycoproteins forming the fusion machinery of the virus [18,116]. Thus, the first candidate and well described glycoprotein involved in both virus entry and syncytium formation in HCMV infection has been identified in the glycoprotein B (gB), encoded by the ORF UL55, a highly polymorphic genetic locus in the HCMV genome. gB usually requires the gH/gL complex, that mediates the binding and triggers the conformational activation of the fusogenic receptor. Recent studies have demonstrated the presence of specific gB fusogenic variants expressed in HCMV strains as well as congenital HCMV isolates [154,155]. One variant of gB present in the laboratory-adapted AD169 strain and in at least two other HCMV isolates, has been reported to promote fusion and facilitate virus entry in fibroblasts [154]. This D275Y amino acid substitution induced a hyperfusogenic gB by promoting direct fusion of the envelope to the plasma membrane rather than mediating entry via macropinocytosis. Another amino acid substitution in gB, S585G, has been reported in the clinical HCMV strain VR1814 and in some congenital HCMV isolates from Italy, and all these viruses showed syncytium formation *in vitro*. Additionally, recent work published by our laboratory has identified five fusogenic variants of gB derived from congenitally infected foetuses isolated in China, suggesting a possible contribution of syncytium formation in HCMV vertical transmission and pathogenicity. Interestingly, the fusogenic variants of gB have been reported to induce cell-cell fusion mainly in fibroblasts, while syncytium formation in other cell types, such as epithelial cells, seems to require additional viral factors. Given the important contribution of the trimer and pentamer in mediating virus entry in several cell types and promoting fusion between virus envelope and plasma membrane [88,156], it is fair to hypothesize a direct contribution of these complexes in syncytium formation. However, no specific fusogenic variants of the two gH/gL complexes have been identified so far.

Nevertheless, it has been proposed the contribution of host cellular factors in syncytium formation as the susceptibility to virus-induced cell-cell fusion greatly varies among different cell types. This variability seems to be dependent on the tissue of origin, cell morphology, motility properties, and physiological functions of the cell. Moreover, the expression levels at the plasma membrane of the receptors used by the virus for entry certainly play a role in syncytium formation. However, until now no host cell factors have been identified in the virus-induced cell-cell fusion.



## 4 Aims of the study

Human cytomegalovirus (HCMV) displays a broad cell and tissue tropism and its ability to infect a wide range of cells supports viral transmission, systemic spread, and pathogenesis in the human host [18,30,76]. Certain HCMV strains not only exhibit a broad cell tropism and capability to be transferred to human leukocytes but induce also cell-cell fusion in infected cells, leading to the formation of multinucleated giant cells known as syncytia. Syncytium formation may reduce virus exposure to host immune factors and influence the pathogenicity. However, the genetic basis of the broad cell tropism and the biological relevance of syncytia in HCMV infection have been poorly investigated. To gain further insights into the genetic factors required for HCMV wide cell tropism and syncytium formation, this study compared the HCMV clinical isolate VR1814 to its bacterial artificial chromosome (BAC) clone, FIX. Previous studies have identified gB variants of congenital HCMV isolates with increased fusogenicity in fibroblasts [155]. However, the same gB variants were unable to cause cell-cell fusion in epithelial cells, indicating that other viral components were involved in the process. Another factor identified as important for syncytium formation in epithelial cells was the pentameric complex, as monoclonal antibodies to proteins encoded by UL128L were shown to inhibit virus-induced cell-cell fusion more potently than monoclonal antibodies directed to the glycoproteins gO, gH, and gB [156].

The first aim of this study was to identify and characterize the viral genetic factors dictating the cell tropism of the HCMV strain VR1814 in epithelial cells and macrophages. In addition, the contribution of VR1814-specific variants on cell-cell fusion and syncytium formation in both cell types was examined. The second aim of this study was to investigate the HCMV trafficking in human neutrophils upon virus uptake from infected endothelial cells. To this end, an *in vitro* system for the HCMV transfer to leukocytes was established and the virus intracellular localization was investigated through several microscopy techniques.

Taken together, the results of this study provide valuable tools to study HCMV infection of biologically relevant cell types and provide new insights on how natural strain variations may influence HCMV infection and pathogenesis in the human host.



## 5 Results

### 5.1 HCMV strain VR1814 shows high infectivity and fusogenicity in several cell types

In previous studies, the HCMV clinical isolate VR1814 was shown to grow efficiently on endothelial cells and to be capable of transferring viral material to polymorphonuclear leukocytes, suggesting a retained broad cell tropism. Thanks to its property, VR1814 has been used in numerous studies that investigated HCMV infectivity in endothelial cells, epithelial cells, and macrophages [68,69,156]. To quantify its infectivity and wide tropism *in vitro*, VR1814 was compared either to another widely used clinical HCMV strain, TB40/E, or to the virus reconstituted from VR1814-derivatived BAC clone, FIX. Human fibroblasts, epithelial cells, endothelial cells, and macrophages were infected at different multiplicities of infection (MOI) according to the cell type. Two days post-infection, cells were fixed, stained with an anti-viral immediate-early 1 and 2 (IE1/IE2) antibody and analyzed by immunofluorescence. The percentage of IE1/IE2-positive cells was determined by using HCS Studio software. As expected, the clinical HCMV strains VR1814 and TB40/E showed similar infectivity in fibroblasts, epithelial, and endothelial cells (Figure 10A to C). Nevertheless, VR1814 infected THP-1-derived macrophages and monocyte-derived M1 macrophages more efficiently than TB40/E, but it showed similar infection rates for monocyte-derived M2 macrophages (Figure 10D to F). Conversely, FIX revealed extremely low infectivity for all cell types except fibroblasts, suggesting an entry defect compared to the parental strain VR1814 (Figure 10).

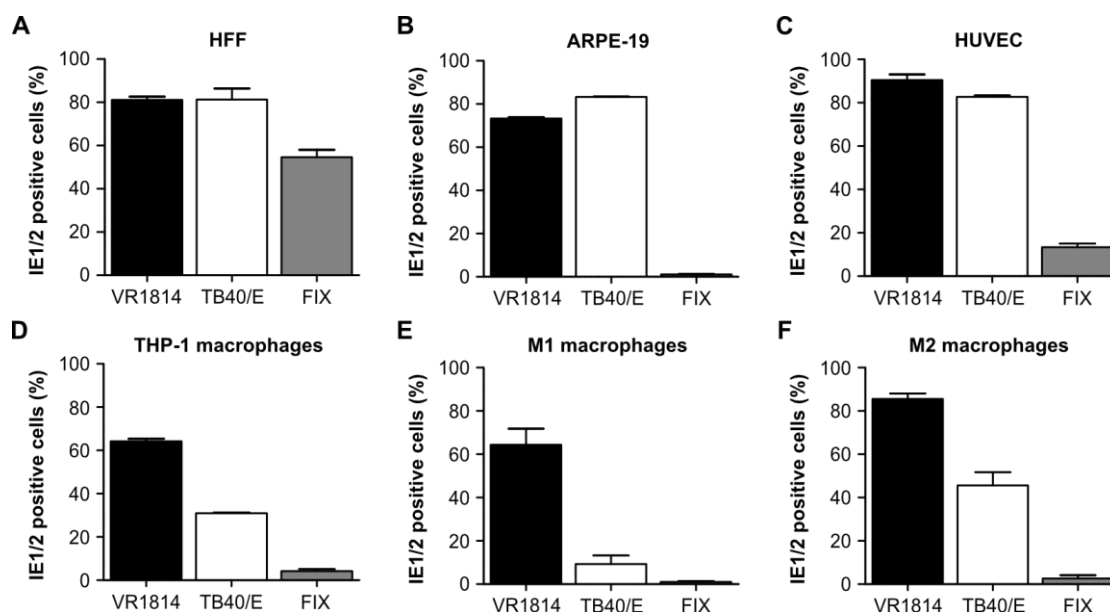


**Figure 10. HCMV infectivity in different cell types.** HFF and ARPE-19 cells were infected with HCMV strains VR1814, TB40/E, and FIX at an MOI of 1. HUVEC cells, THP-1-derived macrophages, and M1 and M2 macrophages were infected at an MOI of 5. The percentage of

infected cells was determined by immunostaining with an antibody recognizing IE1 and IE2. Mean  $\pm$  SEM of three independent experiments are shown.

It has been observed from our laboratory and other researchers that VR1814 caused infected ARPE-19 epithelial cells and MRC-5 fibroblasts to fuse together, resulting in the formation of giant multinucleated cells. Typically, these syncytia have a circular arrangement of nuclei that resembles flower's petals [154–156]. The ability to induce cell-cell fusion and syncytium formation was investigated and compared between the HCMV clinical strains VR1814 and TB40/E. As it has been previously observed that FIX is poorly infectious for almost all cell types (Figure 10) and I hypothesized that its entry defect could also affect its fusogenicity, FIX was not included in this experimental set-up. Fibroblasts, epithelial cells, and macrophages were infected with either VR1814 or TB40/E and incubated for 5 days. At 5 days post-infection, cells were fixed and stained as previously described. The syncytium formation was analyzed by immunofluorescence and imaged by confocal microscopy. Following VR1814 infection, large syncytia were observed in epithelial cells and monocyte-derived macrophages (Figure 11). Fascinatingly, human fibroblasts varied in their susceptibility to cell-cell fusion. Supporting previous findings [154,155], large syncytia were observed in MRC-5 fibroblasts only and not in HFF cells, implying that HFF fibroblasts were less vulnerable to viral-induced cell-cell fusion. On the other hand, TB40/E produced minimal to no syncytium formation in any of the cell type tested (Figure 11).

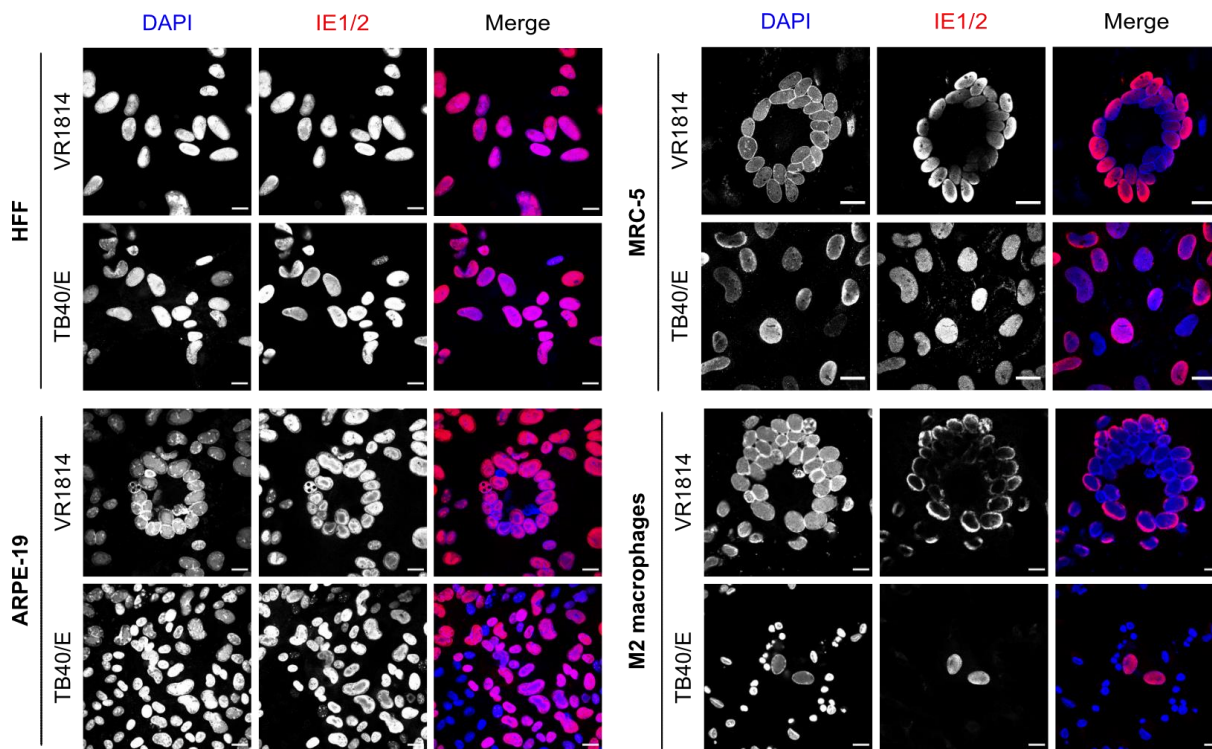


**Figure 11. HCMV syncytium formation in different cell types.** HFF, MRC-5, and ARPE-19 cells were infected with either VR1814 or TB40/E at an MOI of 1. M2 macrophages were infected at an MOI of 5. Syncytium formation was analyzed in the indicated cell types at 5 dpi.



Immunofluorescence staining was performed with anti-IE1/IE2 antibody, and a secondary antibody coupled to AlexaFluor 647. Cell nuclei were counterstained with DAPI. Representative images were taken by confocal microscopy. Scale bar, 20  $\mu$ m.

Altogether, these results indicate that VR1814 retains a broad cell tropism and can be assessed as a useful tool to study HCMV infection of biologically relevant cells, such as myeloid cells. However, the genetic determinants of VR1814 high infectivity and virus-induced cell-cell fusion were still understudied.

## 5.2 Identification of the genetic differences between VR1814 and FIX

The genome of the VR1814 clinical strain was originally cloned as a BAC in *E. coli*, resulting in FIX-BAC. The FIX-BAC reconstituted virus, called FIX, should originally preserve the wild type characteristics of the parental strain [69]. However, FIX has fallen out of favour due to its low infectivity in almost all cell types, as shown in Figure 10. Furthermore, unlike VR1814, FIX does not induce cell-cell fusion and syncytium formation in MRC-5 fibroblasts [154]. Previous work performed in our laboratory has reported that the amino acid exchange in position 585 (S585G) in the UL55 gene, encoding for the glycoprotein B, is responsible of the increased fusogenicity of VR1814 in fibroblasts [154]. This amino acid substitution is not present in the genome of FIX, suggesting that some mutations have occurred during BAC cloning. However, the poor infectivity of FIX and its loss of cell tropism have remained unknown and not further investigated. To identify and characterize the genetic determinants of these differences, we decided to compare the full-length genome sequences of VR1814 and FIX-GFP, a derivative of FIX-BAC containing a GFP expression cassette within the BAC vector backbone [71]. As it is well known and accepted in the literature that *in vitro* passaging of HCMV strains plays a role in selecting certain natural variants and promoting adaptive mutations, we decided to compare the genomes of the isolates present in our laboratory, even though the genome sequences of both viruses were published several years ago [2,70]. The viral genome sequences of our virus isolates were determined by Illumina sequencing. The sequencing depth of FIX-GFP BAC was 2609x  $\pm$ 393x with a genome coverage of 100%, while the sequencing depth of VR1814 was 1429x  $\pm$ 277x with areas of reduced depth: 374x  $\pm$ 91x 452 (GU179289: 849-18593) and 251x  $\pm$ 32x (GU179289: 197622-207977). As expected, the viral sequences of FIX-GFP and FIX-BAC were identical. Interestingly, the VR1814 isolate present in our laboratory revealed a high grade of similarity to an endothelial cell-adapted VR1814 strain described by Dargan *et al.*, called VR1814Ep199 [70]. Except for the known deletion of the genes IRS1 to US6 in FIX, which was added during the BAC cloning [2,69], the VR1814 sequence differed from FIX in several genetic loci. An overview of the variations presents in the coding regions of the genome is listed in Table 1.

**Table 1.** Genetic differences in coding regions of HCMV VR1814 compared to FIX.

<b>GENE</b>	<b>PROTEIN</b>	<b>LOCATION*</b>	<b>SEQUENCE†</b>	<b>CODING EFFECT</b>
<b>UL8</b>	UL8	16499	A	Substitution (E212K)
<b>UL25</b>	UL25	32046	CC+	Frameshift
<b>UL30</b>	UL30	37446	A+	Frameshift
<b>UL31</b>	UL31	38319	C	Substitution (V44A)
<b>UL38</b>	UL38	51477	GGG	In-frame insertion
<b>UL41A</b>	UL41A	54327	T	Substitution (E58K)
<b>UL43</b>	UL43	55889	C	Substitution (T143A)
<b>UL50</b>	NEC2	73746	GAG	In-frame insertion
<b>UL55</b>	gB	82890	C	Substitution (S585G)
<b>UL56</b>	TRM1	85615	T	Substitution (V515M)
<b>UL57</b>	DNBI	89021	C	Substitution (N803S)
<b>UL75</b>	gH	111133	G	Substitution (L43P)
<b>UL76</b>	UL76	111993	C	Substitution (L180P)
<b>UL80.5</b>	APNG	117852	CGC	In-frame insertion
<b>UL89</b>	TRM3	133963	G	Substitution (C547R)
<b>UL95</b>	UL95	140692	GGT+	In-frame insertion
<b>UL98</b>	UL98	144900	G	Substitution (K352E)
<b>UL98</b>	UL98	145063	C	Substitution (D406A)
<b>UL100</b>	gM	147480	C	Substitution (P3R)
<b>UL104</b>	UL104	151475	G	Substitution (L590P)
<b>UL111A</b>	vIL-10	160884	T+	Frameshift
<b>UL111A</b>	vIL-10	160925	GAC	In-frame insertion
<b>UL112</b>	UL112	163725	GGT	In-frame insertion
<b>UL116</b>	UL116	166522	GGC	In-frame insertion
<b>UL121</b>	UL121	170032	C+	Frameshift
<b>UL122</b>	IE2	171135	A	Substitution (S376F)
<b>UL122</b>	IE2	171910	AGG	In-frame insertion
<b>UL128</b>	UL128	176683	C	Substitution (F33V)
<b>UL130</b>	UL130	177250	G	Substitution (P72S)
<b>UL130</b>	UL130	176856	T	Substitution (T203N)
<b>UL147A</b>	UL147A	180059	C	Substitution (Y55X)
<b>UL147</b>	vCXCL2	180375	A+	Frameshift
<b>UL135</b>	UL135	188726	G	Substitution (W284R)
<b>UL135</b>	UL135	189267	CTA	In-frame insertion
<b>UL133</b>	UL133	189770	GTC	In-frame insertion

<b>UL150A</b>	UL150A	193227	GGC	In-frame insertion
<b>US15</b>	US15	209669	G	Substitution (F87L)
<b>US20</b>	US20	214013	T	Substitution (W231X)
<b>US28</b>	US28	225076	GAC	In-frame insertion
<b>US28</b>	US28	225998	TT+	Frameshift
<b>US33A</b>	US33A	230110	C	Substitution (L39P)
<b>US34</b>	US34	230525	GA+	Frameshift
<b>TRS1</b>	TRS1	234246	G	Substitution (E35A)

\* Nucleotide position in the genome sequence of VR1814 (GenBank GU179289).

† The mutated nucleotide at each location is shown.

### 5.3 Role of VR1814-specific glycoprotein variants in the infectivity on epithelial cells

To gain insight into the role of sequence variations listed in Table 1 on VR1814 infectivity and virus-induced cell-cell fusion, the goal was to select few genetic loci that appeared to be valid candidates and test them in the context of epithelial cell infection. A former post-doctoral researcher in our laboratory, Dr. Giada Frascaroli, has generated on the backbone of the HCMV strain FIX-BAC a series of mutants by *en passant* mutagenesis (Figure 12). The genetic candidates we decided to focus on were the following:

- (i) The S585G amino acid exchange in UL55 gene, encoding for the glycoprotein B (gB), which our laboratory already demonstrated to be a fusogenic variant in the context of MRC-5 fibroblast infection [154,155].
- (ii) The three amino acid substitutions in UL128 locus (UL128L), in details F33V in UL128, P72S and T203N in UL130, respectively, as the pentameric glycoprotein complex (gH/gL/UL128/UL130/UL131A) is essential for HCMV entry and infection of epithelial, endothelial, and myeloid cells.
- (iii) The frameshift mutation in US28, leading to a short missense amino acid sequence after the amino acid 314, which was previously described to cause an altered signalling activity of the truncated US28(1-314) protein [157].

Consequently, the recombinant FIX strains carry VR1814-specific variants of UL55/gB (later on called B), the pentameric components UL128 and UL130 (called P), and the truncated version of the chemokine receptor US28 (called C). Three single, two double, and one triple mutants were generated by BAC mutagenesis as shown in Figure 12.

In this work, I evaluated the recombinant FIX strains in terms of infectivity and cell-cell fusion in epithelial cells and macrophages, and compared their replication fitness to the parental strains, VR1814 and FIX.

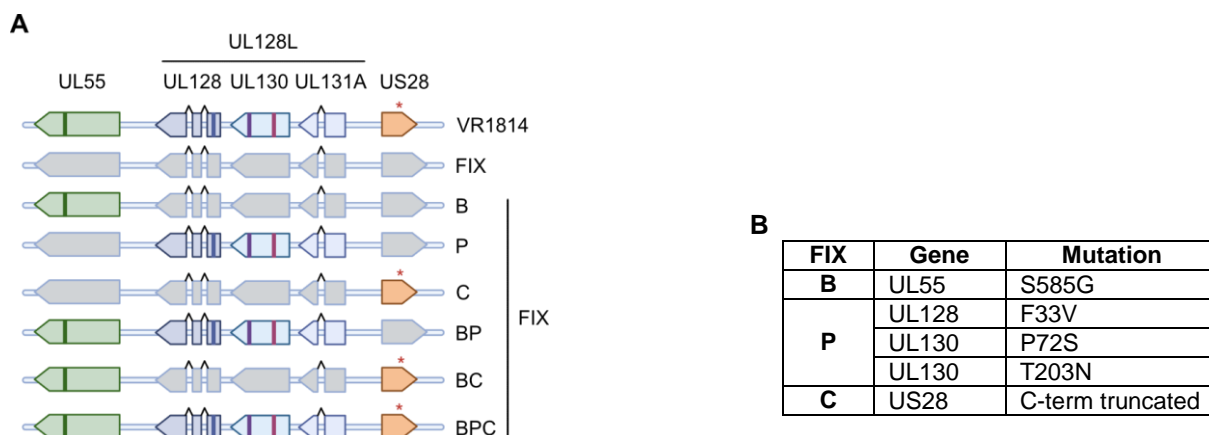


**Figure 12. Generation by BAC mutagenesis of the recombinant FIX strains.** (A) Schematic representation of the FIX derived mutants used in this study. They contain VR1814-specific variants of UL55/gB, the Pentamer proteins UL128 and UL130, and the US28 Chemokine receptor. (B) List of the mutations present in the recombinant FIX strains.

Initially, the replication properties of the recombinant FIX strains were investigated in ARPE-19 epithelial cells by multistep replication kinetics. As shown in Figure 13, ARPE-19 cells were infected at a MOI of 0.5 and infectious supernatants were collected for titration at the indicated time post-infection. Comparison of the single mutants to the parental FIX demonstrated that the insertion of one VR1814-specific variant per time had minimal effect in viral replication and spread in epithelial cells. Specifically, FIX-B and FIX-C replicated to slightly higher titers than the parental FIX strain, while FIX-P even replicated to lower titers and a strictly cell-associated phenotype was observed during virus stock production (Figure 13A). In contrast, the double mutant FIX-BP and the triple mutant FIX-BPC replicated most efficiently, and their titers were at least as high as VR1814 up to day 7 post-infection. However, their peak titers at later time post-infection were approximately 5 to 9-fold lower than those of VR1814 (Figure 13B). Interestingly, the double mutant FIX-BC replicated to slightly higher titers than the parental FIX strain as the single mutants FIX-B and FIX-C did. These results suggested that the VR1814-specific variants of gB and UL128L mostly contribute in a synergistic way to the high infectivity of VR1814 in epithelial cells.

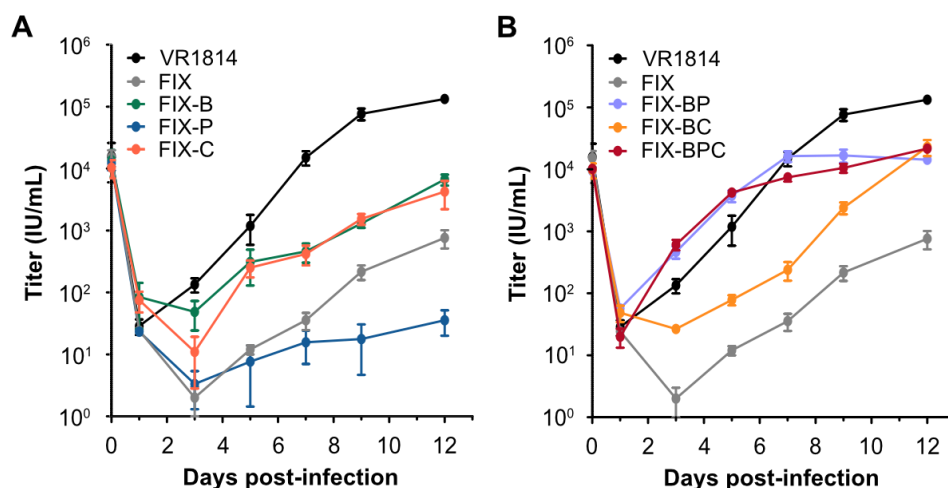


**Figure 13. Replication kinetics of the recombinant FIX strains in ARPE-19 cells.** ARPE-19 cells were infected at an MOI of 0.5. Supernatants from the infected cells were collected at the indicated time points and titered on HFF cells. Viral titers are shown as mean  $\pm$  SEM of three biological replicates. (A) Multistep replication kinetics of FIX single mutants. (B) Multistep replication kinetics of FIX double and triple mutants.

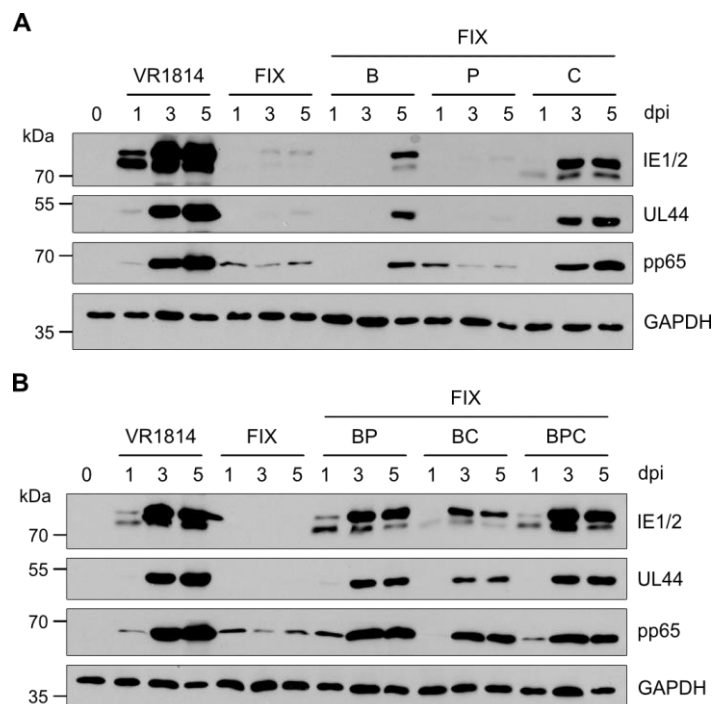


**Figure 14. Expression kinetics of the recombinant FIX strains in ARPE-19 cells.** ARPE-19 cells were infected at an MOI of 1. Whole cell lysates were harvested at 1, 3, and 5 dpi, and the levels of the viral proteins IE1/IE2, UL44, and pp65 were analyzed by immunoblotting. GAPDH was used as loading control. (A) Expression kinetics of FIX single mutants. (B) Expression kinetics of FIX double and triple mutants.

When ARPE-19 cells were infected with the recombinant FIX strains, the viral protein expression on days 1, 3 and 5 post-infection were determined by Western blot. The immediate-early proteins 1 and 2 (IE1/IE2), the early protein UL44, and the late protein pp65 were detected with specific antibodies. As shown in Figure 14, the results were consistent with those of the growth curve kinetics previously shown. The single mutants FIX-B and FIX-P showed a

delayed and strongly reduced expression of viral proteins comparable to the parental FIX. Surprisingly, FIX-C expression kinetics were delayed compared to VR1814, but stronger than FIX (Figure 14A). Among double and triple mutants, FIX-BP and FIX-BPC showed expression levels similar to VR1814 for all immediate-early, early, and late viral proteins, while FIX-BC showed a delayed kinetics (Figure 14B).

Next, the relative infectivity of the recombinant viruses on ARPE-19 epithelial cells was determined at 1 and 5 dpi. The cells were infected at an MOI of 1 and at the indicated time post-infection, cells were fixed, stained with an anti-viral IE1/IE2 antibody and analyzed by immunofluorescence. The percentage of IE1/IE2-positive cells was determined by using HCS Studio software. As expected, VR1814, FIX-BP, and FIX-BPC showed the highest relative infectivity at both 1 and 5 dpi (Figure 15A and B). Nevertheless, FIX, the three single mutants, and FIX-BC showed lower infectivity at 1 dpi. Interestingly, only FIX-P seemed to slowly increase the infection rate over time.

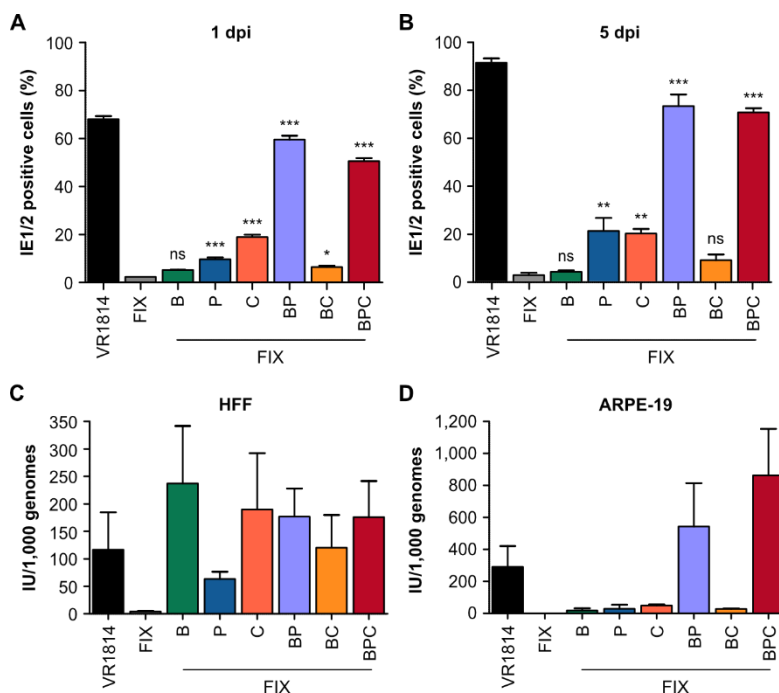


**Figure 15. Infectivity of the recombinant FIX strains in ARPE-19 cells.** (A, B) ARPE-19 cells were infected at an MOI of 1. Relative infectivities of the recombinant FIX strains were determined as percentage of IE1/IE2-positive nuclei at 1 and 5 dpi, respectively. Mean  $\pm$  SEM of three independent experiments are shown. Recombinant FIX strains were compared to FIX. Significance was determined by one-way ANOVA with Dunnett's multiple comparison test. \*,  $P < 0.05$ ; \*\*,  $P < 0.01$ ; \*\*\*,  $P < 0.001$ ; ns, not significant. (C, D) Infectivities of cell-free virus stocks on either HFF cells (C) or ARPE-19 cells (D) were determined by quantifying viral genome copies by qPCR and infectious units (IU) per mL by titration. Infectivity is shown as infectious units (IU) per 1000 viral genomes. Mean  $\pm$  SEM are shown.

Given the variable infectivity of FIX and of the recombinant strains on epithelial cells, I additionally determined the infectivity of each virus stock on either HFF fibroblasts or ARPE-19 epithelial cells as infection units (IU) per 1000 genomes (Figure 15C and D). According to

previous publications, HCMV enters in fibroblasts or epithelial cells through two different mechanisms. HCMV entry into fibroblasts is mediated by the trimeric gH/gL/gO complex in cooperation with gB [158–160], while HCMV infection of epithelial, endothelial, and myeloid cells requires the pentameric gH/gL/UL128/UL130/UL131A complex [148,161,162]. In order to explain the different infectivity according to the cell type shown by VR1814 and FIX (Figure 10), I hypothesized that the ratio IU per genomes of the viruses should be different on either fibroblasts or epithelial cells. Thus, cell-free stocks of VR1814, FIX, and all recombinant FIX strains were analyzed by real-time qPCR to quantify the genome-containing virions, and the viral titers were determined by infectious units (IU) per millilitre on either HFF cells (Figure 15C) or ARPE-19 cells (Figure 15D). The ratio IU per 1000 genomes was then calculated. The measurements on fibroblasts did not significantly vary among all viruses, with FIX having the lowest value (Figure 15C). Notably, FIX-P showed lower value compared to the other FIX single mutants. This modest difference might indicate the non-contribution of the pentameric complex to virus entry and infection of fibroblasts. These results were consistent to previous observations, suggesting that genetic differences in the pentameric proteins UL128 and UL130 did not affect entry and infection in fibroblasts. Nevertheless, as shown in Figure 15D the ratios measured on ARPE-19 epithelial cells were higher, as reported by previous findings [123,163]. HCMV less likely infects epithelial cells than fibroblasts, possibly due to the more complex entry mechanism, which requires endocytosis followed by fusion of the virus envelope with the endosome membranes. These findings demonstrated that all recombinant FIX strains were more infectious than the parental FIX, with VR1814, FIX-BP, and FIX-BPC showing the highest values.

#### **5.4 Role of VR1814-specific glycoprotein variants in cell-cell fusion and syncytium formation in epithelial cells**

Given the findings of the recombinant FIX strains infectivity on epithelial cells, I further investigated their ability to induce cell-cell fusion and syncytium formation in this cell type. ARPE-19 cells were infected at a MOI of 1 and incubated for 5 days. At day 5 post-infection, cells were fixed and stained with an anti-IE1/IE2 antibody. Syncytium formation was analyzed by immunofluorescence and imaged by confocal microscopy (Figure 16). The findings demonstrated that the formation of large multinucleated syncytia was induced only by VR1814,

FIX-BP, and FIX-BPC. Consistently with previous observations, FIX, the three single mutants, and FIX-BC were able to infect very few cells and failed in inducing fusion of epithelial cells.

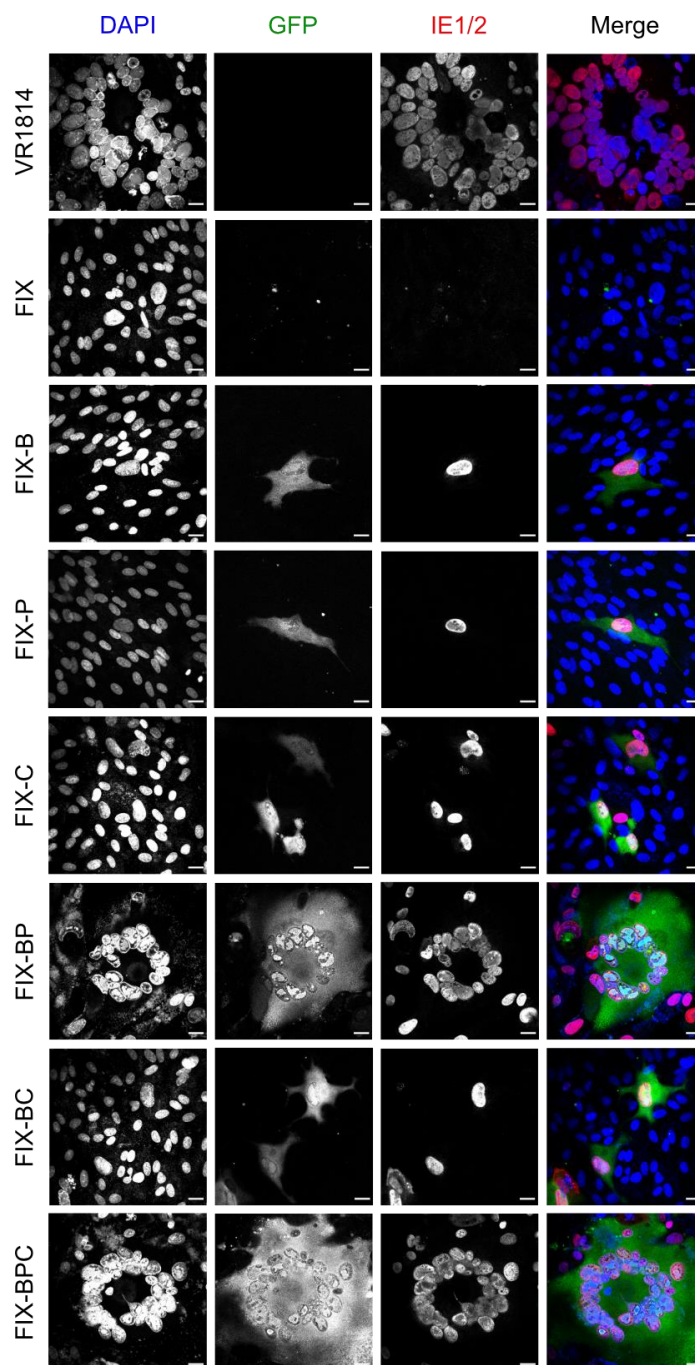


**Figure 16. Epithelial cell fusion induced by the recombinant FIX strains.** ARPE-19 cells were infected at an MOI of 1. At 5 dpi, cells were fixed, and stained with an anti-IE1/IE2 antibody (red). Cell nuclei were counterstained with DAPI (blue). All FIX strains express GFP (green). Syncytium formation was analyzed by microscopic inspection. Representative images were taken by confocal microscopy. Scale bar, 20  $\mu$ m.

To analyze and compare syncytium formation induced by VR1814 and the recombinant FIX strains in infected epithelial cells, I employed a previously developed method that allows an easy and rapid quantification of cell-cell fusion upon HCMV infection [155]. Previous work



performed in our laboratory established and optimized a reporter system based on a dual split protein (DSP) made up of split *Renilla* luciferase (RLuc) and split green fluorescent protein (GFP). As shown in Figure 17A, when cells expressing different DSP fuse together due to viral infection, the two halves of the DSP re-associate and both the GFP fluorescent activity and the *Renilla* luciferase enzymatic activity are restored.

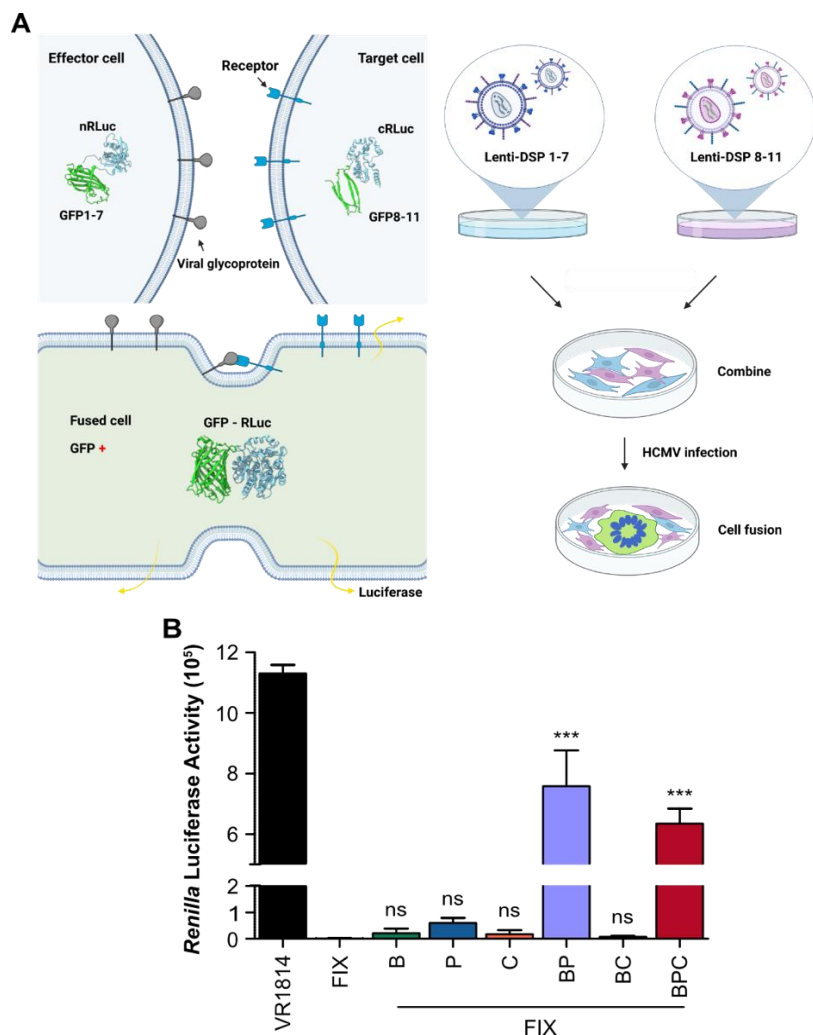


**Figure 17. Fusogenicity of the recombinant FIX strains in ARPE-19 cells.** (A) Schematic representation of the dual split protein (DSP) reporter system used to detect HCMV-induced cell-cell fusion. ARPE-19 cells expressing either DSP1-7 or DSP8-11 were generated by lentiviral transduction [155]. (B) DSP-expressing ARPE-19 cells were infected at an MOI of 1. *Renilla* luciferase activity was measured at 5 dpi. Mean  $\pm$  SEM of three independent experiments are shown. Recombinant FIX strains were compared to FIX. Significance was determined by one-way ANOVA with Dunnett's multiple comparison test. \*\*\*,  $P < 0.001$ ; ns, not significant.

Thus, I transduced ARPE-19 cells with lentiviral vectors expressing either one or the other half of the DSP system. Puromycin was used for selection of the transduced cells. Equal amounts of ARPE-19 cells stably expressing either DSP1-7 or DSP8-11 were combined, seeded in cell culture plates, and infected with the recombinant FIX strains and the parental strains at an MOI of 1. Since all FIX strains already expressed GFP, only the restored activity of *Renilla* luciferase

was used as read-out of cell-cell fusion. On day 5 post-infection, cells were washed with PBS, and incubated with the *Renilla* luciferase substrate, coelenterazine-h, at a final concentration of 2.5 nM. The enzymatic activity was measured using a multi-mode microplate reader (FLUOstar Omega). The results showed that only cells infected with VR1814, FIX-BP, and FIX-BPC had high luciferase levels detected, in line with the previous qualitative analysis made by microscopy (Figure 17B). FIX-B, FIX-P, FIX-C, and FIX-BC showed similar levels as the parental FIX. These findings indicate that VR1814-specific variants of both gB and UL128L are necessary for syncytium formation in ARPE-19 epithelial cells. Furthermore, it is noteworthy that both infectivity and cell-cell fusion of FIX are affected by its poor entry in these cells.

To gain insight into the role of the pentameric complex on cell-cell fusion and syncytium formation in epithelial cells, equal amounts of ARPE-19 cells stably expressing either DSP1-7 or DSP8-11 were combined, seeded in cell culture plates, and infected with either VR1814 or FIX-BP at an MOI of 1. After 3 hours, the virus inoculum was removed, and cells were incubated in fresh medium containing serial dilutions of a neutralizing anti-UL130 antibody for 5 days. On day 5 post-infection, cells were washed with PBS and incubated with coelenterazine-h. The *Renilla* luciferase activity was measured as described above and the percentage of syncytia relative to cells treated with a non-neutralizing anti-pp71 control antibody was calculated. The hybridoma supernatant towards a tegument protein, such as pp71, served as control for any non-specific inhibition. Higher concentrations of the anti-UL130 antibody in the medium prevented either virus from inducing cell-cell fusion in infected epithelial cells (Figure 18B). Furthermore, after luciferase activity quantification, cells were fixed, stained with an anti-IE1/IE2 antibody, and syncytium formation was observed by microscopy. The results were consistent with the luciferase measurements (Figure 18A). Large syncytia were present only in untreated infected cells, and as the concentration of the hybridoma supernatant increased, the size and the quantity of syncytia decreased. These findings confirmed the critical role played by the pentamer in HCMV-induced cell fusion of epithelial cells.

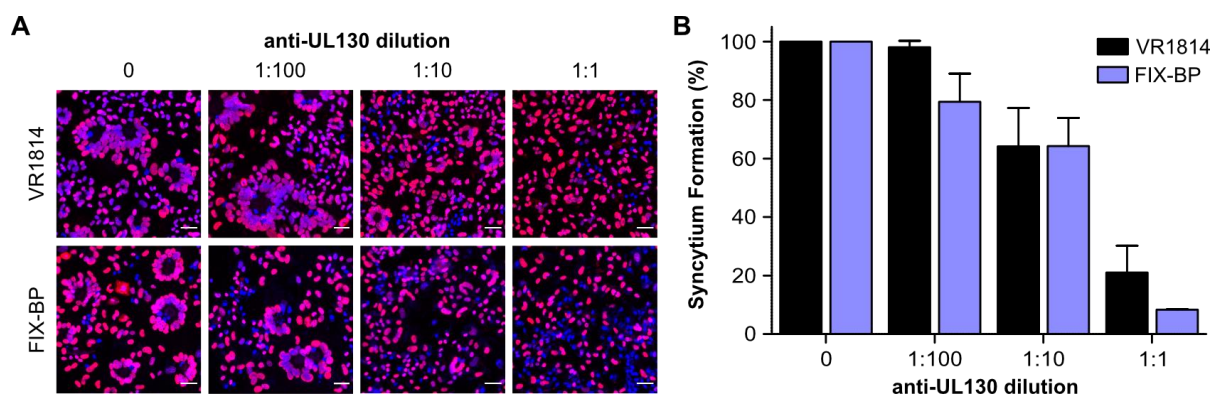


**Figure 18. Contribution of the pentamer in cell-cell fusion on ARPE-19 cells.** DSP-expressing ARPE-19 cells were infected with either VR1814 or FIX-BP at a MOI of 1 and incubated with serial dilutions of an anti-UL130 hybridoma supernatant for 5 days. (A) Syncytium formation was observed microscopically on day 5 post-infection using IE1/IE2

specific antibody. (B) *Renilla* luciferase activity was measured at 5 dpi. Syncytium formation is shown relative to cells treated with a non-neutralizing anti-pp71 hybridoma supernatant. Mean  $\pm$  SEM of two independent experiments performed in triplicate are shown.

### 5.5 Characterization of FIX-derived variants of UL128 and UL130 for the infectivity and cell-cell fusion in epithelial cells

Given the crucial role of UL128L on syncytium formation in infected epithelial cells, VR1814-specific variants may contribute differently to viral infectivity and cell-cell fusion. Considering that FIX-BP carry all the three different amino acid substitutions of VR1814 in UL128L (F33V in UL128, P72S and T203N in UL130), the effect of each single variant was analyzed. Consequently, each of the three positions in FIX-BP were reverted to the variant present in the parental FIX by *en passant* mutagenesis. Three new revertant FIX strains in UL128L were generated by Dr. Giada Frascaroli as shown in Figure 19A.

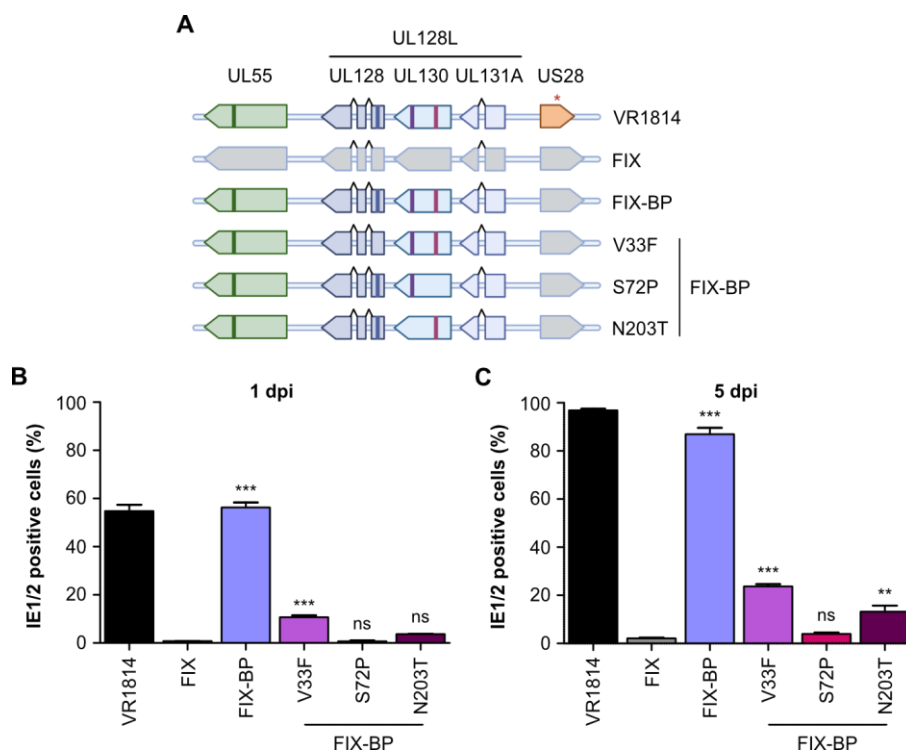


**Figure 19. Infectivity of the revertant FIX strains in UL128L.** (A) Schematic representation of the FIX derived mutants used in this study. They were reverted in either UL128 (V33F) or UL130 (S72P and N203T) as the variants present in FIX. (B, C) ARPE-19 cells were infected at an MOI of 1. Relative infectivities of the recombinant FIX strains were determined as percentage of IE1/IE2-positive nuclei at 1 and 5 dpi, respectively. Mean  $\pm$  SEM of three independent experiments are shown. Recombinant FIX strains were compared to FIX. Significance was determined by one-way ANOVA with Dunnett's multiple comparison test. \*\*,  $P < 0.01$ ; \*\*\*,  $P < 0.001$ ; ns, not significant.

First, the relative infectivity of the three revertant strains FIX-BP(V33F), FIX-BP(S72P), and FIX-BP(N203T) on ARPE-19 epithelial cells was determined at 1 and 5 dpi. Cells were infected at an MOI of 1, and at the indicated time post-infection were fixed, stained with an anti-IE1/IE2 antibody, and analyzed by immunofluorescence. The percentage of IE1/IE2-positive cells was

determined by using HCS Studio software. Consistent with previous observation (Figure 15A and B), VR1814 and FIX-BP had similar infectivity on ARPE-19 cells at 1 dpi, that increased over time. In comparison to FIX-BP, the three revertant FIX strains showed lower infectivity at early and late time post-infection (Figure 19B and C). Interestingly, FIX-BP(S72P) showed the strongest decrease in infectivity at 1 and 5 dpi, very similar to those shown by FIX.

Next, the syncytium formation of the three revertant strains FIX-BP(V33F), FIX-BP(S72P), and FIX-BP(N203T) on ARPE-19 epithelial cells was analyzed at 5 dpi by using either microscopy or the DSP reporter system. On the one hand, ARPE-19 cells were infected at an MOI of 1 and incubated for 5 days for qualitative analysis of cell-cell fusion. On day 5 post-infection, cells were fixed, stained with an anti-IE1/IE2 antibody and syncytium formation was analyzed by confocal microscopy. The results confirmed that the three revertant FIX viruses caused minimal or no cell-cell fusion compared to VR1814 and FIX-BP, whose induced the largest syncytia (Figure 20A). On the other hand, equal amounts of ARPE-19 cells stably expressing either DSP1-7 or DSP8-11 were combined and infected at an MOI of 1 for quantitative evaluation. On day 5 post-infection, cells were washed with PBS, and incubated with coelenterazine-h. The enzymatic activity of the restored *Renilla* luciferase was then measured. Once more, VR1814 showed the highest values, followed by FIX-BP, FIX-BP(V33F), and FIX-BP(N203T) (Figure 20B). Interestingly, the S72P substitution in UL130 of FIX completely abolished the cell-cell fusion of infected epithelial cells, suggesting a negative impact of this variant on either infectivity or fusogenicity.

It is known that mutations in genes encoding for viral envelope glycoproteins can cause amino acid exchanges leading to an altered incorporation into viral particles or a defective interaction with cell receptors. Considering that, I hypothesized that alterations in the pentameric complex may affect virus entry and infectivity in epithelial cells. To assess the incorporation of the pentamer in the virion envelopes, cell-free viruses of the revertant FIX strains were analyzed by non-reducing Western blotting and compared to the parental strains. The gH/UL128 disulfide-linked complex was used as surrogate for the pentamer, separated by non-reducing SDS-PAGE and analyzed by Western blotting using an anti-UL128 antibody. The UL130 protein was detected by standard SDS-PAGE and with an anti-UL130 antibody. The gel loads were normalized to the tegument protein pp150. The findings revealed that small amounts of the pentamer were present in FIX and FIX-BP(S72P) virions (Figure 20C), in line with previous studies [164].

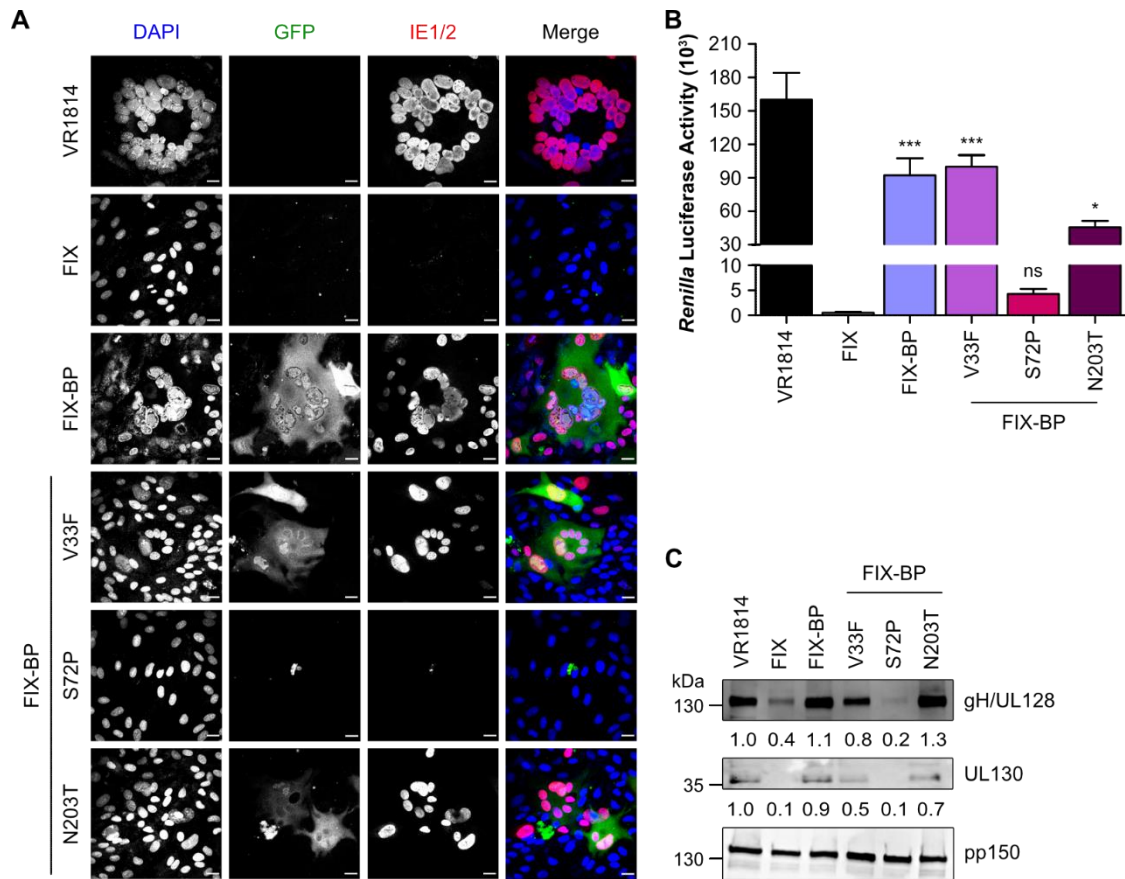


**Figure 20. Epithelial cell fusion induced by the revertant FIX strains in UL128L.** ARPE-19 cells were infected at an MOI of 1. At 5 dpi, cells were fixed, and stained with an anti-IE1/IE2 antibody (red). Cell nuclei were counterstained with DAPI (blue). All FIX strains express GFP (green). Syncytium formation was observed at 5 dpi. Representative images were taken by confocal microscopy. Scale bar, 20  $\mu$ m. (B) DSP-expressing ARPE-19 cells were infected at an MOI of 1. *Renilla* luciferase activity was measured at 5 dpi. Mean  $\pm$  SEM of three independent experiments are shown. Recombinant FIX strains were compared to FIX. Significance was determined by one-way ANOVA with Dunnett's multiple comparison test. \*,  $P < 0.05$ ; \*\*\*,  $P < 0.001$ ; ns, not significant. (C) Lysates of purified virions were analyzed by immunoblot. The gH/UL128 disulfide-linked complex, separated on a non-denaturing gel, was detected with an anti-UL128 antibody. UL130 and pp150 were separated on a denaturing gel and detected with specific antibodies. The gel loads were normalized to equal pp150 and the numbers below the blots indicate band intensity analysis, normalized to VR1814 band on the same blot.

Together, these analyses indicate that the amino acid exchange S72P in UL128 of FIX mostly contributes to impair infectivity and cell-cell fusion in epithelial cells due to a limited incorporation of the pentamer on the viral envelope.

## 5.6 Role of VR1814-specific glycoprotein variants in the infectivity on macrophages

Even though the findings obtained with FIX-BP and FIX-BPC recombinant viruses suggested that both gB and UL128L fusogenic variants were important for infectivity and syncytium

formation in epithelial cells, it was crucial to identify the effects of these VR1814-specific variants on infectivity in macrophages. To investigate this aspect, the infectivity and replication kinetics of the recombinant FIX strains were analyzed in THP-1-derived macrophages, an established model to study HCMV infection of macrophages [165–167]. THP-1 cells were seeded in cell culture plates and treated with phorbol 12-myristate 13-acetate (PMA) for 3 days at a final concentration of 50 nM to induce their differentiation into macrophages. THP-1-derived macrophages were then washed with fresh medium, infected at an MOI of 5, and infectious supernatants were collected for titration at the indicated time post-infection. Overall, the release of infectious supernatants from infected macrophages was lower than in epithelial cells. FIX, FIX-B, and FIX-P replicated very poorly in macrophages and their spread never increased over time (Figure 21A). Interestingly, FIX-C spread to higher titers than the parental FIX. Contrary, VR1814, FIX-BP, FIX-BC, and FIX-BPC showed comparable replication kinetics, with similar titers up to day 5 post-infection. However, VR1814 was the only virus to show an increasing titer up to day 7 post-infection in infected macrophages (Figure 21B). These results were consistent with what previously described in ARPE-19 epithelial cells and confirmed the essential role played by VR1814-specific variants of gB and UL128L in increasing virus infectivity. Furthermore, VR1814-specific mutation in US28 seemed to promote viral replication in THP-1-derived macrophages.

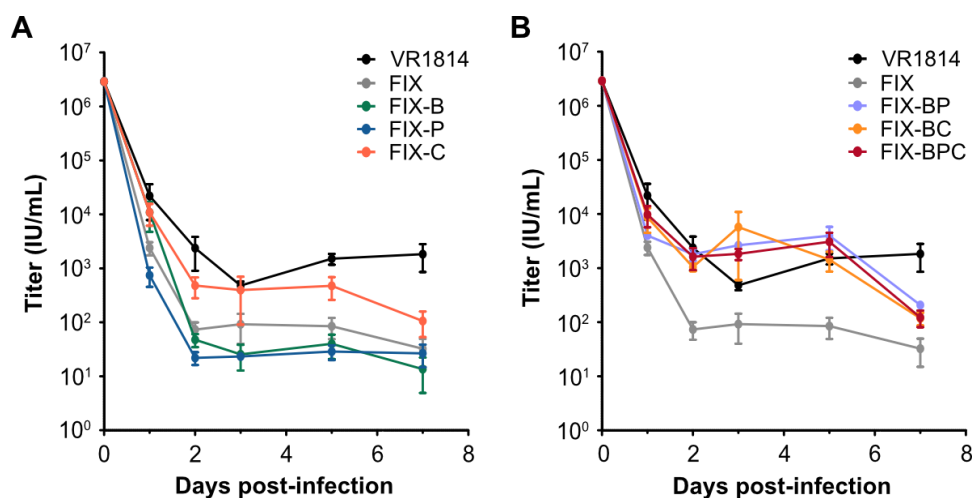


**Figure 21. Replication kinetics of the recombinant FIX strains in THP-1-derived macrophages.** THP-1 cells were differentiated into macrophages by PMA treatment for 3 days and infected at an MOI of 5. Supernatants from the infected cells were collected at the indicated time points and titered on HFF cells. Viral titers are shown as mean  $\pm$  SEM of three biological replicates. (A) Single step replication kinetics of FIX single mutants. (B) Single step replication kinetics of FIX double and triple mutants.

When THP-1-derived macrophages were infected with the recombinant FIX strains, the viral protein expression on days 1, 3 and 5 post-infection were determined by Western blot. The immediate-early proteins 1 and 2 (IE1/IE2), and the proteins UL44 and pp65 were expressed with similar kinetics in FIX-BP and FIX-BPC as well as in VR1814 (Figure 22B). FIX-BC



showed a delayed viral protein kinetics compared to VR1814. On the contrary, the three single mutants and FIX exhibited a strongly reduced viral protein expression profile (Figure 22A). These data confirmed previous observations and suggested that gB, UL128L, and US28 genes are important for macrophages infection.

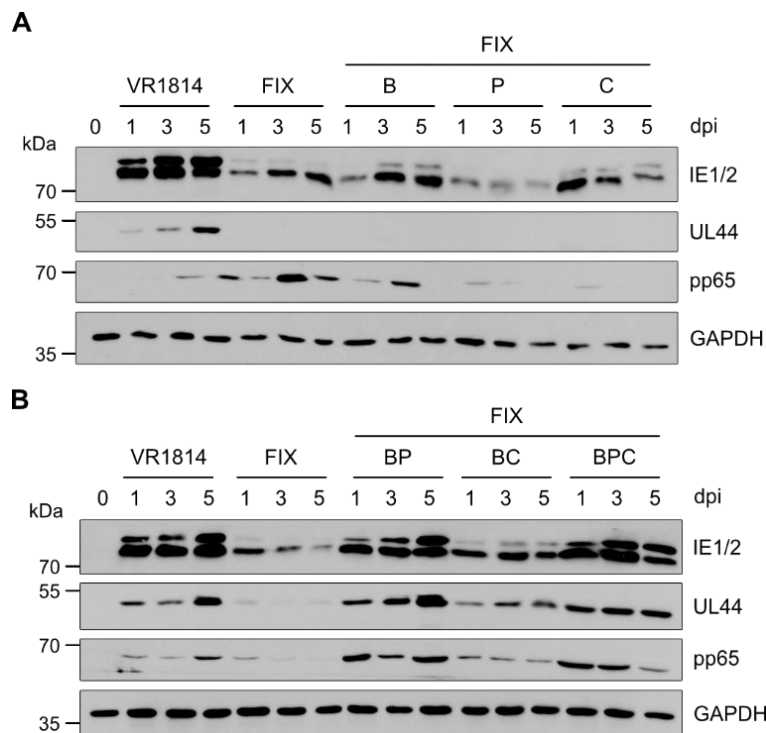


**Figure 22. Expression kinetics of the recombinant FIX strains in THP-1-derived macrophages.** THP-1-derived macrophages were infected at an MOI of 5. Whole cell lysates were harvested 1, 3, and 5 dpi, and the levels of the viral proteins IE1/IE2, UL44, and pp65 were analyzed by immunoblotting. GAPDH was used as loading control. (A) Expression kinetics of FIX single mutants. (B) Expression kinetics of FIX double and triple mutants.

Subsequently, the relative infectivity of the recombinant FIX viruses on THP-1-derived macrophages was determined. Cells were differentiated for 3 days by adding PMA, infected at an MOI of 5 and on days 1 and 5 post-infection, cells were fixed, stained with an anti-viral IE1/IE2 antibody, and analyzed by immunofluorescence to determine the percentage of IE1/IE2-positive cells. Consistent with previous observations in ARPE-19 epithelial cells, VR1814, FIX-BP, and FIX-BPC had the highest infectivity at both 1 and 5 dpi (Figure 15A and B). Surprisingly, FIX-BC showed higher infection rates for macrophages compared to epithelial cells, implying that the C-terminally shortened US28 protein could facilitate infection and particularly the immediate-early gene expression in this specific cell type. FIX and the three single mutants infected with very low efficiency THP-1-derived macrophages at 1 dpi (Figure 23A), while the infectivity of FIX-B, FIX-P, and FIX-C increased later on (Figure 23B). As described by Kim *et al.*, a delayed virus entry via endocytosis could be the reason of this discrepancy [112].

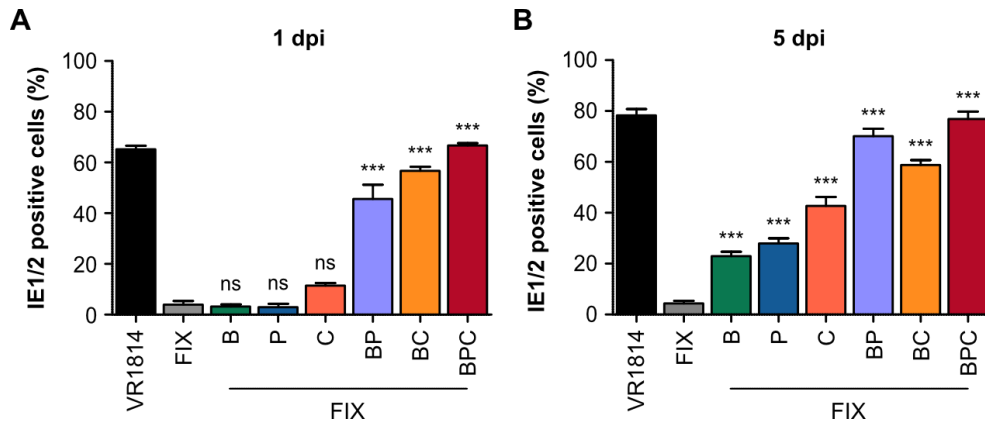


**Figure 23. Infectivity of the recombinant FIX strains in THP-1-derived macrophages.** (A, B) THP-1-derived macrophages were infected at an MOI of 5. Relative infectivities of the recombinant FIX strains were determined as percentage of IE1/IE2-positive nuclei at 1 and 5 dpi, respectively. Mean  $\pm$  SEM of three independent experiments are shown. Recombinant FIX strains were compared to FIX. Significance was determined by one-way ANOVA with Dunnett's multiple comparison test. \*\*\*,  $P < 0.001$ ; ns, not significant.

As the absolute infectivity of VR1814 and FIX significantly differed according to the cell types (Figure 15C and D), I hypothesized that infecting macrophages with VR1814 or FIX at the same MOI would not correspond to add the same amount of infectious viral particles to the cells. Thus, I tested whether infecting THP-1-derived macrophages with the same genome copy numbers would modify the infection outcome previously observed. THP-1-derived macrophages were infected with either VR1814 or FIX using 5 genomes per cell based on viral genome copies per mL detected in the virus stocks. The viral input was then quantified again via quantitative real-time PCR as control (Figure 24A). On day 2, 3, and 5 post-infection, cells were scraped, and viral DNA was extracted in order to quantify intracellular viral genome copy numbers by qPCR. GAPDH was used as endogenous control for relative quantification analysis. As shown in Figure 24B, even though THP-1-derived macrophages were infected with the same amount of infectious viral particles, intracellular viral genome copy numbers significantly differed between the two viruses. Although the genome copies per cell at 2 dpi were similar, starting from 3 dpi VR1814 showed an efficient viral DNA replication with increasing genome copies per cell. In contrast, FIX intracellular viral genome copies did not increase over time. These findings suggested that FIX showed a growth defect in THP-1-derived macrophages, possibly due to an abortive replicative cycle.



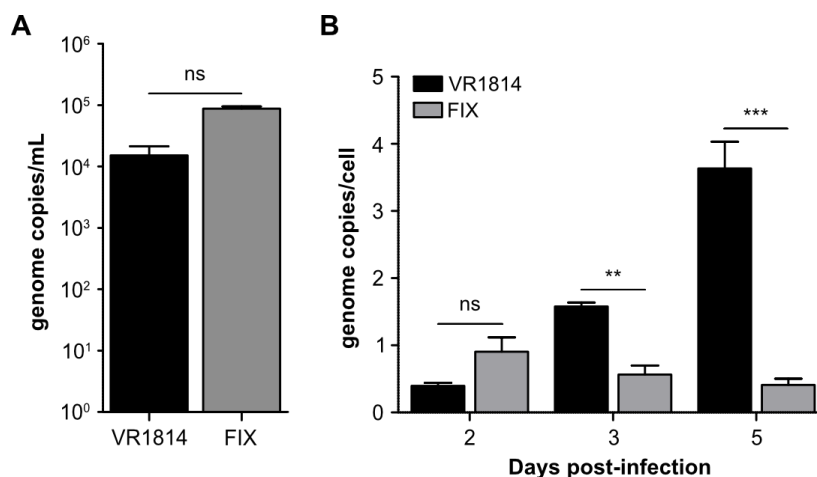


**Figure 24. Replication of VR1814 and FIX in THP-1-derived macrophages.** THP-1-derived macrophages were infected with either VR1814 or FIX using 5 genomes/cell. (A) Viral input used for the infection was quantified by qPCR. Significance was determined by two-tailed unpaired *t*-test. (B) The intracellular viral genome copies at 2, 3, and 5 dpi was determined by qPCR. GAPDH was used as endogenous control. Mean  $\pm$  SEM of two biological replicates are shown. Significance was determined by two-way ANOVA with Bonferroni post-test. \*\*,  $P < 0.01$ ; \*\*\*,  $P < 0.001$ ; ns, not significant.

### 5.7 Role of VR1814-specific glycoprotein variants in cell-cell fusion and syncytium formation in macrophages

To assess the ability of the recombinant FIX strains to induce cell-cell fusion in macrophages, THP-1-derived macrophages were infected at an MOI of 5 and syncytium formation was investigated at day 5 post-infection by microscopy analysis. In line with previous findings, syncytia were observed only in VR1814, FIX-BP, and FIX-BPC infected cells (Figure 25A), suggesting that the truncated US28 protein plays a role in infectivity, but it is not involved in the virus-induced cell-cell fusion in macrophages.

The reporter DSP system used to quantify HCMV-induced cell-cell fusion in ARPE-19 epithelial cells was initially used in THP-1 cells as well. The DSP system was cloned in a different lentiviral vector, called pLeGO, containing a SFFV promoter optimal for the transduction of myeloid and B cells. The monocytic cell line was then transduced with this system and selected by puromycin resistance. Equal amounts of THP-1 cells stably expressing either DSP1-7 or DSP8-11 were combined, differentiated for 3 days in presence of PMA, and infected at an MOI of 5. On day 5 post-infection, cells were washed with PBS, and incubated with coelenterazine-h prior to measurement of the *Renilla* luciferase activity. The results showed that cells infected with VR1814, FIX-BP, and FIX-BPC had high luciferase levels detected (Figure 25B). By contrast, FIX, the three single mutants, and FIX-BC showed similar low luciferase activity indicating a reduced cell-cell fusion. However, a massive cell death and consequently cell detachment was observed in infected cells with FIX, FIX-B, and FIX-P at 5 dpi, as shown in Figure 25C. As the cell density of ARPE-19 cells upon HCMV infection remained stable over time contrary to what I had observed in THP-1-derived macrophages, I concluded that the DSP

system did not work reliably in this cell type. Thus, syncytium formation was evaluated also by microscopic inspection and manual counting. The IE1/IE2 staining was used to define infected cells and syncytia were counted when contained at least three IE1/IE2-positive nuclei in the characteristic circular arrangement akin to flower petals. Once again, FIX-BP and FIX-BPC showed the highest numbers of syncytia among the recombinant FIX strains, as VR1814 did (Figure 25D). This data confirmed that VR1814-specific variants of gB and UL128L played a crucial role in inducing cell-cell fusion in macrophages.

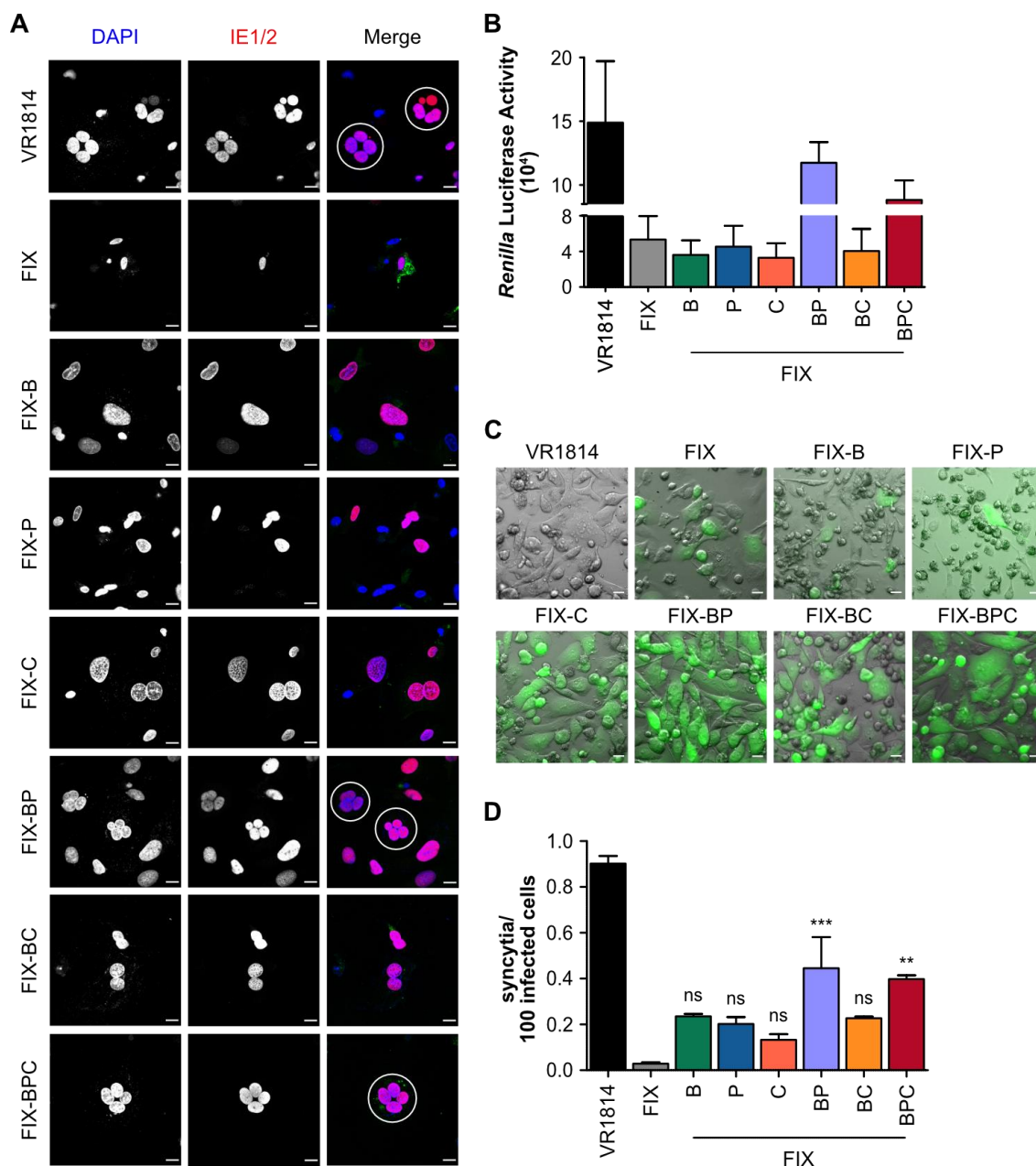


**Figure 25. Fusogenicity of the recombinant FIX strains in THP-1-derived macrophages.** (A) THP-1-derived macrophages were infected at an MOI of 5, and syncytium formation was analyzed at 5 dpi. Cells were stained with an anti-IE1/IE2 antibody and nuclei were counterstained with DAPI. Syncytia are marked by white circles. Representative images were taken by confocal microscopy. Scale bar, 20  $\mu$ m. (B) DSP-expressing THP-1-derived macrophages were infected at an MOI of 5. *Renilla* luciferase activity was measured at 5 dpi.

Mean  $\pm$  SEM of three independent experiments are shown. (C) After fusion assay, cells were fixed, and the cell monolayer was observed by microscopy analysis. All FIX strains express GFP. Representative images were taken by microscopy. Scale bar, 20  $\mu$ m. (D) Syncytium formation was quantified at 5 dpi by microscopic inspection and counting in infected THP-1-derived macrophages. Mean  $\pm$  SEM of three independent experiments are shown. Recombinant FIX strains were compared to FIX. Significance was determined by one-way ANOVA with Dunnett's multiple comparison test. \*\*,  $P < 0.01$ ; \*\*\*,  $P < 0.001$ ; ns, not significant.

### **5.8 Role of VR1814-specific glycoprotein variants in determining human primary macrophage tropism of HCMV**

Although THP-1-derived macrophages are considered an established model to study HCMV infection in myeloid cells, I verified whether the findings in THP-1-derived macrophages could be translated in human monocyte-derived macrophages. Human peripheral blood monocytes were differentiated and polarized into M1 or M2 macrophages by incubation for 7 days in the presence of granulocyte-macrophage colony-stimulating factor (GM-CSF) or macrophage-colony stimulating factor (M-CSF), respectively. Monocyte-derived macrophages were then infected at a MOI of 5 and analyzed on day 1 and 5 post-infection by immunofluorescence to determine the percentage of IE1/IE2-positive cells. Only double and triple mutants were investigated in monocyte-derived macrophages, and their infectivity was compared to the parental viruses, VR1814 and FIX. As shown in Figure 26, FIX-BP and FIX-BPC displayed the highest relative infectivities on both M1 and M2 macrophages at early and late time points, nearly reaching VR1814. It is worth noted that FIX-BC showed higher infectivity for M2 macrophages than M1 macrophages at both 1 and 5 dpi. This finding raised the possibility that

the truncated US28 protein could exert a different function in HCMV infection depending on the polarization state of macrophages.

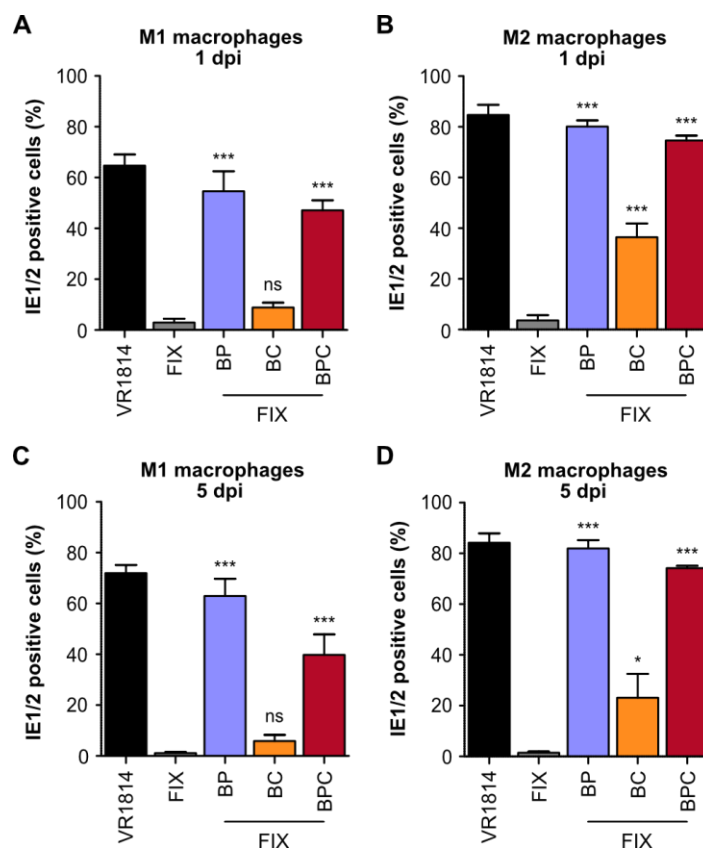


**Figure 26. Infectivity of the recombinant FIX strains in monocyte-derived macrophages.** M1 and M2 macrophages were infected at an MOI of 5. (A, C) Relative infectivities of the recombinant FIX strains were determined in M1 macrophages as percentage of IE1/IE2-positive nuclei at 1 and 5 dpi, respectively. (B, D) Relative infectivities of the recombinant FIX strains were determined in M2 macrophages as percentage of IE1/IE2-positive nuclei at 1 and 5 dpi, respectively. Mean  $\pm$  SEM obtained with cells from four different blood donors are shown. Recombinant FIX strains were compared to FIX. Significance was determined by one-way ANOVA with Dunnett's multiple comparison test. \*,  $P < 0.05$ ; \*\*\*,  $P < 0.001$ ; ns, not significant. These data were generated by Dr. Giada Frascaroli.

As FIX displayed a growth defect in THP-1-derived macrophages (Figure 24B) and failed to infect monocyte-derived macrophages (Figure 26), I hypothesized that the reduced IE1/IE2 expression was caused by a delayed virus entry and replication in this cell type. It is known that the viral tegument protein pp65 is released into the cytoplasm after virus entry and translocated to the nucleus early in infection. However, when DNA replication occurred, pp65 localized again in the cytoplasm, where new viral particles are assembled and released. Indeed, the gene encoding for pp65, UL83, exhibited a late kinetics and dependency on viral DNA replication, with its highest relative expression at 48-72 hours post-infection [168]. In order to determine the subcellular localization of pp65 later in infection, M2 macrophages were infected with either VR1814, FIX, or FIX-BP and analyzed by immunofluorescence. As shown in Figure 27, while pp65 was detected in the cytoplasm of VR1814 and FIX-BP infected M2

macrophages, the viral tegument protein showed predominately a nuclear localization in FIX infected cells. Strikingly, pp65 mainly localized in a disperse fashion in the cytoplasm of FIX-BP infected cells, while it was also found in dot-like structures in the large syncytia induced by VR1814, indicating a productive release of newly assembled viral particles. Nevertheless, the nuclear localization of pp65 at 5 dpi suggested a delayed or even aborted replicative cycle of FIX in M2 macrophages.

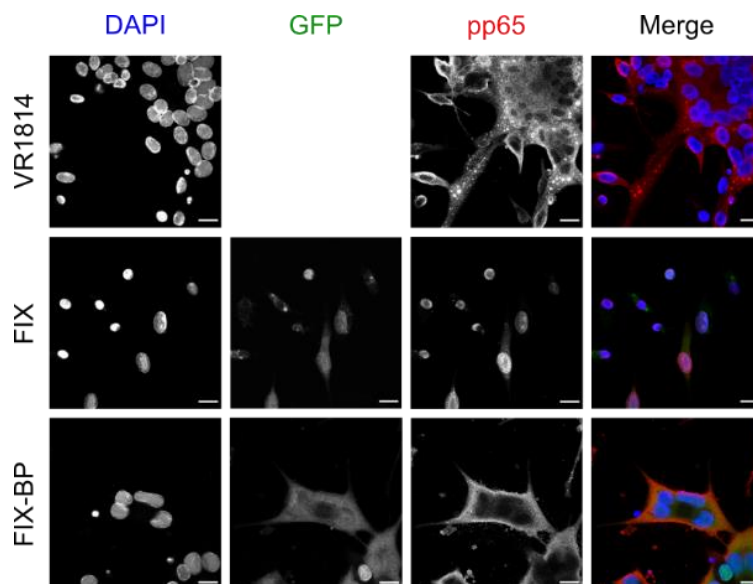


**Figure 27. Intracellular localization of pp65 in infected M2 macrophages.** M2 macrophages were infected at an MOI of 5. The intracellular localization of the viral tegument protein pp65 was detected by indirect immunofluorescence at 5 dpi. Cells were stained with an anti-pp65 antibody (red), and nuclei were counterstained with DAPI (blue). All FIX strains express GFP (green). Representative images were taken by confocal microscopy. Scale bar, 20  $\mu$ m.

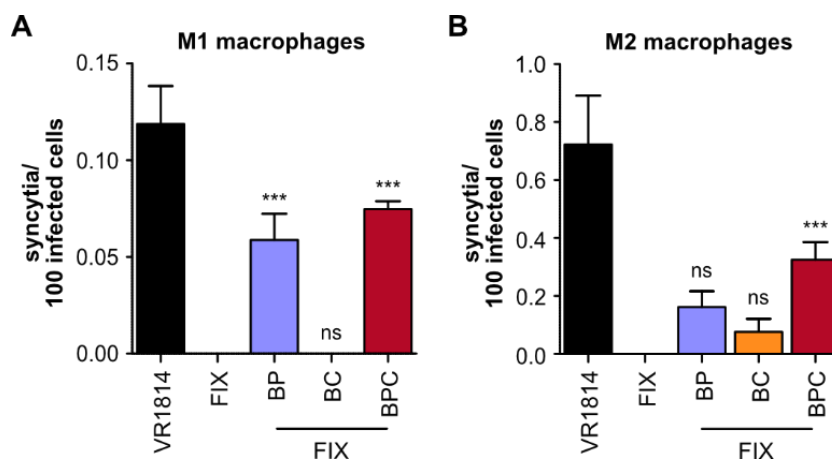


**Figure 28. Fusogenicity of the recombinant FIX strains in monocyte-derived macrophages.** (A, B) M1 and M2 macrophages were infected at an MOI of 5 and syncytium formation was quantified at 5 dpi by microscopic inspection and counting in both cell types. Mean  $\pm$  SEM obtained with cells from four different blood donors are shown. Recombinant FIX strains were compared to FIX. Significance was determined by one-way ANOVA with Dunnett's multiple comparison test. \*\*\*,  $P < 0.001$ ; ns, not significant.

Finally, the ability to induce syncytium formation of the recombinant FIX strains was evaluated by microscopic inspection and manual counting as previously done in THP-1-derived macrophages. The IE1/IE2 staining was used to define infected cells and syncytia were counted when contained at least three IE1/IE2-positive nuclei. These results confirmed that VR1814 and FIX-BPC displayed the strongest induction of cell-cell fusion in both M1 and M2 macrophages (Figure 28). Interestingly, syncytium formation induced by FIX-BP was significantly stronger in M1 macrophages than in M2 macrophages at 5 dpi.

### 5.9 Strategies for HCMV transfer to neutrophils

The broad cell tropism of VR1814 is also displayed by its capability of transferring viral material to polymorphonuclear leukocytes, a feature retained only by clinical HCMV isolates and lost in laboratory-adapted HCMV strains. To investigate the neutrophils uptake of clinically relevant HCMV strains, I first optimized a cell culture model previously established for the PMN-mediated virus dissemination *in vivo* [169]. To best simulate the hematogenous spread in the infected host, I decided to use endothelial cells as donor cultures for cell-associated HCMV transfer to PMNs. As shown in Figure 29A, HUVEC endothelial cells were seeded in 6-well plates a day prior to infection and subsequently infected at a MOI of 5 with either VR1814 or TB4-UL83-EYFP, a TB40E-BAC4-derived virus expressing a fluorescent pp65. At 6 dpi, freshly isolated PMNs were incubated with the donor cultures at a ratio of 10:1 for 5 hours at 37°C to allow viral transfer. After co-culture, PMNs were carefully collected, avoiding detachment of the donor culture layer, and a fraction of the recollected PMNs was sorted via FACS using a two-colour sorting strategy (Figure 29B). Briefly, a Brilliant Violet 421-conjugated anti-human CD66b antibody was used as specific cell marker for neutrophils, while TB4-UL83-EYFP was used to select HCMV-positive PMNs. The sorted CD66b<sup>+</sup>/GFP<sup>+</sup> PMNs were then prepared for microscope analysis by centrifugation in a Cytospin 4 centrifuge at 450 × g for 5 minutes. The remaining fraction of PMNs that have been incubated with VR1814-infected donor cells, as they did not express any fluorescent pp65 useful for cell sorting, were directly prepared for microscope analysis and subsequently stained with an anti-pp65 antibody. Cell nuclei were counterstained with DAPI, and all samples were analyzed by confocal microscopy (Figure 29C). The viral tegument protein pp65 was used as readout for the HCMV transfer to PMNs. The viral pp65 was detected in about 5% of the PMNs that had been incubated with infected endothelial cells and displayed a diffuse nuclear localization with some cytoplasmic dots.

These results confirmed HCMV uptake by PMNs from infected donor cultures, but the low percentage of HCMV-positive PMNs suggested that this event hardly occurred *in vitro*.

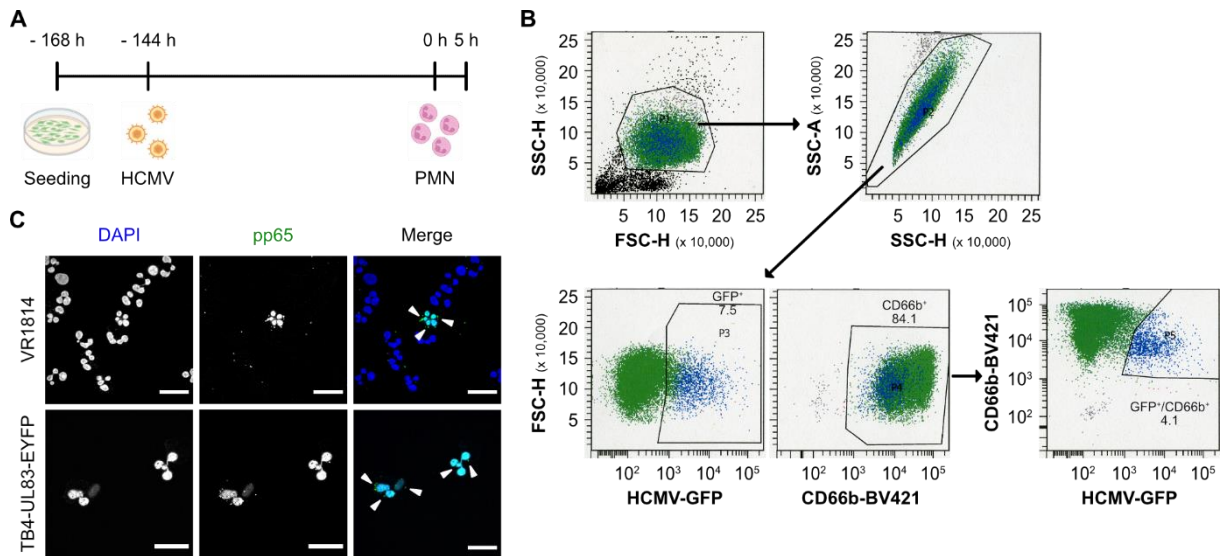


**Figure 29. Strategy for HCMV transfer to PMNs.** (A) Schematic of the workflow for HCMV uptake by PMNs from infected HUVEC endothelial cells. (B) Representative flow cytometry plots showing PMN identification by FSC and SSC characteristics, followed by cell sorting via pp65-EYFP and CD66b-BV421 double positive selection. (C) Representative cytoplots of HCMV-positive PMNs were taken by confocal microscopy. Cell nuclei were counterstained with DAPI (blue). pp65 (green) cytoplasmic dots are marked by white arrowheads. Scale bar, 10 µm.

In addition, to assess the infectivity of the donor culture, after co-culture HUVEC cells were fixed and stained either for the viral IE1/IE2 or pp65 antigens by indirect immunofluorescence. VR1814 and TB4-UL83-EYFP showed high infectivity in HUVEC cells as indicating by >98% of IE1/IE2-positive cells, consistent with the late stage of infection (Figure 30A). Induction of cell-cell fusion was observed by either virus, with formation of large syncytia in VR1814-infected HUVEC cells. As shown in Figure 30B, the viral tegument protein pp65 mainly localized in the cytoplasm of infected cells, with an accumulation in the viral assembly compartment. pp65 was also found in dot-like structures in the large syncytia induced by VR1814, consistent with previous results shown in M2 macrophages (Figure 27). Few infected endothelial cells showed a nuclear localization of pp65, indicating probably infection by the newly produced viral particles. Interestingly, the few PMNs left after recollection were mainly found clustering in the centre of the large syncytia induced by VR1814 or in close proximity to



infected endothelial cells, suggesting a possible attachment to the donor culture after chemoattraction exerted by HCMV-infected HUVEC cells.

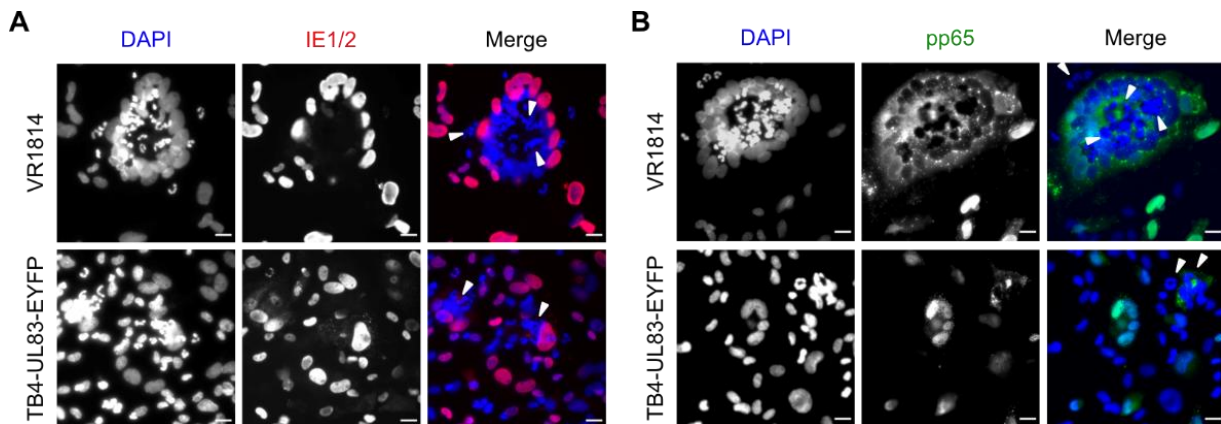


**Figure 30. Infected HUVEC cells as donor culture.** HUVEC cells were infected at a MOI of 5 for 6 days and served as donor cultures. After co-culture with PMNs, cells were fixed and stained with either an anti-IE1/IE2 antibody (red) (A) or an anti-pp65 antibody (green) (B). Nuclei were counterstained with DAPI (blue). PMN nuclei are marked by white arrowheads. Representative images were taken by microscopy. Scale bar, 20  $\mu\text{m}$ .

### 5.10 HCMV viral particles localization in neutrophils

Having established that I could recapitulate the HCMV uptake by PMNs *in vitro*, I next investigated the HCMV intracellular localization in neutrophils that have been co-cultured with donor cells. Recollected PMNs were pelleted down and resuspended in 2% PFA/2.5% GA in PBS. The samples were then prepared and analyzed in transmission electron microscopy (TEM) (Figure 31). All PMNs analyzed showed a strong activation after co-culture as suggested by their cytoplasm highly enriched in granules and vesicles content. Tegumented and enveloped viral particles were visible in large vesicles in the cytoplasm of PMNs, suggesting HCMV uptake via endocytosis (Figure 31A and B). Some PMNs displayed also large vesicles of pinocytosis and efferosomes, due to efferocytosis of apoptotic cellular bodies (Figure 31B). Interestingly, intracellular accumulations of virus appeared to localize in large membrane-bound compartments with a wide size range. These multivesicular structures contained heterogeneous viral material, such as enveloped viral particles, dense bodies (viral tegument particles without capsid and genome), and other viral structures (Figure 31C).



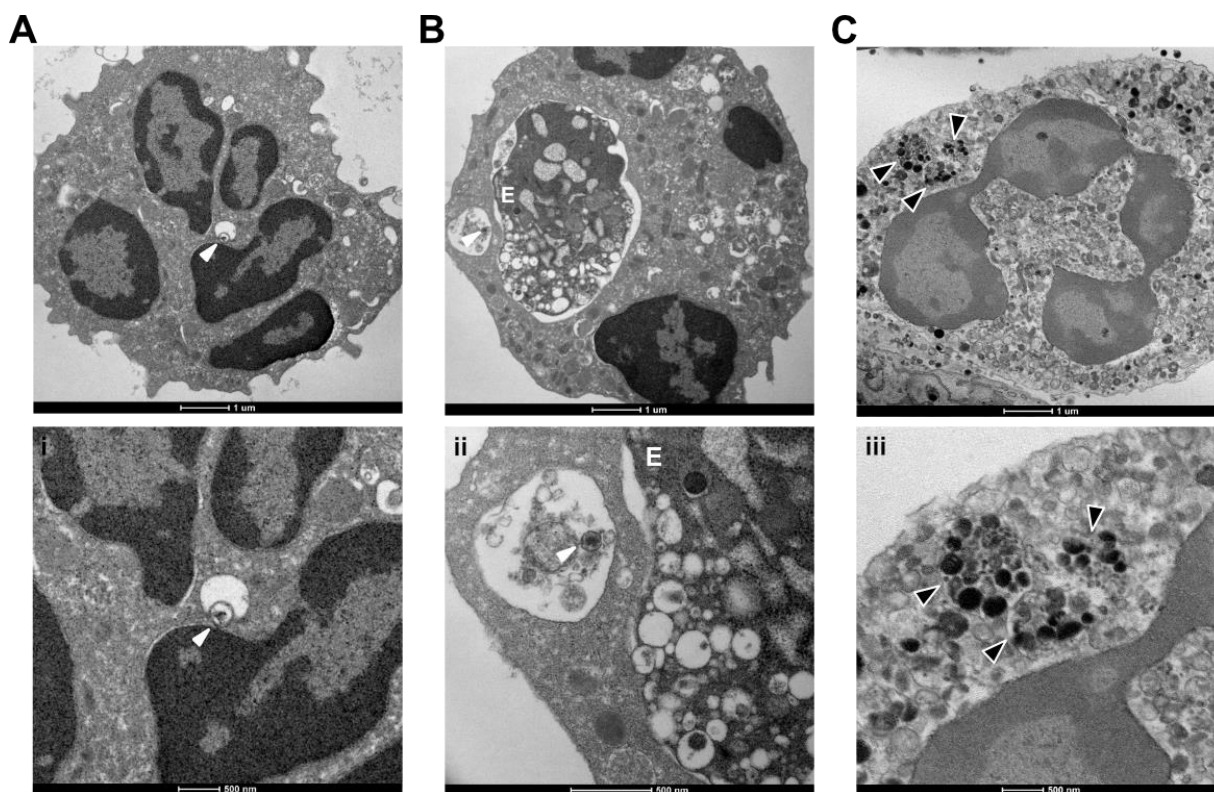


**Figure 31. HCMV intracellular localization in PMNs.** Ultrathin (50 nm) sections of PMNs after recollection from donor cultures were observed by TEM. Scale bars, 1  $\mu\text{m}$ . (i-iii) Magnifications of the same cells. Scale bars, 500 nm. (A) A single viral particle (white arrowhead) was observed in an intact large vesicle in the cytoplasm. (B) An efferosome (E), revealing the engulfment of an apoptotic cellular body, was found in an activated PMN and in proximity to another large vesicle of pinocytosis containing a viral particle (white arrowhead). (C) Large vesicles (white contoured black arrowheads) containing heterogenous viral material, such as virions, dense bodies, and other vesicles, were found in the cytoplasm. Representative electron micrographs of HCMV-positive PMNs were taken with the help of Carola Schneider (LIV Microscopy and Image Analysis facility).

Furthermore, to assess the HCMV transfer to PMNs, the co-culture of infected donor cells and PMNs were directly fixed in  $\mu$ -dishes with imprinted grids and analyzed by electron microscopy (Figure 32). Viral particles release by HCMV-infected HUVEC cells to the extracellular space was observed in the samples and PMNs were found in close proximity to the infected donor cells (Figure 32A and B). The diversity of material found in the extracellular viral accumulations showed the presence of enveloped and non-enveloped capsids, dense bodies, and other vesicles. These large amounts of HCMV viral material have been previously described to be released from large multivesicular structures in infected fibroblasts, resulting in extracellular viral accumulations at the surface of infected cells [170]. Several vesicles containing enveloped viral particles and many dense bodies were observed in the cytoplasm of PMNs.

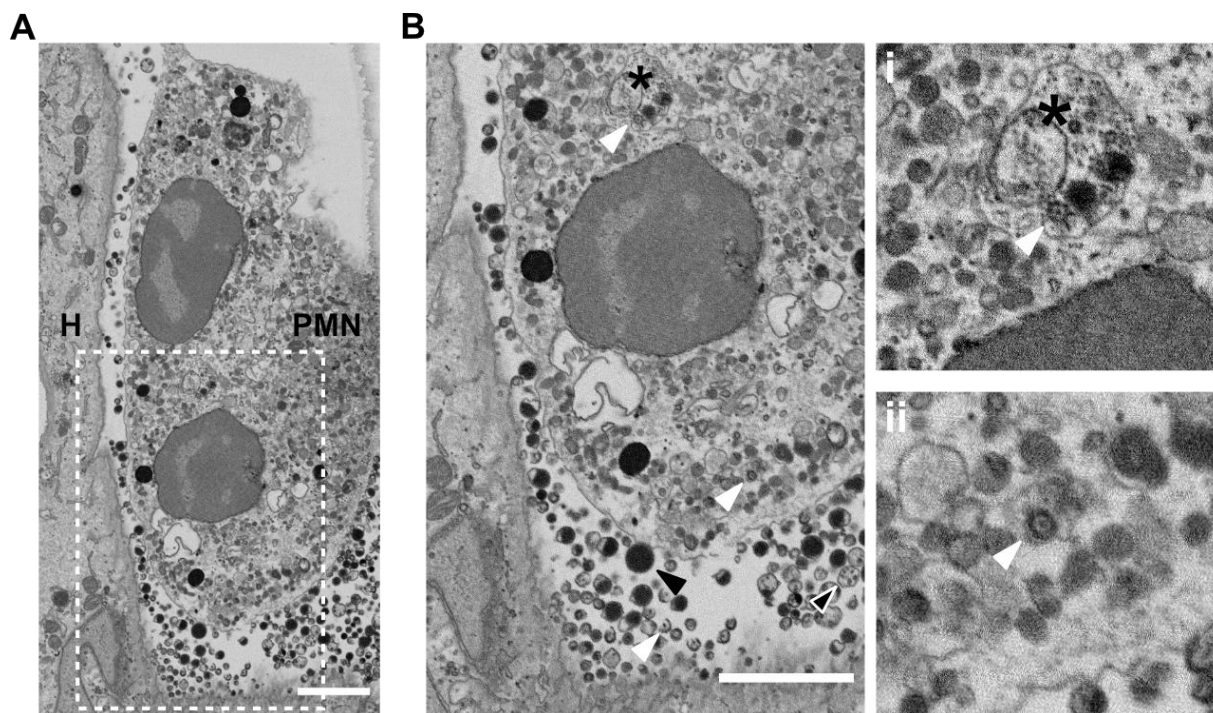


**Figure 32. HCMV transfer to PMNs.** Single section of co-cultured cells observed by EM. Scale bars, 500 nm. (A) A neutrophil (PMN) was found in proximity to an HCMV-infected HUVEC cell (H). (B) Magnification of the selected area, revealing an extracellular accumulation of viral material released by the infected HUVEC cell. The viral material is highly heterogeneous, containing virions (white arrowheads), dense bodies (black arrowheads), and other vesicles (white contoured black arrowheads). Magnifications (i, ii) illustrate the viral particles engulfed by PMN and localized in vesicle (\*). The EM images were obtained with the help of Dr. Felix J. Flomm.

### 5.11 Characterization of the interaction of neutrophils and donor cells

The interaction between HCMV-infected donor cells and neutrophils were further characterized by Correlative Light and Electron Microscopy (CLEM), a technique that combines fluorescence microscopy with electron microscopy [171]. In order to visualize HCMV viral particles by light microscopy, a TB4-UL83-EYFP carrying the viral tegument protein pp65 conjugated with a fluorescent protein was used for infection of donor cells. After co-culture for 5 hours with freshly isolated PMNs, cells were fixed, stained with Hoechst 33342 (nuclear DNA), and imaged with fluorescence microscopy (Figure 33A and B). Areas of interest containing pp65-positive PMNs were selected and subsequently analyzed by electron microscopy (Figure 33B to D). The HCMV pp65-EYFP was used as marker to enable accurate overlaying of fluorescence and electron microscopy images. The intracellular accumulations of virus were visible as round bodies highly variable in size and positive for pp65-EYFP in the cytoplasm of the donor cells (Figure 33A). These accumulations were revealed to be large accumulations of viral particles, dense bodies, and other viral material in the electron microscopy dataset (Figure 33B), similar to what previously described (Figure 31C). Interestingly, the lack of an intact plasma

membrane around the nucleus of the PMN suggested that the cell completely fused with the syncytium formed by HCMV-infected endothelial cells. In addition, the dense regions positive for pp65-EYFP, which either resided in the cytoplasm of the syncytium or accumulated in the nucleus of the PMN, could be resolved in electron microscopy (Figure 33C). A pp65-EYFP dot detected in the nucleus of the PMN was disclosed to co-localize to an electron dense structure in the electron photograph. Other round electron dense structures present in the cytoplasm co-localized to dense bodies full of pp65 and enclosed in double-membrane vesicles. Furthermore, many structures were revealed to be closed multivesicular structures filled with virions, dense bodies, and other vesicles. These vesicles were very heterogeneous in size and viral composition. Notably, these large vesicles were present throughout the entire volume of the syncytium from top to bottom, where they opened to the extracellular space releasing viral material (Figure 33D).

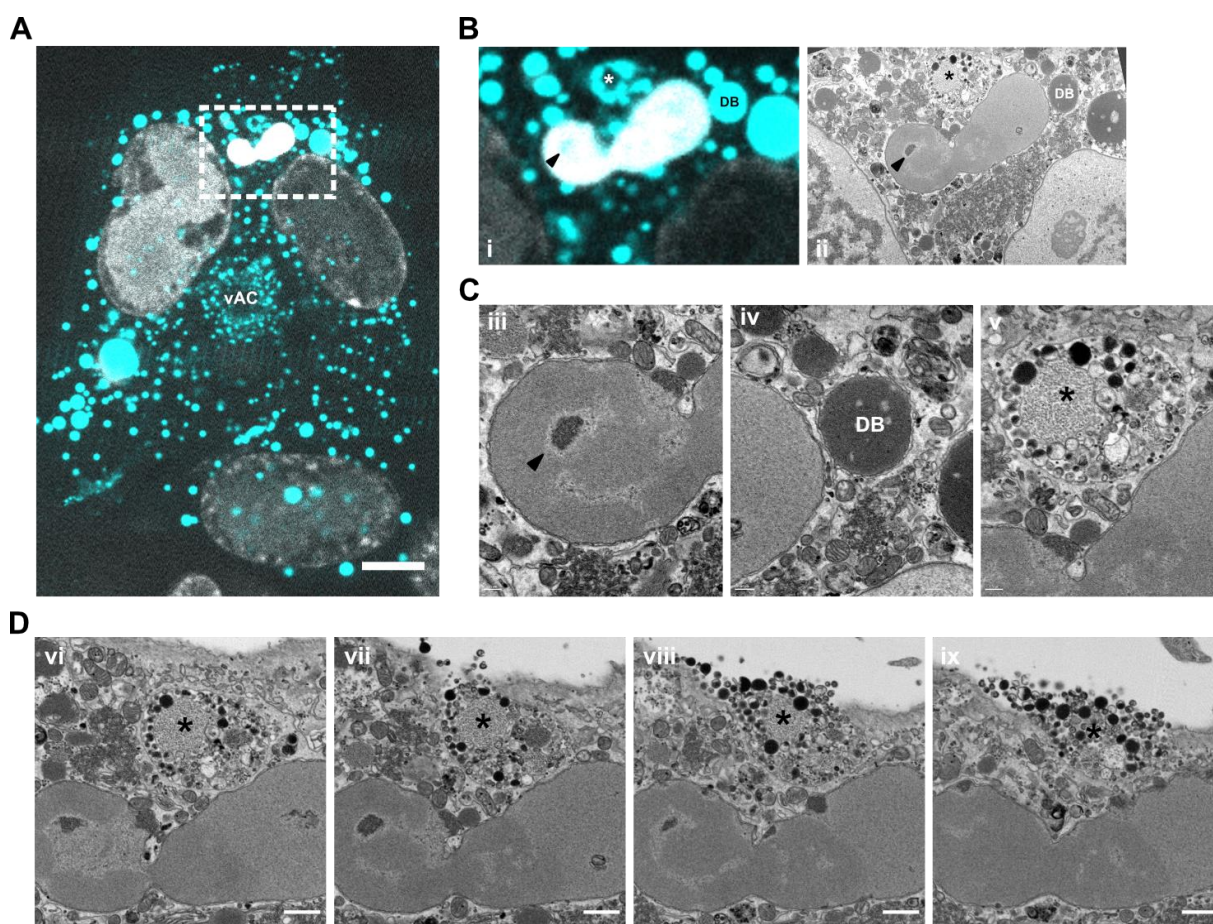


**Figure 33. CLEM of infected HUVEC cells co-cultured with PMNs.** (A and B-i) Confocal images of HCMV-infected HUVEC cells co-cultured with PMNs. The signal of pp65-EYFP is rendered in cyan and cell nuclei in grey. vAC indicates the viral assembly compartment. Scale bar, 10  $\mu$ m. (B-ii to D) Single sections of PMN observed by EM. (C) Magnification of an area of the same cell containing an accumulation of protein (iii), which correlates to a pp65-EYFP dot (arrowhead) localized in the PMN nucleus. Magnification of a dense body (DB) localized in a double-membrane vesicle (iv), which correlates to a pp65-EYFP dot in the cytoplasm. Magnification of a large vesicle (\*) containing heterogeneous viral material positive for pp65-EYFP (v). (D) Magnification of the same vesicle (\*), present throughout the entire volume of

the cell from top (vi) to bottom (ix), where it opens and releases viral material. Scale bars, 500 nm. The EM images were obtained with the help of Dr. Felix J. Flomm.

Collectively these data showed that large and heterogenous amounts of HCMV viral material are released by HCMV-infected endothelial cells and uptaken by PMNs probably via endocytosis. Electron microscopy showed the presence of large multivesicular bodies in either the extracellular space or the cytoplasm of PMNs in close proximity to donor cells.

## 6 Discussion

### 6.1 HCMV strain VR1814 shows broad cell tropism and induction of cell-cell fusion

Despite its large dsDNA genome, HCMV shows a remarkable degree and complexity of genetic variability *in vivo*, dictated by high frequency of multiple strain co-infections, *de novo* mutations, and virus reactivation from latency [58]. Moreover, it has been demonstrated that HCMV propagation *in vitro* leads to accumulation of several genetic alterations as a consequence of either selection and adaptation in cell culture or natural variability. Mutations in RL13 and UL128L have been shown to occur early in passaging, by facilitating viral replication in fibroblasts but limiting infection of many other cell types [172]. Thus, the ability of HCMV to efficiently enter and replicate in epithelial, endothelial, and myeloid cells strongly defines systemic spread and viral dissemination in the human host.

This study aimed to identify and characterize specific envelope glycoprotein variants in promoting HCMV tropism for epithelial cells and macrophages and to investigate the role of neutrophils in HCMV dissemination. The HCMV strain VR1814 has been propagated in endothelial cells since its isolation to preserve its broad cell tropism and its capability to be transferred to human leukocytes and, to allow molecular research and genetic engineering it was cloned as BAC, resulting in FIX-BAC [15]. Unfortunately, the virus reconstituted from FIX-BAC, called FIX, has lost the tropism for non-fibroblastic cells and poorly grew *in vitro* due to either mutations occurred during BAC cloning or its propagation in cell culture. In this study, the high infectivity of VR1814 was assessed in a very diverse set of human cells, including fibroblasts, epithelial cells, endothelial cells, and macrophages differentiated from either THP-1 cells or human peripheral blood monocytes, and compared to its BAC clone FIX or to another widely used laboratory-adapted HCMV strain, TB40/E (Figure 10). The wide tropism of VR1814 was confirmed for all the cell types tested, while TB40/E showed high infectivity for fibroblasts, epithelial cells, endothelial cells, and only M2 polarized macrophages among all myeloid cells tested. Notably, the virus-induced cell-cell fusion was much higher in the context of VR1814 infection than in TB40/E, suggesting the presence of some fusogenic variants in the genome of the first (Figure 11). Thus, the genome sequences of the endothelial cell-passaged VR1814 and FIX were compared, and several genetic differences were identified (Table 1). Mutations in the envelope glycoprotein genes were further characterized as promising candidates for the phenotype of VR1814. A previous systematic genetic study has shown that extensive passaging of VR1814 in endothelial cells and fibroblasts may be related to genetic changes [70]. However, little research has been done on how these selective and adaptive mutations could affect the virus phenotype. To elucidate how strain-specific variations

in envelope glycoproteins contribute to the underlying viral tropism for epithelial cells and macrophages, recombinant FIX strains were generated and investigated during this study.

## **6.2 VR1814-specific gB and UL128L variants increase the infectivity of FIX in epithelial cells**

HCMV infection of epithelial cells is predominant *in vivo* in patients with disseminated infection [15,76]. Interestingly, epithelial cell susceptibility *in vitro* is retained in HCMV strains with high expression of the pentameric gH/gL/UL128/UL130/UL131A complex in viral particles. Indeed, the tropism for this cell type greatly varies among HCMV isolates and mainly depends on the pentamer, as major mediator of virus entry in epithelial cells. The pentameric complex recognizes and binds the cellular receptors Neuropilin-2 and OR1411 to allow virus entry in epithelial and endothelial cells and acts in cooperation with the envelope glycoprotein B (gB). It has been shown that the relative amount of pentamer is dependent on both virus strain and producer cell type and it is one of the first genomic regions to undergo to selective pressure *in vitro* [66,173]. Previous findings of our laboratory have identified fusogenic variants of gB that promote virus entry and infectivity in fibroblasts [154,155]. Moreover, based on published data, several mutations in UL128L led to loss of the pentameric complex and consequently loss of tropism for epithelial and endothelial cells [88,94,172]. The introduction of VR1814-specific variants of gB and UL128L into the backbone of FIX resulted in significantly increased viral replication and release in epithelial cells (Figure 13 and 14). FIX single mutants replicated less efficiently than the parental VR1814 in ARPE-19 epithelial cells. This observation is noteworthy because it suggests that the two genetic loci, UL55/gB and UL128L, cooperate in a concerted way in promoting HCMV tropism, while the chemokine receptor US28 seems not to be involved in the epithelial cell infectivity. The recombinant FIX viruses carrying both gB and UL128L specific variants of VR1814 displayed also the highest relative infectivity in epithelial cells, confirming the importance of the two genetic loci in the regulation of HCMV infectivity (Figure 15A and B). It is worth noting that FIX-BP and FIX-BPC showed higher infectivity and replication kinetics than the parental FIX in epithelial cells, however these recombinant viruses never reached the same levels shown by VR1814. These results indicate that other viral factors remained to be characterized as possible players in VR1814 wide tropism.

Once I confirmed the importance of specific variants of gB and UL128L for an efficient replication and high infectivity in epithelial cells, I compared the absolute infectivity of all FIX strains in fibroblasts and epithelial cells. It is known that the composition of HCMV virions within a population is extremely various, and this heterogeneity may affect the capability of each viral particle to initiate and complete a full replicative cycle in infected cells [163,174]. Moreover, cell susceptibility and permissiveness to HCMV differ among cell types, possibly due to a different mechanism used for virus internalization. Altogether these discrepancies reflect a



highly variable ratio between infectious units (IU) and viral particles. This study showed that the IU per 1000 genomes ratios were generally higher on fibroblasts for all strains analyzed, consistent with the fact that this cell type requires an easy virus entry mediated by direct fusion of the viral envelope to the plasma membrane. Only FIX and FIX-P showed low ratios on fibroblasts, confirming the non-essential role of the pentamer in mediating virus entry in this cell type (Figure 15C). Contrary, the virus internalization in epithelial cells requires endocytosis-like processes and occurs via macropinocytosis in a pH-independent manner [16,123]. This study confirmed low ratios of IU per 1000 genomes showed by poorly infectious FIX strains, validating the importance of VR1814-specific variants of gB and UL128L in HCMV tropism in epithelial cells (Figure 15D).

### **6.3 VR1814-specific gB and UL128L variants promote cell-cell fusion and syncytium formation in epithelial cells**

The core fusion machinery of HCMV formed by gB and the two gH/gL complexes is essential for infectivity. Once the fusogenic activity of gB is activated by membrane binding of gH and gL complexes, the fusion of two adjacent membranes is induced [175]. Thus, the HCMV envelope glycoprotein gB and the gH/gL complexes not only are major determinants of virus entry and tropism in different cell types, but play also a crucial role in cell-cell fusion and formation of syncytia, which is induced to a variable degree by some HCMV strains [152]. HCMV-induced syncytia have been also reported *in vivo* in the organs of patients with HCMV disseminated infection, in the retina of individuals affected by CMV retinitis, and after isolation and propagation of congenital HCMV isolates derived from infected newborns [176,177]. Moreover, syncytium formation has been observed to occur *in vitro* at late time post-infection, after *de novo* expression of viral glycoproteins by the infected cells [156]. Based on this evidence, it has been hypothesized that the physiological process involved in the HCMV-induced cell-cell fusion may be the fusion from within (FFWI), which requires accumulation of newly synthesized viral glycoproteins on the plasma membrane of infected cells. Anyway, the mechanisms of formation and the clinical relevance of those structures *in vivo* have not been completely investigated. It appears likely that an extremely reactive fusion machinery may allow a more effective HCMV entry in specific cells and tissues, a rapid dissemination through tissue barriers, and protection from host immune factors. The results showed in this study demonstrate that the combination of gB and UL128L specific variants of VR1814 are associated with increased cell-cell fusion and appearance of large syncytia in infected epithelial cells (Figure 16 and 17). The selection of specific glycoprotein variants may facilitate the accumulation of fusogenic proteins and complexes to the plasma membrane, thereby promoting the direct transfer of viral particles between fused cells. The incubation of HCMV-infected epithelial cells with neutralizing antibodies to UL130, component of the pentamer,

drastically reduced syncytium formation and inhibited cell-cell fusion, confirming the crucial contribution played by UL128L in the virus-induced cell-cell fusion in this cell type (Figure 18). Overall, this process may play a pro-viral role in HCMV infection, and syncytium-forming HCMV strains might be associated with increased viral transmission and pathogenicity in the host.

#### **6.4 FIX-derived variants of UL128 and UL130 impair infectivity and cell-cell fusion in epithelial cells**

Given the importance of the pentameric complex in epithelial cell tropism and syncytium formation, the role of strain-specific variations in UL128L was further investigated. Several studies have shown that single polymorphisms in UL128L region could lead to alteration of the pentamer complex expression, due to an incorrect incorporation of the complex in the viral particles or failure in the cellular receptor binding with impairment and inhibition of syncytium formation. Other mutations in UL128L have been also demonstrated to induce the appearance of hypersyncytial variants [150,164,178]. However, high expression levels of the pentamer were shown to correlate with strongly cell-associated HCMV growth *in vitro* [179]. The data presented in this thesis support that an amino acid substitution S72P in UL130 present in FIX completely disrupts virus infectivity and abolished cell-cell fusion in epithelial cells, by reducing the incorporation of the pentameric complex into viral particles (Figure 19 and 20).

These specific variants of envelope glycoproteins in VR1814 were compared by alignment to all HCMV sequences deposited in GenBank to determine whether they were naturally occurring variations selected by propagation in endothelial cells rather than adaptive mutations. The S72P substitution in UL130 was found in FIX only and in any other HCMV strain, indicating that this mutation likely occurred during BAC cloning of VR1814 [70]. Interestingly, the S585G substitution in UL55 and the T203N substitution in UL130 were common to VR1814 and three other HCMV strains isolated in northern Italy (GenBank MT070138, MT070141, MT070142). Two of the clinical HCMV strains from Italy displayed syncytium formation *in vitro* as VR1814 did [149]. These findings rise the hypothesis that fusogenic variants of HCMV glycoproteins may be native of specific geographical area.

#### **6.5 Role of VR1814-specific glycoprotein variants in promoting macrophage tropism**

The susceptibility and permissiveness to HCMV infection displayed by myeloid cells strongly support the extent of viral systemic spread and dissemination from the site of infection to several organs and tissues as well as viral persistence in the host. Myeloid cells play an important dichotomic role in HCMV infection, balancing between immune protection and viral pathogenesis. CD34+ hematopoietic progenitor cells (HPCs) and monocytes are the major



reservoir of latent HCMV. As sites of viral persistence, these cells contribute to viral dissemination by circulating in the bloodstream and migrating into tissues [15,180–182]. Infected circulating monocytes act as vehicles for viral spread, and their differentiation into macrophages or dendritic cells causes virus reactivation from latency and establishment of a lytic replicative cycle followed by *de novo* production of infectious viral particles. This virus reactivation allows the HCMV transfer to other permissive cells in the tissues [32,43,183,184]. HCMV tropism in myeloid cells is once again driven by the glycoprotein B and the pentameric complex, which interact with EGFR and  $\beta_1/\beta_3$  integrins, respectively, mediating virus entry in the cells and monocyte differentiation into macrophages [185–188]. Furthermore, HCMV encodes for a G-protein-coupled receptor homolog, US28, present on the envelope and that has been suggested to be crucial for the recruitment of susceptible cells [62,189]. This chemokine receptor plays an important role in the establishment and long-term maintenance of HCMV latency and its activated signalling leads to increased intracellular  $Ca^{++}$  fluxes [42,190]. Several studies have demonstrated that a carboxy-terminal domain truncation of the chemokine receptor US28 led to an altered signalling activity and the deletion of the gene caused failure in latency maintenance in CD34+ HPCs [157,191,192]. Interestingly, VR1814 shows a frameshift mutation in US28 gene that causes a truncated US28 protein similar to the one described by Stropes and colleagues [157]. In this study the cooperation between the two genetic loci of VR1814, UL55/gB and UL128L, has been confirmed promoting viral replication, infectivity, and cell-cell fusion in human macrophages (Figure 21, 22, 23, 25, 26, 28). Although, HCMV susceptibility was higher in THP-1-derived macrophages and M2 macrophages, the virus established a productive infection in all types of macrophages tested (Figure 23 and 26). It is worth noted that FIX single mutants showed a recovered infectivity in THP-1-derived macrophages later in infection compared to the parental FIX, whose infectivity was extremely low even at 5 dpi (Figure 25). These findings may indicate a delay in either virus internalization or nuclear translocation of viral genomes in the differentiated macrophages. Interestingly, the data in this study demonstrated also that the C-terminal truncation of US28 increased the IE1 and IE2 gene expression in differentiated THP-1 and M2 macrophages (Figure 23 and 26). No increased infectivity of FIX recombinant viruses carrying US28 specific variant of VR1814 was observed in M1 macrophages, indicating that the promotion of lytic infection may be influenced by the state of polarization of the cells (Figure 26). These findings arise the hypothesis that the promotion of IE gene expression in differentiated macrophages may facilitate the lytic cycle with failure in maintaining latency. Therefore, HCMV must enter efficiently in macrophages and the viral genome should be translocated to the nucleus in order to carry out the promotion of IE gene expression. Altogether, the results shown in this study demonstrated that specific variants of the envelope glycoproteins gB, UL128, UL130, and US28 act in a concerted way in promoting HCMV macrophage tropism. Lastly, VR1814 variant of US28 was also compared to

other HCMV sequences in GenBank, but no similar mutation was found in any other strain. This observation indicates that could be either a minor natural variant or an adaptive mutation occurred after propagation in cell culture.

Once I confirmed the importance of gB, UL128L, and US28 for HCMV tropism in macrophages, I investigated the poor infectivity of FIX in this cell type. It is known that the nuclear translocation of viral genomes in myeloid cells is delayed compared to other permissive cells, such as fibroblasts, epithelial cells, and endothelial cells. This delay in macrophages is due to a complex intracellular trafficking process after virus internalization, that involves the recycling of endosomes. Thus, the viral genome nuclear translocation does not occur before 48-72 hours post-infection in human macrophages [112]. The data in this thesis revealed that FIX showed an extremely low entry efficiency in macrophages due to the low expression of the pentameric complex in the viral particles, and the few viral particles that enter in the cells failed to initiate a replicative cycle (Figure 24). Moreover, I investigated the intracellular localization of the viral tegument protein pp65 at late time post-infection. In FIX-infected macrophages pp65 was found mainly in the nucleus, while in macrophages infected by VR1814 or other infectious FIX strains pp65 was detected in the cytoplasm of the syncytia, suggesting once again an abortive infection of FIX in differentiated macrophages (Figure 27).

### **6.6 Interaction of HCMV-infected endothelial cells and neutrophils *in vitro***

The ability of HCMV to infect and replicate in endothelial cells defines the extent of viral spread in the human host. In the bloodstream, peripheral blood leukocytes, such as neutrophils and monocytes, were documented to be the major carrier of HCMV infectious particles and viral products in patients with disseminated infection [103]. These immune cells have been proposed to spread the virus to new tissues, facilitating HCMV transfer to other permissive cells. The model of HCMV dissemination proposed by the scientific community describes epithelial cells as the first target of HCMV infection *in vivo*. In this cell type, HCMV spreads mainly in a cell-associated way to the surrounding uninfected fibroblasts and endothelial cells [15,76,87,193]. Thus, infected endothelial cells produce chemoattractants, such as IL-8, to recruit monocytes and neutrophils from the bloodstream to the infection site and transfer the virus to them. In those cells, the virus is carried throughout the blood to new organs and tissues, where it can be transferred again to other permissive cells. Although the role of endothelial cell tropism and neutrophil-mediated transfer displayed by clinical HCMV isolates potentially correlate to high pathogenesis and dissemination *in vivo*, the molecular mechanism and relevance of this process have been poorly characterized. Neutrophils do not support a viral replicative cycle, but act as vehicles for HCMV dissemination. How neutrophils are able to uptake virus and other viral material from infected endothelial cells has been remained unclear for long time. A reason of so few research lines that aim at investigating this process

can be found in the difficulty to establish a robust cell system *in vitro*. The capability of transfer viral material to human leukocytes is retained only by clinical HCMV isolates and is lost in laboratory-adapted HCMV strains. Previous publications have demonstrated that neutrophils-mediated virus transmission requires contact and adhesion mediated by ICAM-1 and its ligand LFA-1 between the two cell populations, and strictly depends on an intact viral tegument and a functional pentamer [92,156,169,194]. Thus, the genetic locus UL128L was described to be essential in endothelial and epithelial cell tropism as well as in leukocyte-mediated transmission of HCMV [88,94,123,195].

In this study, I established a cell system to allow the investigation of HCMV uptake by neutrophils *in vitro* (Figure 29). Endothelial cells were used as donor cells for the HCMV transfer to best mimic the viral dissemination *in vivo*. The results confirmed the uptake of HCMV particles and other viral material by neutrophils (Figure 31 and 32). Heterogenous viral material was released in the extracellular space by infected endothelial cells and was mainly observed in large vesicles in the cytoplasm of neutrophils, suggesting an intense activity of endocytosis. These findings show a correlation with the virus entry mode mediated by the pentameric complex, which requires endocytosis of viral particles followed by low-pH fusion. An interesting follow-up would be to determine the fate of these multivesicular bodies containing viral particles by using inhibitors to block either endocytosis or phagocytosis. Therefore, the cell culture model established in this study could serve as valuable asset to investigate neutrophils-mediated viral dissemination *in vitro* and could enable to evaluate the effects of entry inhibitors on this specific transmission mode. Furthermore, neutrophils were strongly activated after co-culture, as observed by many vesicles and granules in their cytoplasm (Figure 31). Additionally, an increased survival of neutrophils during HCMV infection has been described by previous studies [107,196,197]. Together these findings raise the hypothesis that neutrophils could act as a trojan horse to facilitate viral spread and infection to other cells, for example after being engulfed by macrophages and dendritic cells [198,199]. Thus, the virus could reach its cell niche without being exposed to neutralizing antibodies in the extracellular space. In addition, although published data reported that HCMV transfer from infected endothelial cells to neutrophils is mediated by microfusion events [92], I could not observe any fusion points between the two plasma membranes. However, a massive recruitment of neutrophils was observed in close proximity to the viral assembly compartment of large HCMV-induced syncytia (Figure 30), and the presence of neutrophils fused to syncytia of infected endothelial cells was also confirmed by EM investigations (Figure 33). It would be interesting to know whether the fusion between infected endothelial cells and neutrophils may facilitate viral dissemination rather than viral clearance. A possible strategy would be using the recombinant FIX-GFP viruses generated in this study to conduct further investigations.

## 6.7 Summary

In the present study, the role of HCMV-specific glycoprotein variants in promoting viral tropism in epithelial cells and leukocytes was investigated. VR1814-specific variants of the envelope glycoproteins gB, UL128, and UL130 were shown to be essential for high infectivity in epithelial cells and macrophages as well as for syncytium formation in both cell types. Those variants increased the infectivity of FIX by promoting virus entry and replication in the cells under investigation. The pentameric complex was described to play a crucial role in the virus-induced cell-cell fusion in epithelial cells and to act in a cooperative way with a fusogenic variant of gB in syncytium formation. Moreover, a specific amino acid substitution in UL130 was identified as main responsible of the impaired infectivity and abolished cell-cell fusion of FIX, by reducing pentamer expression in viral particles. Additionally, a C-terminally truncated US28 protein appeared to increase significantly HCMV infectivity in macrophages, by promoting IE gene expression and consequently lytic infection rather than latency in differentiated myeloid cells. Ultimately, this study established a cell culture system to investigate the uptake of cell-associated HCMV strains by neutrophils after co-culture with infected endothelial cells. The data showed that HCMV-infected endothelial cells released large amount of viral particles into the extracellular space and neutrophils were able to uptake this material by endocytosis. Virus and other viral material, such as dense bodies, were found in large vesicles in the cytoplasm of neutrophils and the tegument protein pp65 displayed a nuclear accumulation in these cells. However, the survival of neutrophils after HCMV uptake from infected endothelial cells and their role in viral dissemination remains to be identified. Taken together, the results of this study reveal the viral genetic determinants of increased HCMV tropism in epithelial cells and macrophages and provide valuable tools to study HCMV infection and dissemination in human leukocytes.

## 7 Material

### 7.1 Cells

Name	Description	Reference
HFF-1	Primary human foreskin fibroblasts	ATCC (SCRC-1041)
MRC-5	Primary human embryonic lung fibroblasts	ATCC (CCL-171)
ARPE-19	Human retinal pigmented epithelial cells	ATCC (CRL-2302)
ARPE-19_DSP1-7	Human retinal pigmented epithelial cells expressing dual split protein (DSP) 1-7	[155]
ARPE-19_DSP8-11	Human retinal pigmented epithelial cells expressing dual split protein (DSP) 8-11	[155]
HUVEC	Human primary umbilical vein endothelial cells	ATCC (PCS-100-010)
THP-1	Human acute leukemia monocytic cell line	DSMZ (ACC 16)
THP-1_DSP1-7	Human acute leukemia monocytic cell line expressing dual split protein (DSP) 1-7	This study
THP-1_DSP8-11	Human acute leukemia monocytic cell line expressing dual split protein (DSP) 8-11	This study
HEK-293T	Human embryonic kidney cells transformed with SV40 T-antigen	ATCC (CL-11268)
M1 macrophages	Human monocyte-derived macrophages isolated from CMV-seronegative individuals, GM-CSF polarized	This study
M2 macrophages	Human monocyte-derived macrophages isolated from CMV-seronegative individuals, M-CSF polarized	This study
Neutrophils	Human neutrophils isolated from CMV-seronegative individuals	This study

### 7.2 Viruses

Name	Description	Reference
TB40/E	HCMV clinical strain TB40/E	[200]
TB4-UL83-EYFP	HCMV strain TB40E-BAC4, cloned as BAC, expressing pp65-EYFP	[201]
VR1814	HCMV clinical strain VR1814	[68]

FIX-GFP	HCMV strain FIX-BAC, cloned as BAC, expressing GFP	[69]
---------	--	------

The following virus mutants were generated by Dr. Giada Frascaroli.

Name	Description	Reference
FIX-B	FIX-GFP with S585G mutation introduced into UL55	This study
FIX-P	FIX-GFP with the entire UL128L replaced by UL128L from VR1814	This study
FIX-C	FIX-GFP with US28 replaced by US28 from VR1814	This study
FIX-BP	FIX-GFP with S585G mutation introduced into UL55 and the entire UL128L replaced by UL128L from VR1814	This study
FIX-BC	FIX-GFP with S585G mutation introduced into UL55 and the US28 replaced by US28 from VR1814	This study
FIX-BPC	FIX-GFP with S585G mutation introduced into UL55 and the entire UL128L and US28 replaced by UL128L and US28 from VR1814	This study
FIX-BP(V33F)	FIX-BP with V33F mutation introduced into UL128	This study
FIX-BP(S72P)	FIX-BP with S72P mutation introduced into UL130	This study
FIX-BP(N203T)	FIX-BP with N203T mutation introduced into UL130	This study

### 7.3 Bacteria

Strain	Growth t°	Description	Reference
<i>E. coli</i> DH10B	37°C	F- mcrA Δ(mrr-hsdRMS-mcrBC) Φ80dlacZΔM15 ΔlacX74 endA1 recA1 deoR Δ(ara,leu)7697 araD139 galU GalK nupG rpsL λ-	Life Technologies
<i>E. coli</i> GS1783	30°C	H10B   cl857 Δ(cro-bioA) <> araC-PBADI-scel	[202]

### 7.4 Plasmids

Name	Description	Reference
pcDNA3	expression vector, ampR, neoR	Life Technologies
pEPkan-S	template plasmid for <i>en passant</i> mutagenesis, containing I-Sce-aphA1 cassette, kanR	[202]
pCGN-pp71	pCGN plasmid expressing HCMV tegument protein pp71	[203]

pdl	expression lentiviral vector, ampR	Dalan Bailey (The Pirbright Institute, UK)
pdl-DSP1-7	pdl lentiviral vector expressing the dual split protein (DSP) 1-7	Dalan Bailey (The Pirbright Institute, UK)
pdl-DSP8-11	pdl lentiviral vector expressing the dual split protein (DSP) 8-11	Dalan Bailey (The Pirbright Institute, UK)
pLeGO-iPuro2	expression lentiviral vector, ampR	Kristoffer Riecken (UKE, Germany)
pLeGO-DSP1-7	pLeGO lentiviral vector expressing the dual split protein (DSP) 1-7	This study
pLeGO-DSP8-11	pLeGO lentiviral vector expressing the dual split protein (DSP) 8-11	This study
pMD-G	Packaging vector, lentiviral gag, pol, rev encoding vector, ampR	Dalan Bailey (The Pirbright Institute, UK)
pCMVR8.91	Envelope vector, encoding VSV-G protein, ampR	Dalan Bailey (The Pirbright Institute, UK)

## 7.5 Primers

### 7.5.1 Molecular cloning primers

Name	Sequence (5'-3')	Application
N-F1	CACCATGGCTTCCAAGGTGT	To clone DSP1-7 into pLeGO vector [155]
N-R2	GCGAGCCCACCACTGAGGCC	
N-F2	GTGAACAGAATCGAGCTGAA	
N-R1	CACTTGTCGGCGGTGATGTA	
C-F1	CAGAAGAACGGCATCAAGGCC	To clone DSP8-11 into pLeGO vector [155]
C-F2	AAGCCCGACGTCGTCCAGATT	
C-R1	TTACTGCTCGTTCTTCAGCAC	
Seq-SFFV FWD	CTGCTTCCCGAGCTCTATA	To sequence verify the DSP insertions into pLeGO vector
pLeGO-seq4 REV	AAGACAGGGCCAGGTTTC	

### 7.5.2 BAC mutagenesis primers

The following primers were designed by Dr. Giada Frascaroli.

Name	Sequence (5'-3')	Application
gB_PCR_C REV	CATGCAGCACCTAGATATCCAG	To PCR amplify UL55

gB_PCR_N REV	GTACTGCACGTACGAGCTGT	To sequence verify UL55
gB_PCR_C FWD	GTCAAGGTGCTGCGTGATAT	
gB_PCR_N FWD	TGTCCAGACCGGATGAGAGT	
gB-C-seq2 FWD	CAATGGCTACGCCAACGGCC	
gB-C-seq1 REV	CCGCCCTACCTCAAGGGTCT	
gB-N-seq4 FWD	CGTTCCGAGGCTTCCCAGAA	
gB-N-seq2 REV	TTCTGGGAAGCCTCGGAACG	
gB-N-seq3 FWD	TGAATCTCCCACATAGGAGG	
gB-N-seq1 REV	ACCACTTATCTGCTGGGCAG	
gB-PM FWD	TGCTACTCACGACCCGTGGTCA TCTTTAATTTCTCAACGGCTCG TACGTGCAGTTAGGGATAACAG GGTAATCGATTT	To introduce S585G mutation in UL55 of FIX
gB-PM REV	GTCCTCACCCAGTTGACCGTAC TGCACGTACGAGCCGTTGACGA AATTAAAGATGGCCAGTGTTACA ACCAATTAACC	
gB_kan_b	CGTTTCCCGGAGGGTCCGCGC AACACGCAAGAGACCACGACGC GCCTCATCGCTGCTGGATTTGG CCCGCGACGAACATGGAATCCA GGATCTGGTGCCT	To insert kanamycin cassette into UL55
gB_kan_c	CAGCACCTAGATATCCAGTTTAA CCCCGTATATCACAAGTCTCTGT GTCACTTTTTTTTGTCTGTTTTTTT TTTCTTCTCCTGGTTCAGACGTT CTCTTCT	
UL128 locus FWD	TCGGCGATAAACACCACTATC	To PCR amplify UL128L
UL128 locus REV	TCAGAGATCCCGAGTACGAC	
UL128_3seq	AACGGCGTCAGGTTTTTTGG	To sequence verify UL128L
UL128_5seq	ACCCATCCCAATCTCATCGT	
UL130_3seq	AACGGCGTCAGGTTTTTTGG	
UL130_5seq	CCAACAAAAGGACCACGTTT	
UL131_3seq	ACAGAAGCAGGCAGTGAAAG	
HR_UL128locus FWD	TCACGGGAAATAATATGCTACG GCTTCTGCTTCGTCACCACTTTC	To delete UL128L in FIX, selected by zeocin



	ACTGCTGTTGACAATTAATCATC GGCAT	
HR_UL128locus REV	CACCGCAGCCTGTGGATTCATG AAAATCTACTCTGGCATTCCCGA GGATCTCAGTCCTGCTCCTCGG CCA	
UL128locus_Frg1 FWD	CCCAAGCTTGGTACCGAGCTCG GATCTGCCAACTAGCCTGCGTC A	To generate VR1814- UL128L-pcDNA by Gibson cloning
UL128locus_Frg1 REV	CACACATCTGATAACGTGTGCC	
UL128locus_Frg2 FWD	GATGGCACACGTTATCAGATGT GTGTGATGAAACTGGAGAGCTG GGCCCACGTCTTCCGGTAGGGA TAACAGGGTAATCGATTT	
UL128locus_Frg2 REV	TCGGTGAACGTCAATCGCACCT GAAAAGACACGCTGTAGTCCCG GAAGACGTGGGCCAGCTCTCC AGTTTCATCAGCCAGTGTTACAA CCAATTAACC	
UL128locus_Frg3 FWD	TTCAGGTGCGATTGACGTTT	
UL128locus_Frg3 REV	CAGTGTGATGGATATCTGCAGA ATTCACCGCAGCCTGTGGATTC AT	
UL128locus_FR FWD	TGCCAACTAGCCTGCGTCA	To PCR amplify UL128L containing kanamycin cassette from pcDNA
UL128locus_FR REV	CACCGCAGCCTGTGGATTCAT	
PCR_US28 FWD	CCCAAGCTTACGTGGTGAACCG CTCATATAG	To PCR amplify and clone US28 into pcDNA
PCR_US28 REV	CATGCTCGAGTGTGAGACGCGA CACACCT	
Seq_US28_N-term	TGAAGCAGGAGATACCTTAC	To sequence verify US28
HR_US28 FWD	ACGTGGTGAACCGCTCATATAG ACCAAACCGGACGCTGCCTCAG TCTCTCTGTTGACAATTAATCAT CGGCAT	To delete US28 in FIX, selected by zeocin

HR_US28 REV	TGTGAGACGCGACACACCTCGT CGGACAGCGTGTTCGGAAGATGT CTCTCTTCAGTCCTGCTCCTCG GCCA	
Kan_US28 FWD	CGGCGGCCGCCGATTTGCTTTT CGTTTGTACTACTCTGTGG ATGCAATACTAGGGATAACAGG GTAATCGATTT	To insert kanamycin cassette into VR1814-US28-pcDNA
Kan_US28 REV	CGCGGCCGCGCCAGTGTTACAA CCAATTAACC	
Rev1_UL128_HR FWD	CAGCCGCGTGCCGCGGGTACG CGCAGAAGAATGTTGCGAATTC ATAAACGTCAACCTAGGGATAA CAGGGTAATCGATTT	To introduce F33V mutation in UL128 of FIX
Rev1_UL128_HR REV	GTAACAGCGTTCCGGCGGGTG GTTGACGTTTATGAATTCGCAAC ATTCTTCTGCGCGCCAGTGTTA CAACCAATTAACC	
Rev2_UL130_HR FWD	TTTTCTCTATCCCTCGCCCCAC GGTCCCCCTCGCAATTCCCGGG GTTCCAGCGGGTAGGGATAACA GGGTCATCGATTT	To introduce P72S mutation in UL130 of FIX
Rev2_UL130_HR REV	ACACTCGGGACCCGTTGATACC CGCTGGAACCCCGGGAATTGC GAGGGGGACCGTGGCCAGTGT TACAACCAATTAACC	
Rev3_UL130_HR FWD	TTTCAGGTGCGATTGACGTTCA CCGAGGCCAATAACCAGACTTA CACCTTCTGACTAGGGATAACA GGGTAATCGATTT	To introduce T203N mutation in UL130 of FIX
Rev3_UL130_HR REV	AAACGATGAGATTGGGATGGGT GCAGAAGGTGTAAGTCTGGTTA TTGGCCTCGGTGGCCAGTGTTA CAACCAATTAACC	

### 7.5.3 qPCR primers

Name	Sequence (5'-3')	Application
UL36 FWD	ACGCAAAGAGTTCCTCGTAC	To PCR amplify UL36 ORF
UL36 REV	TGAACATAACCACGTCCTCG	
GAPDH FWD	TGATGACATCAAGAAGGTGTTGAA	To PCR amplify GAPDH [204]
GAPDH REV	TCCTTGGAGGCCATGTGGGCCAT	

## 7.6 Antibodies

### 7.6.1 Primary Antibodies

Antigen	Clone	Species	Application (dilution)	Reference
IE1/IE2	3H4	Mouse	IF (1:3) WB (1:15)	Thomas Shenk (Princeton University, USA)
pp65	8F5	Mouse	IF (1:15) WB (1:100)	Thomas Shenk (Princeton University, USA)
pp71	2H10-9	Mouse		Thomas Shenk (Princeton University, USA)
pp150	XPA 36-14	Mouse	WB (1:3)	William Britt (University of Alabama, USA)
UL44	10D8	Mouse	WB (1:2000)	Virusys
UL128	4B10	Mouse	WB (1:30)	Barbara Adler (University of Munich, Germany)
UL130	3E3	Mouse	WB (1:30)	Barbara Adler (University of Munich, Germany)
GAPDH	14C10	Rabbit	WB (1:1000)	Cell signalling
CD66b-BV421	6/40c	Mouse	FC (1:20)	BioLegend

### 7.6.2 Secondary Antibodies

Antigen	Conjugate	Species	Application (dilution)	Reference
Mouse Ig	HRP	goat	WB (1:5000)	Dako Cytomation
Rabbit Ig	HRP	goat	WB (1:5000)	Dako Cytomation
Mouse Ig	Alexa Fluor 488	goat	IF (1:1000)	Invitrogen
Mouse Ig	Alexa Fluor 555	goat	IF (1:1000)	Invitrogen
Mouse Ig	Alexa Fluor 647	goat	IF (1:1000)	Invitrogen

### 7.6.3 Nuclear dyes

Antigen	Application (dilution)	Reference
DAPI	IF (1:1000)	Roche
Hoechst 33342	IF (1:1000)	Thermo Fisher Scientific

## 7.7 Chemical and reagents

### 7.7.1 Antibiotics

Name	Application	Concentration	Reference
Ampicillin	Selection of bacteria	100 µg/mL	Roth
Chloramphenicol	Selection of bacteria	15 µg/mL	Roth
Kanamycin	Selection of bacteria	50 µg/mL	Roth
Zeocin	Selection of bacteria	25 µg/mL	Thermo Fisher Scientific
Penicillin	Cell culture supplement	100 U/mL	Sigma-Aldrich
Streptomycin	Cell culture supplement	100 µg/mL	Sigma-Aldrich
Puromycin	Selection transduced cells	1.5 µg/mL	Sigma-Aldrich

### 7.7.2 Enzymes

Name	Reference
DreamTaq Green DNA polymerase and buffer	Thermo Fisher Scientific
Fast Digest restriction enzymes and buffer	Thermo Fisher Scientific
PRECISOR High-Fidelity DNA polymerase and buffer	BioCat
Q5 High-Fidelity DNA polymerase and buffer	NEB
PowerTrack™ SYBR Green Mastermix	Thermo Fisher Scientific
T4 DNA ligase and buffer	Thermo Fisher Scientific
Turbo™ DNase	Thermo Fisher Scientific

### 7.7.3 Molecular mass standard

Name	Reference
O'GeneRuler™ DNA Ladder mix	Thermo Fisher Scientific
PageRuler™ Prestained protein ladder	Thermo Fisher Scientific

### 7.7.4 Other reagents and chemicals

Name	Reference
Polyethylenimine (PEI)	Sigma-Aldrich
PolyFect® Transfection reagent	Qiagen
Polybrene	Millipore
Protease inhibitor cocktail cOmplete™ mini, EDTA free	Roche
Dithiothreitol (DTT)	Sigma-Aldrich
Albumin Fraction V pH 7.0 (BSA)	Applichen Panreac
Pierce™ ECL Western Blotting Substrate	Thermo Fisher Scientific
Nitrocellulose membrane (0.45 µm)	GE Healthcare Life Science
Polyvinylidenedifluoride (PVDF) membrane (0.2 and 0.45 µm)	Immobilon
Whatman® gel blotting paper, Grade GB003	Sigma-Aldrich
Ponceau S	Sigma-Aldrich
Coelenterazine-h	Promega
Blue bromophenol	Roth
β-mercaptoethanol	Roth
L-(+)-Arabinose	Sigma-Aldrich
Dimethyl sulfoxide (DMSO)	Roth
phorbol 12-myristate 13-acetate (PMA)	Sigma-Aldrich
Collagen Type I	Sigma-Aldrich
Trypan Blue	Bio-Rad
Paraformaldehyde (PFA)	Roth
Glutaraldehyde (GA) 25% aqueous EM grade	Ladd Research Industries
AEC Chromogen concentrate and Substrate buffer	Biolegend
Epredia™ Shandon™ Double Cytofunnel™	Thermo Fisher Scientific
Epredia™ Shandon™ Double Cytoslides™	Thermo Fisher Scientific
Mounting medium	Polysciences
Giemsa's azur eosin methylene blue solution	Merck Millipore

### 7.8 Media and buffers

#### 7.8.1 Cell culture media and buffers

Name	Reference
Dulbecco's Modified Eagle's Medium (DMEM) with glucose	PAN Biotech
DMEM/F-12, GlutaMAX™ Supplement	Gibco

RPMI 1640, GlutaMAX™ Supplement	Gibco
Dulbecco's Phosphate Buffer Saline (PBS)	Sigma-Aldrich
Endothelial Cell Growth Medium Kit	PromoCell
Foetal calf serum (FCS)	PAN Biotech
Trypsin-EDTA	Sigma-Aldrich
Opti-MEM	Thermo Fisher Scientific
HEPES	Gibco
Sodium Pyruvate	Gibco
β-mercaptoethanol	Gibco
Recombinant human fibroblast grow factor-basic (FGF-basic)	Peprotech
Recombinant human granulocyte-macrophage colony-stimulating factor (GM-CSF)	R&D Systems
Recombinant human macrophage-colony stimulating factor (M-CSF)	R&D Systems
UltraPure™ 0.5 M EDTA	Thermo Fisher Scientific
Bovine Serum Albumin (BSA) solution	Sigma-Aldrich
10X PBS	Sigma-Aldrich
Ficoll®-Paque Premium	Sigma-Aldrich
Histopaque®-1119	Sigma-Aldrich
Percoll™	GE Healthcare

Growth media for cell culture were prepared as follow:

Media	Components	Cell type
DMEM 5% FCS	5% (v/v) FCS	HFF cells
	1% (v/v) penicillin/streptomycin	
	0.5 ng/mL FGF-basic	
DMEM 10% FCS	10% (v/v) FCS	MRC-5 cells
	1% (v/v) penicillin/streptomycin	
DMEM/F-12 10% FCS	10% (v/v) FCS	ARPE-19 cells
	1% (v/v) penicillin/streptomycin	
	15 mM HEPES	
	0.5 mM sodium pyruvate	
RPMI 10% FCS Complete medium	10% (v/v) FCS	THP-1 cells
	1% (v/v) penicillin/streptomycin	
	10 mM HEPES	
	1 mM sodium pyruvate	

	50 $\mu$ M $\beta$ -mercaptoethanol	
RPMI 10% FCS Blood medium	10% (v/v) FCS	Human
	1% (v/v) penicillin/streptomycin	leukocytes

### 7.8.2 Bacteria growth media

Name	Reference
Luria Bertani (LB) liquid medium	Roth
Luria Bertani (LB) agar medium	Roth

### 7.8.3 Agarose gel electrophoresis buffers

Name	Components	Application
50X TAE buffer	2 M Tris, pH 8.0	Diluted to 1X with ddH <sub>2</sub> O before using. Applied for preparing agarose gel and as running buffer
	50 mM EDTA	
	5.7 % (v/v) acetic acid	
10X TBE buffer	990 mM Tris, pH 8.0	Diluted to 0.5X with ddH <sub>2</sub> O before using. Applied for preparing agarose gel and as running buffer
	40 mM EDTA	
	990 mM boric acid	

### 7.8.4 SDS polyacrylamide gel electrophoresis (SDS-PAGE) and western blot buffers

Name	Components	Application
8% SDS-Resolving gel	46% (v/v) ddH <sub>2</sub> O	Used as resolving gel
	26.7% (v/v) Bis-acrylamide	
	25% (v/v) 1.5 M Tris, pH 8.8	
	1% (v/v) 10% SDS	
	1% (v/v) 10% APS	
	0.06% (v/v) TEMED	
10% SDS-Resolving gel	40% (v/v) ddH <sub>2</sub> O	Used as resolving gel
	33% (v/v) Bis-acrylamide	
	25% (v/v) 1.5 M Tris, pH 8.8	
	1% (v/v) 10% SDS	
	1% (v/v) 10% APS	
	0.04% (v/v) TEMED	
12% SDS-Resolving gel	33% (v/v) ddH <sub>2</sub> O	Used as resolving gel
	40% (v/v) Bis-acrylamide	

	25% (v/v) 1.5 M Tris, pH 8.8	
	1% (v/v) 10% SDS	
	1% (v/v) 10% APS	
	0.04% (v/v) TEMED	
5% SDS-Stacking gel	56% (v/v) ddH <sub>2</sub> O	Used as stacking gel
	17% (v/v) Bis-acrylamide	
	25% (v/v) 0.5 M Tris, pH 6.8	
	1% (v/v) 10% SDS	
	1% (v/v) 10% APS	
	0.08% (v/v) TEMED	
RIPA lysis buffer	50 mM Tris, pH 8	Used for lysing cell samples after adding 5X DTT (optional) and 7X protease inhibitors
	150 mM NaCl	
	1 mM EDTA	
	1% (v/v) NP40	
	0.1% (v/v) SDS	
	0.5% (w/v) DOC	
4X SDS sample loading buffer	0.5 M Tris-HCl, pH 6.8	Diluted to 1X with ddH <sub>2</sub> O before using as loading buffer
	20% (v/v) Glycerol	
	4% (v/v) SDS	
	10% (v/v) β-mercaptoethanol	
	0.1% (v/v) Blue Bromophenol	
10X Laemmli running buffer	250 mM Tris	Diluted to 1X with ddH <sub>2</sub> O before using. Applied for Laemmli gel running buffer
	1.92 M Glycine	
	1% (w/v) SDS	
WB Transfer buffer	50 mM Tris	Used for semi-dry blot transfer
	40 mM Glycine	
	0.04% (v/v) SDS	
	20% (v/v) Methanol	
10X TBS-T	100 mM Tris-HCl, pH 7.5	Diluted to 1X with ddH <sub>2</sub> O before using. Applied for antibody dilutions and washing of membranes
	1.5 mM NaCl	
	1% (v/v) Tween20	



### 7.8.5 Immunofluorescence buffers

Name	Components
Fixation buffers	1-4% PFA in PBS or ice-cold methanol or ice-cold methanol/acetone (1:1)
Permeabilization buffers	0.2% (v/v) Triton-X in PBS or 10% (w/v) sucrose, 1% (v/v) FCS, 0.5% (v/v) in PBS
Blocking buffers	1% (w/v) BSA in PBS or 5% (v/v) FCS in PBS

### 7.8.6 DNA preparation from bacteria (Mini Prep) buffers

Name	Components	Application
S1 buffer	50 mM Tris-HCl, pH 8.0	Used to resuspend bacteria pellet
	100 µg/mL RNase A	
	10 mM EDTA	
S2 buffer	200 mM NaOH	Used for bacteria lysis
	1% (v/v) SDS	
S3 buffer	2.8 M calcium acetate, pH 5.1	Used to neutralize
Tris-HCl	10 mM Tris, pH 8.0	Used to dissolve DNA

### 7.8.7 FACS buffers

Name	Components
Staining buffer	5% (v/v) FCS, 5 mM EDTA in PBS
FACS buffer	10% (v/v) FCS in PBS

### 7.9 Kits

Name	Reference
BCA Protein Assay Kit	Thermo Fisher Scientific
innuPREP DNA mini kit	Analytik Jena
mi-Plasmid Miniprep kit	Metabion
NucleoBond Gel and PCR clean-up	Macherey-Nagel
NucleoBond Xtra Midi	Macherey-Nagel
Trans-Blot Turbo RTA mini Transfer kit	Bio-Rad
Gibson Assembly Ultra Master Mix A and Mix B	Synthetic Genomics Inc.
Pan Monocyte Isolation Kit	Miltenyi Biotec



## 8 Methods

### 8.1 Molecular biology methods

#### 8.1.1 Preparation of *E. coli* DH10B electrocompetent bacteria

A single colony of *E. coli* DH10B was inoculated into 10 mL of pre-warmed LB medium and cultured overnight at 37°C with continuous shaking. The following day, 5 mL of the bacteria pre-culture was added to 200 mL of LB medium and incubated at 37°C with continuous shaking. The OD600 was continually measured using a cell density meter Ultrospec 10 (Amersham Biosciences). Once the OD600 reached 0.5–0.6, the bacteria culture was immediately transfer on ice and chilled for 20 minutes. Bacteria were further pelleted by centrifugation at 5,000 × g for 10 minutes at 4°C. The pellet was then resuspended in 100 mL of ice-cold sterile water and pelleted again. After a second washing step with ice-cold sterile water, the bacteria pellet was resuspended in 10 mL of 10% (v/v) ice-cold glycerol and pelleted again. Lastly, the bacteria pellet was dissolved in 1 mL of 10% ice-cold glycerol, immediately aliquoted and stored at -80°C.

#### 8.1.2 Preparation of *E. coli* GS1783 electrocompetent bacteria

A single colony of *E. coli* GS1783 with the respective BAC clone was inoculated in 10 mL of pre-warmed LB medium with 15 µg/mL chloramphenicol and cultured overnight at 30°C with continuous shaking. The overnight culture was diluted at 1:50 ratio in LB medium containing 15 µg/mL chloramphenicol and incubated at 30°C with continuous shaking. Once the OD600 reached 0.5–0.6, the culture was immediately transferred into a water bath shaker at 42°C for 13 minutes. Subsequently, the bacteria culture was chilled down on ice for 20 minutes. The bacteria were further pelleted by centrifugation at 5,000 × g for 10 minutes at 4°C. The pellet was then resuspended in 100 mL of ice-cold sterile water and pelleted again. After a second washing step with ice-cold sterile water, the bacteria pellet was resuspended in 10 mL of 10% (v/v) ice-cold glycerol and pelleted again. Lastly, the bacteria pellet was dissolved in 1 mL of 10% (v/v) ice-cold glycerol, immediately aliquoted and stored at -80°C.

#### 8.1.3 Transformation of bacteria

Electrocompetent bacteria were transformed by electroporation. 50 µL of frozen bacteria were thawed on ice and mixed with either 150 ng of purified PCR-amplified DNA fragment (*E. coli* GS1783), 1-10 ng of plasmids or 4 µL of ligation product (*E. coli* DH10B). After 10-15 minutes of incubation on ice, the mixture was transferred into pre-chilled 2 mm electroporation cuvettes

and pulsed using the Gene Pulser XCell (Bio-Rad) with the settings of 2,500 V, 25  $\mu$ F and 200  $\Omega$ . Immediately after electroporation, 900  $\mu$ L of warm LB medium were added to the bacteria and transferred into a microcentrifuge tube. Bacteria were then incubated for 1 hour at 30°C (*E. coli* GS1783) or 37°C (*E. coli* DH10B). Next, the bacteria were pelleted by centrifugation at 500  $\times$  g for 5 minutes. The bacteria pellet was resuspended and plated on LB agar plates with the corresponding antibiotics and incubated overnight at the appropriate temperature in a bacteria incubator.

#### 8.1.4 Extraction of plasmid DNA and BAC DNA (Mini Prep)

Single clone bacteria containing the plasmid or BAC of interest were inoculated in 5 mL of LB medium supplemented with the required antibiotics and incubated overnight at proper condition. Plasmid DNA was extracted from *E. coli* DH10B bacteria using the Mi-Plasmid MiniPrep Kit according to the manufacturing protocol. BAC DNA was extracted from *E. coli* GS1783 as follow: 10 mL of the overnight culture were centrifuged at 11,000  $\times$  g for 1 minute at 4°C and the pellet was resuspended with 400  $\mu$ L of ice-cold S1 buffer. 400  $\mu$ L of ice-cold S2 buffer were then added to the mixture and gently inverted for three times. After 4 minutes of incubation at RT, 400  $\mu$ L of ice-cold S3 buffer were added and the tubes were gently inverted for five times. The samples were incubated on ice for 7 minutes and then centrifuged at 11,000  $\times$  g for 20 minutes at 4°C. The clear supernatant was transferred into a new tube and mixed with 0.8X volume of isopropanol by inversion for three times. The tube was centrifuged at 11,000  $\times$  g for 30 minutes at 4°C. The pellet was then washed with 500  $\mu$ L of 70% (v/v) ethanol and centrifuged again at 11,000  $\times$  g for 5 minutes at 4°C. The DNA pellet was dried and then dissolved in 25  $\mu$ L of 10 mM Tris-HCl (pH 8.0). To facilitate the resuspension of the DNA pellet, the tubes were incubated at 37°C with continuous shaking for 1 hour.

#### 8.1.5 Extraction of plasmid DNA and BAC DNA (Midi Prep)

Bacteria were incubated in 200 mL of LB medium supplemented with the required antibiotics overnight at the appropriate temperature. The DNA was extracted using the NucleoBond Midi Xtra Kit according to the manufacturing protocol. The high-copy protocol was used for plasmid DNA extraction, while the low-copy protocol was used for the extraction of BAC DNA. The plasmid DNA pellet was dissolved using 200-400  $\mu$ L of Tris-HCl buffer (pH 8.0), while BAC DNA was dissolved using 50-150  $\mu$ L of Tris-HCl buffer (pH 8.0).

#### 8.1.6 Storage of bacteria

For long-term storage of bacteria, 700  $\mu$ L of an overnight culture were mixed with 300  $\mu$ L of sterile 86% (v/v) glycerol and frozen at -80°C.

### **8.1.7 Polymerase chain reaction (PCR)**

PCR was performed by using DreamTaq (Thermo Fisher Scientific), Precisor (BioCat) or Q5 (NEB) High-Fidelity DNA polymerases according to the manufacturer's protocol. DreamTaq polymerase was used for colony PCR. Precisor and Q5 polymerases were used for cloning and sequencing purposes.

### **8.1.8 Restriction enzyme digestion of DNA**

DNA restriction digestion was performed using FastDigest restriction enzymes (Thermo Fisher Scientific) according to the manufacturer's protocol. 1 µg of plasmid DNA was used for analytical plasmid restriction and 2 µg of plasmid DNA were used for cloning procedures. Plasmid DNA was digested at 37°C for 20 minutes using the reaction set up according to the manufacturer's instructions. For analytical BAC restriction, 1-3 µg of BAC DNA were digested at 37°C for 1 hour.

### **8.1.9 Agarose gel electrophoresis**

PCR products and plasmid fragments were analyzed on 0.8-1.5% (w/v) TAE agarose gels and run at 120 V for 30-60 minutes. BAC DNA fragments were analyzed on 0.6% (w/v) TBE agarose gels and run at 50 V overnight, followed by 100 V for 4 hours. All gels contained 0.5 µg/mL of ethidium bromide. The O'GeneRuler (Thermo Fisher Scientific) was used as DNA size ladder. DNA bands were visualized with GelDoc XR+ (Bio-Rad) and analyzed with Image Lab software.

### **8.1.10 Purification of DNA fragments**

DNA bands of interest were cut out from TAE agarose gels and DNA fragments were then purified from the agarose gel using a NucleoSpin Gel and PCR clean up kit according to the manufacturer's protocol. Purified DNA was quantified by a NanoDrop-1000 (Peglab) photometer. DNA was stored at 4°C for short-term usage and at -20°C for long-term usage.

### **8.1.11 DNA ligation**

DNA ligations were performed using T4 DNA ligase according to the manufacturer's protocol. The molecular ratio of vector and insert was 1:5. Ligation reactions were performed at 22°C for 1 hour or at 16°C overnight.

### 8.1.12 Quantitative polymerase chain reaction (qPCR)

Total DNA was extracted from either HCMV-infected cells or cell-free virus stocks using innuPrep-DNA Mini Kit according to the manufacturing instructions and added to the SYBR Green Mastermix (Thermo Fisher Scientific) mixed with specific primers (10  $\mu$ M each). Each DNA was measured in triplicate. Quantitative polymerase chain reaction (qPCR) was performed in MicroAmp™ Fast Optical 96-Well Reaction Plate (Thermo Fisher Scientific) on a QuantStudio 3 (Thermo Fisher Scientific) qPCR machine. Viral genome copy numbers per cell were quantified using the  $\Delta\Delta$ Ct method and normalized to the GAPDH housekeeping gene. For determination of viral genome copy numbers per millilitre (mL), serial dilutions of a FIX-BAC DNA were used as reference for the standard curve.

### 8.1.13 DNA sequencing

PCR products and plasmid DNA were sequenced by SEQLAB (Sequence Laboratories, Göttingen, Germany). HCMV genome sequences were determined by Illumina sequencing at the Next Generation Sequencing facility of the Leibniz Institute of Virology (LIV, Hamburg, Germany).

### 8.1.14 *En Passant* BAC mutagenesis

The modifications of HCMV viral genome cloned into the bacterial artificial chromosome (BAC) were performed by Dr. Giada Frascaroli using *en passant* mutagenesis according to the protocols published by Tischer *et al.* [202]. Briefly, for each mutagenesis primers were designed in order to generate short linear DNA fragments with homologs of the viral genome and used for PCR amplifying the I-SceI-aphAI-cassette from the pEP-Kan-S plasmid containing the kanamycin resistance gene. The plasmid template was removed from the PCR product by DpnI digestion. The digestion reaction was run in TAE agarose gel and purified by NucleoSpin Gel and PCR clean up kit following the manufacturing protocol. For the first recombination, 150 ng of purified DNA were transformed into competent *E. coli* GS1783 carrying the appropriate viral genome by electroporation in a 2 mm cuvette at 2,500 V using a GenePulser Xcell (Bio-Rad). Bacteria were first recovered in 1 mL of LB medium and cultured in a Thermomixer (Eppendorf) at 30°C for 1 hour with continuous shaking. Afterwards, bacteria were plated in a LB agar plate containing appropriate antibiotics and incubated overnight at 30°C. Ten resulting colonies were picked, further inoculated in LB medium containing chloramphenicol and either kanamycin or zeocin and incubated overnight at 30°C to prepare BAC DNA mini preps. Resulting bacteria clones were checked via enzymes restriction digestion, analytical PCR, colony PCR, and sequencing. Two positive clones were then

selected for the second Red-recombination procedure. A single colony was inoculated into 2 mL of LB medium containing chloramphenicol and cultured at 30°C for 60-90 minutes until medium turning cloudy. 2 mL of LB medium containing 2% (w/v) L-arabinose was added and cultured for another hour. The culture was then immediately transferred into a shaking incubator with water bath at 42°C to induce the expression of the red recombinase. After 30 minutes, the culture was transferred back into a 30°C shaker for 1 hour. The bacteria density was determined by OD600 using a cell density meter Ultrospec 10 (Amersham Biosciences). The culture was diluted with LB medium at 1:1000 (OD600<0.5). 100 µL of the diluted culture were plated onto an agar plate containing chloramphenicol and 1% (w/v) L-arabinose and incubated for at least 20 hours at 30°C. Resulting colonies were picked and checked for loss of kanamycin resistance by enzyme restriction digestion, analytical PCR, and sequencing of the modified region. Two selected positive clones were grown in 200 mL of LB medium containing chloramphenicol for BAC DNA Midi preps. Purified DNA was finally used to reconstitute BAC-derived viruses in human fibroblasts.

#### **8.1.15 Gibson assembly cloning**

The UL128 locus of VR1814 was cloned into pcDNA3 plasmid and used to replace the entire UL128L in FIX, essentially as described [154]. The Gibson assembly cloning was performed by Dr. Giada Frascaroli. Briefly, pcDNA3 plasmid was digested using BamHI and EcoRI and used as template. Then, three DNA fragments containing overlapping sequences with the adjacent DNA fragments were PCR-amplified: (i) fragment containing the UL131A and UL130 from VR1814; (ii) fragment containing the selection marker (kanamycin) and the homology sequences for the second recombination of BAC mutagenesis; (iii) fragment containing the UL128 from VR1814. After gel purification, the fragments were ligated following the Gibson Assembly Ultra Master Mix A and Mix B manufacturing instructions.

### **8.2 Cell biology and virology methods**

#### **8.2.1 Cell culture**

All cells were maintained in culture flasks (T25, T75 or T175) or plates (6-well, 12-well, 24-well, 48-well or 96-well) and incubated in a Hera Cell CO<sub>2</sub> incubator (Heraeus) at 37°C, 80% relative humidity and 5% CO<sub>2</sub>. All cell culture work was done using a sterile bench (HeraSafe, Heraeus). Specific growth media were used according to the cell type as described in 7.8.1. Adherent cells were passaged at 80-90% of confluence by removing the media, washing with PBS and adding 0.25% (v/v) trypsin-EDTA solution. The trypsin was then neutralized with double the volume of FCS supplemented medium and split 1:3 to 1:10. Cells in suspension

were collected and centrifuged at  $250 \times g$  for 7 minutes at RT. The cell pellet was then resuspended in fresh growth medium. Human leukocytes were isolated from buffy coats of healthy HCMV-seronegative blood donors, obtained from the Transfusion Center of the University Medical Center Hamburg-Eppendorf (Hamburg, Germany). Peripheral blood mononuclear cells (PBMC) were isolated by negative selection (Pan monocyte isolation kit) with magnetic microbeads according to the manufacturer's instructions. A total of  $3 \times 10^6$  monocytes/mL were seeded in hydrophobic Lumox dishes (Sarsted) and differentiated into M1 or M2 macrophages by incubation at  $37^\circ\text{C}$  for 7 days in the presence of 100 ng/mL recombinant human granulocyte-macrophage colony-stimulating factor (GM-CSF) or macrophage-colony stimulating factor (M-CSF), respectively. Polymorphonuclear neutrophils (PMN) were purified by density centrifugation at  $800 \times g$  for 20 minutes at RT using Histopaque-1199, followed by an isotonic discontinuous Percoll density gradient (85%, 80%, 75%, 70%, 65%) centrifugation at  $800 \times g$  for 20 minutes at RT as described before [205]. PMNs were isolated to a purity of  $>95\%$  as assessed by Giemsa staining.

For seeding the cells, the cell number was determined by counting 10  $\mu\text{L}$  of cell suspension using an automated cell counter (TC20, Bio-Rad). Cell viability was assessed using Trypan Blue.

For freezing the cells, the cell suspension was centrifuge at  $250 \times g$  for 5 minutes at RT. The obtained cell pellet was resuspended in freezing media containing 90% FCS and 10% DMSO to prevent mechanical damage to the cells due to the freezing process. The cells were then aliquoted into cryotubes and immediately frozen at  $-80^\circ\text{C}$  using a freezing box (CoolCell LX). The cells were further transferred to liquid nitrogen for long-term storage.

For thawing the cells, aliquots of frozen cells were kept shortly at  $37^\circ\text{C}$  in the water bath, and then suspended gently in 9 mL of growth media. After a centrifugation at  $125 \times g$  for 5 minutes at RT, cell pellet was resuspended in a proper volume of complete growth medium and incubated at  $37^\circ\text{C}$ .

### **8.2.2 Transfection of plasmid DNA**

Plasmid DNA was transfected to cells using polyethylenimine (PEI).  $4 \times 10^6$  cells were seeded in a  $10\text{-cm}^2$  dish and transfected using 8  $\mu\text{g}$  of plasmid DNA. The plasmid and PEI (32  $\mu\text{L}$  considering a ratio with the DNA of 1:4) were first resuspended in separate tubes in 100  $\mu\text{L}$  of DMEM without supplements. After 5 minutes of incubation, they were mixed together by vortexing, incubated for 15 minutes at RT and delivered to the cells. The medium was changed 6-8 hours post-transfection. The supernatant was collected at 48 and 72 hours post-transfection for further using.



### 8.2.3 Transfection of BAC DNA

HCMV BAC DNA was transfected into human fibroblasts by electroporation for reconstitution of HCMV viruses. For each transfection,  $1 \times 10^7$  cells were pelleted by centrifugation at  $180 \times g$  for 8 minutes at RT. Cell pellet was resuspended with 10 mL of OptiMEM and pelleted again at  $180 \times g$  for 8 minutes at RT. Supernatant was discarded and the cell pellet was resuspended in 250  $\mu$ L of OptiMEM. During centrifugation, 3  $\mu$ g of HCMV BAC DNA and 1.5  $\mu$ g of pCGN-pp71 plasmid DNA were diluted in OptiMEM and mixed by gently pipetting. The cells and DNA were then combined, gently mixed and transferred into a 4 mm electroporation cuvette. Electroporation was performed using a GenePulser Xcell (Bio-Rad) with the setting of 220 V and 950  $\mu$ F. After a short incubation of 5 minutes at RT, 1 mL of OptiMEM was slowly added into the cuvette. The floated viscous material was carefully removed, and the leftover was gently resuspended by pipetting and transferred to a 10-cm<sup>2</sup> dish with fresh growth medium. The medium was changed after an overnight incubation and transfected cells were monitored every 2-3 days by detection of GFP expression or cytopathic effects (CPE). The infectious supernatant was harvested for virus stock preparation.

### 8.2.4 Production of lentivirus

Lentivirus was produced from HEK-293T cells. Transfection was done in 10-cm<sup>2</sup> dishes. 4.5  $\mu$ g of recombinant lentiviral expression vector (pdl for epithelial cells transduction and pLeGO for monocytic cell line transduction) encoding the protein of interest were mixed with 3  $\mu$ g of packaging plasmid pCMVR8.91 and 3  $\mu$ g of envelope plasmid pMD-G in 1 mL of serum-free medium and co-transfected to cells as described in 8.2.2. The supernatant containing lentivirus was harvested at 48 and 72 hours post-transfection. The supernatant was filtered through a 0.45  $\mu$ m filter and used directly or stored at -80°C.

### 8.2.5 Transduction of cells

To transduce adherent cells,  $3 \times 10^5$  of ARPE-19 cells were seeded on a 6-well plate the day before transduction. The medium was replaced by 3 mL of the filtered supernatant containing lentivirus mixed with Polybrene (5  $\mu$ g/mL). The cells were incubated for 2 hours at 37°C, then supplemented with the appropriate growth medium and incubated at 37°C for further 48 hours. Transduced cells were trypsinized and transferred to a 10-cm<sup>2</sup> dish and selected by application of 1.5  $\mu$ g/mL of puromycin every third day. Non-transduced cells were treated by puromycin and used as control.

To transduce cells in suspension, THP-1 cells were diluted to  $5 \times 10^5$  cells in 1 mL of medium and mixed with 500  $\mu$ L of the filtered supernatant containing lentivirus into a 2 mL Eppendorf

tube. Polybrene to a final concentration of 8 µg/mL was added to the mixture, and incubated for 6 hours at 37°C. The mixture was then centrifuge at 250 × g for 7 minutes at RT, and the cell pellet was resuspended in 3 mL of complete growth medium. Cells were transferred into a 6-well plate and incubated for 48 hours at 37°C. Transduced cells were finally selected using 1.5 µg/mL of puromycin applied every third day until complete selection.

### 8.2.6 Preparation of HCMV stocks

For the preparation of cell-free virus stocks, HFF cells were co-cultured with late-stage infected HUVEC cells at a ratio of roughly 50:1. Supernatant was collected from infected cultures showing 100% CPE, stored at -80°C or directly concentrated by centrifugation. Cell debris were first removed by centrifugation at 5,500 × g for 15 minutes at 4°C, then virus particles were pelleted by ultracentrifugation at 23,000 × g for 1 hour at 4°C. The virus pellet was resuspended in DMEM medium containing a cryopreserving sucrose phosphate buffer (74.62 g/L sucrose, 1.218 g/L K<sub>2</sub>HPO<sub>4</sub>, 0.52 g/L KH<sub>2</sub>PO<sub>4</sub>) for 2 hours at 4°C with continuous shaking. After resuspension, the virus was aliquoted and stored at -80°C.

### 8.2.7 Titration of HCMV stocks

The virus was titrated in either HFF or ARPE-19 cells and the virus titer was determined by calculating the infectious units (IU) per mL. 2 × 10<sup>4</sup> cells were plated in 96-well plate and after an overnight incubation were infected with log<sub>10</sub> serial dilutions (10<sup>-1</sup> up to 10<sup>-7</sup>) prepared in DMEM containing serum. Each dilution was done in triplicate. 100 µL of virus dilution were added to the cells. After 48 hours, the cells were fixed with methanol/acetone for 10 minutes at -20°C, blocked with 1% (w/v) milk in PBS for 15 minutes at 37°C, and incubated with an anti-IE1/IE2 antibody for 2 hours at 37°C and an HRP-conjugated rabbit anti-mouse secondary antibody for 45 minutes at 37°C. Staining was done with 3-amino-9-ethylcarbazole (AEC) as HRP substrate. IE1/IE2-positive nuclei were counted, and viral titers were determined as infectious units per millilitre (IU/mL).

### 8.2.8 Viral infections

Cells were infected with HCMV using different multiplicities of infection (MOI) based on the IU/mL of a virus stock. To determine the volume of virus stock needed to infect cells at a given MOI the following equation was used:

$$\frac{\text{number of cells} * \text{MOI}}{\text{IU/mL}} = \text{volume of virus stock (mL)}$$

The required volume of the virus stock was first diluted in growth medium supplemented only with FCS and antibiotics and then added to cells. The virus inoculum was removed after 3 hours and replaced with fresh growth medium.

### 8.2.9 Viral replication kinetics

Viral replication kinetics were determined by single step and multiple step replication curves. Cells ( $1.2 \times 10^5$  ARPE-19 cells per well in 6-well plates or  $1.5 \times 10^5$  THP-1-derived macrophages per well in 48-well plates) were infected with a defined MOI. Three biological replicates were prepared for each virus. After 3 hours, the supernatant was removed, cells were washed with PBS, and fresh medium was added. The supernatants were harvested at different time points post-infection and titrated on HFF cells as described in 8.2.7.

### 8.2.10 Cell-cell fusion assay

Equal numbers of cells stably expressing DSP1-7 or DSP8-11 ( $1 \times 10^4$  ARPE-19 cells,  $1.5 \times 10^5$  THP-1-derived macrophages) were seeded in black-walled, transparent-bottomed 96-well plates. The cells were infected with a defined MOI for 3 hours at 37°C. The virus inoculum was then removed, the cells were washed with PBS and new fresh growth medium was added. At 5 dpi, cells were washed with PBS, and incubated with coelenterazine-h (Promega) at a final concentration of 2.5 nM. To quantify *Renilla* luciferase activity, luminescence was measured on a multi-mode microplate reader (FLUOstar Omega).

### 8.2.11 Syncytium formation inhibition assay

Equal numbers of DSP-expressing ARPE-19 cells were seeded in black-walled, transparent-bottomed 96-well plates at a density of  $1 \times 10^4$  cells/well. The following day, cells were infected at an MOI of 1 for 3 hours at 37°C, washed with PBS, and incubated with fresh medium containing serial dilutions of anti-UL130 antibody (3E3 hybridoma supernatant). At 5 dpi, *Renilla* luciferase expression was quantified as described in 8.2.10, and the percentage of syncytia relative to cells treated with a non-neutralizing anti-pp71 control antibody (2H10-9 hybridoma supernatant) was calculated. After luciferase activity quantification, cells were fixed in methanol/acetone for 10 minutes at -20°C, blocked with 1% (w/v) milk in PBS for 15 minutes at 37°C, and incubated with an anti-IE1/IE2 antibody for 2 hours at 37°C and an anti-mouse IgG secondary antibody coupled to AlexaFluor 555 for 1 hour at 37°C. Nuclear DNA was stained with 1 µg/mL of DAPI (4',6-diamidino-2-phenylindole). Images of IE1/IE2-positive cells were acquired using CellInsight CX5 High-Content Screening Platform (Thermo Fisher Scientific).

### 8.2.12 Cytospin and Giemsa staining

Freshly isolated PMNs ( $1 \times 10^5$  cells per 100  $\mu\text{L}$ ) were spread on microscope slides by cytocentrifugation at  $450 \times g$  for 5 minutes at RT, and air dried completely. The samples were then fixed in ice-cold methanol for 1 minute and subsequently stained with a Giemsa solution diluted 1:10 in PBS for 3 minutes at RT. The samples were finally washed with water, one drop of mounting medium was poured on the glass slides and the cover slips were mounted onto them. The neutrophil purity (>95%) was evaluated using a PrimoVert Zeiss cell culture microscope.

### 8.2.13 Uptake of cell-associated HCMV by PMNs

HUVEC endothelial cells infected with HCMV were used as donor cultures for PMN-mediated transmission. HUVEC cells were seeded in 6-well plates (pre-treated with 1 mg/mL of collagen type I for 30 minutes at  $37^\circ\text{C}$ ) at a density of  $2 \times 10^5$  cells/well. The following day, cells were infected at an MOI of 5 for 3 hours at  $37^\circ\text{C}$ , washed with PBS, and incubated in endothelial growth medium at  $37^\circ\text{C}$ . At 6 dpi, the infected HUVEC cells were washed in PBS and freshly isolated PMNs were added at a ratio of 10:1 to the donor culture. After co-culturing for 5 hours at  $37^\circ\text{C}$ , PMNs were collected, carefully avoiding detachment of the donor culture layer. One fraction of the recollected PMNs was used for cytospot preparations in order to determine the pp65 uptake during the previous incubation of the PMNs with the donor cells. In addition, the donor cultures were fixed and stained for viral IE1/IE2 or pp65 antigens by indirect immunofluorescence to determine the number of infected donor cells. The staining protocols used for the immunofluorescence analysis of PMNs and donor cultures are described in 8.4.1.

### 8.2.14 Fluorescence-activated cell sorting (FACS)

Fluorescence activated cell sorting (FACS) was used to select HCMV-positive PMNs. PMNs were carefully collected after co-culture with infected endothelial cells and pelleted by centrifugation at  $250 \times g$  for 5 minutes at RT.  $1 \times 10^6$  cells were suspended in 100  $\mu\text{L}$  of staining buffer containing 5  $\mu\text{L}$  of anti-human CD66b-BV421 antibody and incubated for 20 minutes at  $4^\circ\text{C}$ . After incubation, 1.5 mL of staining buffer was added to the mixture and cells were pelleted by centrifugation at  $350 \times g$  for 5 minutes at RT. The cell pellet was washed a second time in 2 mL of staining buffer and finally resuspended in 1 mL of FACS buffer. The cells were then transferred into 5 mL FACS tubes with cell-strainer cap (Falcon) and sorted using a FACS Aria-Fusion flow cytometer (BD Biosciences) at the LIV FACS facility (Hamburg, Germany). Cells were initially gated on the basis of forward and side scatter (granulocytes), the granulocytes were then gated based on CD66b-BV421 (neutrophil cell marker) and GFP

(HCMV pp65) fluorescence. The instrument setting was performed using unstained PMNs as negative control. After cell sorting, the CD66b<sup>+</sup>/GFP<sup>+</sup> cells were collected in 5 mL of RPMI supplemented with 20% FCS.

### **8.3 Protein biochemistry methods**

#### **8.3.1 Cell lysis for immunoblotting**

For protein analysis of the whole cell lysates, cells were washed with PBS and lysed in RIPA buffer supplemented with cOmplete Mini Protease Inhibitor Cocktail (Roche). Cell-free virions were further cleared of debris by centrifugation at 1,000 × g for 5 minutes at 4°C and resuspended in RIPA buffer supplemented with cOmplete Mini Protease Inhibitor Cocktail. Insoluble material from all lysate samples was removed by centrifugation at 16,000 × g for 10 minutes, and the cleared extracts were boiled in 4X SDS-PAGE loading buffer at 95°C for 5 minutes. For reducing blots, extracts were supplemented with 1% β-mercaptoethanol. Lysate samples were either used directly or stored at -20°C.

#### **8.3.2 Protein concentration measurement**

Protein concentration was measured using BCA Protein assay kit (Thermo Fisher Scientific). Protein lysates were diluted at the ratio 1:10 in PBS in triplicate in 96-well plate. BSA standard curve was prepared using the dilutions of BSA (2.0 mg/mL) in PBS. 100 μL of a 50:1 mix of the BCA solutions A and B were added to each sample and standards. After 30 minutes of incubation at 37°C, the absorbance at 562 nm was measured using FLUOstar Omega reader (BMG Labtech). The BSA standard curve was used to calculate the protein concentration.

#### **8.3.3 SDS polyacrylamide gel electrophoresis (SDS-PAGE) and immunoblot**

Laemmli-SDS-PAGE was used to analyze protein expression in this study. Proteins (20 μg) were separated according to their molecular weight by using a lysis buffer containing sodium dodecyl sulphate (SDS) and β-mercaptoethanol. The protein separation occurred into a polyacrylamide gel formed by two different phases: stacking gel (loading gel) containing 5% of acrylamide and resolving gel (separation gel) containing 8-12% of acrylamide. The run was performed in Laemmli running buffer at 60-120 V. PageRuler (Thermo Fisher Scientific) was used as size ladder. Once the proteins were separated in the SDS-PAGE, they were transferred on a nitrocellulose or polyvinylidenedifluoride (PVDF) membrane by semi-dry blotting in a Trans Blot Turbo Transfer System (Bio-Rad). Transfer was done by applying 100 mA per gel for 60-75 minutes. When suitable, the blot transfer was performed using a ready-to-assemble transfer kit (Bio-Rad) according to the manufacturing protocol. Afterwards, the

transfer efficiency was quickly evaluated using a Ponceau S staining solution and then the membranes were blocked using 5% (w/v) non-fat milk powder or BSA in TBS-T buffer for 45 minutes at RT on a shaking platform. Membranes with primary antibodies were incubated overnight at 4°C on a shaking platform. The following day, the membranes were washed three times for 5 minutes each with TBS-T buffer and incubated with specific secondary antibodies coupled with Horseradish peroxidase (HRP) for 1 hour at RT on a shaking platform. Primary and secondary antibodies were diluted in 5% (w/v) non-fat milk powder or BSA in TBS-T buffer according to the requirement of the antibody. Afterwards, the membranes were washed three times for 5 minutes each in TBS-T buffer and incubated with Pierce™ ECL Western Blotting Substrate (Thermo Fisher Scientific) for 4 minutes in the dark. The chemiluminescent signal was detected and imaged using X-ray films or Fusion Capture Advance FX7 16.15 (Peqlab) device.

## **8.4 Microscopy methods**

### **8.4.1 Immunofluorescence (IF)**

Cells were seeded on 8-well  $\mu$ -slides (Ibidi) and infected with HCMV specific viruses with a defined MOI. At the indicated time points, cells were fixed accordingly to the datasheet of the primary antibody either with methanol/acetone for 10 minutes at -20°C or with 4% paraformaldehyde (PFA) in PBS for 20 minutes at RT, followed by two times washing with PBS and a permeabilization with 0.2% (v/v) TritonX-100 in PBS for 2 minutes at RT. The cells were then blocked in 1% (w/v) milk in PBS for 15 minutes at 37°C. Primary antibodies were diluted in 1% (w/v) BSA in PBS and incubated for 2 hours at 37°C or overnight at 4°C. After three times washing with PBS, specific secondary antibodies coupled to AlexaFluor diluted in 1% (w/v) BSA in PBS were applied to the cells for 1 hour at 37°C. After three times washing with PBS, the cell nuclei were counterstained with 1  $\mu$ g/mL of DAPI for 10 minutes in the dark.

For the detection of pp65 in cytocentrifuged PMN preparations, the dried cytosspots were fixed in 1% PFA in PBS for 10 minutes at RT, permeabilized with 10% sucrose, 1% FCS and 0.5% Nonidet P40 for 10 minutes at RT, and blocked in 5% (v/v) FCS in PBS for 30 minutes at 37°C. The detection of viral pp65 antigen was then performed using the previously described antibodies, each applied for 45 minutes at 37°C. Nuclei were counterstained with DAPI for 10 minutes at RT. The samples were finally washed with water, one drop of mounting medium was poured on the glass slides and the cover slips were mounted onto them.

All fluorescence images were acquired with a Nikon A1+ confocal laser scanning microscope (cLSM).

#### 8.4.2 Transmission electron microscopy (TEM)

After co-culture with donor cells, sorted CD66b<sup>+</sup>/GFP<sup>+</sup> PMNs were pelleted by centrifugation at 350 × g for 5 minutes at RT and resuspended in 100 μL of 2% (v/v) PFA + 2.5% (v/v) glutaraldehyde (GA) in PBS and incubated overnight at 4°C. For ultrastructural analysis in the transmission electron microscope (TEM), the cells were encapsulated in capillary microtubes and processed for ultrathin sectioning technique with the help of Carola Schneider (LIV Microscopy and Image Analysis facility, Hamburg, Germany). After fixation with 2.5% GA, the microtubes (200 μm diameter) were filled with the solutions by capillary attraction and mechanically sealed at both ends by a scalpel. The cells within the tubes were fixed *in situ* from the outside through the highly porous tube walls (molecular weight cut-off: 10 kDa) by successive immersion into 1% OsO<sub>4</sub> in PBS and 1% uranyl acetate for 30 minutes each, followed by dehydration in a graded series of ethanol. For ultrathin sectioning, the microtubes were embedded in EPON (Carl Roth) resin. Ultrathin 50 nm sections were prepared using a Leica Ultracut Microtome and counterstained with 1% uranyl acetate. Electron micrographs were obtained with a 2K wide angle CCD camera (Veleta) attached to a FEI Tecnai G 20 Twin transmission electron microscope (FEI) at 80 kV.

#### 8.4.3 Correlative light and electron microscopy (CLEM)

For combined confocal laser scanning microscopy (CLSM) and ultrastructural analysis by electron microscopy (EM), HUVEC cells were infected with TB4-UL83-EYFP at a MOI of 5 and cultured for 6 days in pre-coated 35-mm μ-dishes with imprinted grids (Ibidi) before addition of freshly isolated PMNs as described in 8.2.13. Fluorescence microscopy was performed with a Nikon spinning disk system consisting of Yokogawa CSU-W camera. A Nikon 100x 1.49 NA Apo-TIRF objective was used resulting in 130 nm pixel size. The image acquisition was run in NIS-Elements (Nikon), post-processing and image analysis were performed in Fiji and Imaris softwares. For serial block-face scanning electron microscopy (SBF-SEM), samples were processed, and EM images were acquired with the help of Dr. Felix J. Flomm (LIV, Hamburg, Germany). Briefly, before spinning disk microscopy, the cells were fixed with 4% PFA in PBS for 10 minutes at RT and cell nuclei were stained with Hoechst 33342 for 10 minutes at RT. Afterwards, the cells were post-fixed with ice-cold 4% (m/v) OsO<sub>4</sub> + 5% (m/v) GA in PBS directly on the dish and stained essentially as described [153]. The washing steps were carried out carefully to avoid neutrophils detachment from the dishes. Single parts of the culture dishes containing cells of interest were cut out after Epon embedding. Serial block-face scanning electron microscopy was performed using a Jeol JSM-7100F scanning electron microscope (Jeol) equipped with a Gatan 3view stage (Gatan). Imaging was performed with a beam acceleration voltage of 3 kV. ROIs were defined manually, and the pixel size was set to 3 nm.





## 9 References

- (1) Davison, A. J.; Eberle, R.; Ehlers, B.; Hayward, G. S.; McGeoch, D. J.; Minson, A. C.; Pellett, P. E.; Roizman, B.; Studdert, M. J.; Thiry, E. The Order Herpesvirales. *Arch. Virol.* **2009**, *154* (1), 171–177. <https://doi.org/10.1007/s00705-008-0278-4>.
- (2) Murphy, E.; Yu, D.; Grimwood, J.; Schmutz, J.; Dickson, M.; Jarvis, M. A.; Hahn, G.; Nelson, J. A.; Myers, R. M.; Shenk, T. E. *Coding Potential of Laboratory and Clinical Strains of Human Cytomegalovirus*; 2003. [www.pnas.org/cgi/doi/10.1073/pnas.2136652100](http://www.pnas.org/cgi/doi/10.1073/pnas.2136652100).
- (3) Dunn, W.; Chou, C.; Li, H.; Hai, R.; Patterson, D.; Stolc, V.; Zhu, H.; Liu, F. Functional Profiling of a Human Cytomegalovirus Genome. *Proc. Natl. Acad. Sci.* **2003**, *100* (24), 14223–14228. <https://doi.org/10.1073/pnas.2334032100>.
- (4) Yu, D.; Silva, M. C.; Shenk, T. Functional Map of Human Cytomegalovirus AD169 Defined by Global Mutational Analysis. *Proc. Natl. Acad. Sci.* **2003**, *100* (21), 12396–12401. <https://doi.org/10.1073/pnas.1635160100>.
- (5) Wilkinson, G. W. G.; Davison, A. J.; Tomasec, P.; Fielding, C. A.; Aichele, R.; Murrell, I.; Seirafian, S.; Wang, E. C. Y.; Weekes, M.; Lehner, P. J.; Wilkie, G. S.; Stanton, R. J. Human Cytomegalovirus: Taking the Strain. *Med. Microbiol. Immunol. (Berl.)* **2015**, *204* (3), 273–284. <https://doi.org/10.1007/s00430-015-0411-4>.
- (6) Cunningham, C.; Gatherer, D.; Hilfrich, B.; Baluchova, K.; Dargan, D. J.; Thomson, M.; Griffiths, P. D.; Wilkinson, G. W. G.; Schulz, T. F.; Davison, A. J. Sequences of Complete Human Cytomegalovirus Genomes from Infected Cell Cultures and Clinical Specimens. *J. Gen. Virol.* **2010**, *91* (3), 605–615. <https://doi.org/10.1099/vir.0.015891-0>.
- (7) Sijmons, S.; Van Ranst, M.; Maes, P. Genomic and Functional Characteristics of Human Cytomegalovirus Revealed by Next-Generation Sequencing. *Viruses* **2014**, *6* (3), 1049–1072. <https://doi.org/10.3390/v6031049>.
- (8) Dhuruvasan, K.; Sivasubramanian, G.; Pellett, P. E. Roles of Host and Viral microRNAs in Human Cytomegalovirus Biology. *Virus Res.* **2011**, *157* (2), 180–192. <https://doi.org/10.1016/j.virusres.2010.10.011>.
- (9) Gibson, W. Structure and Formation of the Cytomegalovirus Virion. In *Human Cytomegalovirus*; Shenk, T. E., Stinski, M. F., Eds.; Compans, R. W., Cooper, M. D., Honjo, T., Koprowski, H., Melchers, F., Oldstone, M. B. A., Olsnes, S., Vogt, P. K., Series Eds.; Current Topics in Microbiology and Immunology; Springer Berlin Heidelberg: Berlin, Heidelberg, 2008; Vol. 325, pp 187–204. [https://doi.org/10.1007/978-3-540-77349-8\\_11](https://doi.org/10.1007/978-3-540-77349-8_11).
- (10) Varnum, S. M.; Streblow, D. N.; Monroe, M. E.; Smith, P.; Auberry, K. J.; Paša-Tolić, L.; Wang, D.; Camp, D. G.; Rodland, K.; Wiley, S.; Britt, W.; Shenk, T.; Smith, R. D.; Nelson, J. A. Identification of Proteins in Human Cytomegalovirus (HCMV) Particles: The HCMV Proteome. *J. Virol.* **2004**, *78* (20), 10960–10966. <https://doi.org/10.1128/JVI.78.20.10960-10966.2004>.
- (11) Kalejta, R. F. Tegument Proteins of Human Cytomegalovirus. *Microbiol. Mol. Biol. Rev.* **2008**, *72* (2), 249–265. <https://doi.org/10.1128/MMBR.00040-07>.
- (12) Terhune, S. S.; Schröer, J.; Shenk, T. RNAs Are Packaged into Human Cytomegalovirus Virions in Proportion to Their Intracellular Concentration. *J. Virol.* **2004**, *78* (19), 10390–10398. <https://doi.org/10.1128/JVI.78.19.10390-10398.2004>.
- (13) Irmiere, A.; Gibson, W. Isolation and Characterization of a Noninfectious Virion-like Particle Released from Cells Infected with Human Strains of Cytomegalovirus. *Virology* **1983**, *130* (1), 118–133. [https://doi.org/10.1016/0042-6822\(83\)90122-8](https://doi.org/10.1016/0042-6822(83)90122-8).
- (14) Schleiss, M. R. Cytomegalovirus. In *Maternal Immunization*; Elsevier, 2020; pp 253–288. <https://doi.org/10.1016/B978-0-12-814582-1.00013-9>.
- (15) Sinzger, C.; Digel, M.; Jahn, G. Cytomegalovirus Cell Tropism. In *Human Cytomegalovirus*; Shenk, T. E., Stinski, M. F., Eds.; Compans, R. W., Cooper, M. D., Honjo, T., Koprowski, H., Melchers, F., Oldstone, M. B. A., Olsnes, S., Vogt, P. K.,

- Series Eds.; Current Topics in Microbiology and Immunology; Springer Berlin Heidelberg: Berlin, Heidelberg, 2008; Vol. 325, pp 63–83. [https://doi.org/10.1007/978-3-540-77349-8\\_4](https://doi.org/10.1007/978-3-540-77349-8_4).
- (16) Vanarsdall, A. L.; Johnson, D. C. Human Cytomegalovirus Entry into Cells. *Curr. Opin. Virol.* **2012**, *2* (1), 37–42. <https://doi.org/10.1016/j.coviro.2012.01.001>.
- (17) Kinzler, E. R.; Compton, T. Characterization of Human Cytomegalovirus Glycoprotein-Induced Cell-Cell Fusion. *J. Virol.* **2005**, *79* (12), 7827–7837. <https://doi.org/10.1128/JVI.79.12.7827-7837.2005>.
- (18) Nguyen, C. C.; Siddiquey, M. N. A.; Zhang, H.; Li, G.; Kamil, J. P. Human Cytomegalovirus Tropism Modulator UL148 Interacts with SEL1L, a Cellular Factor That Governs Endoplasmic Reticulum-Associated Degradation of the Viral Envelope Glycoprotein gO. *J. Virol.* **2018**, *92* (18), e00688-18. <https://doi.org/10.1128/JVI.00688-18>.
- (19) Isaacson, M. K.; Compton, T. Human Cytomegalovirus Glycoprotein B Is Required for Virus Entry and Cell-to-Cell Spread but Not for Virion Attachment, Assembly, or Egress. *J. Virol.* **2009**, *83* (8), 3891–3903. <https://doi.org/10.1128/JVI.01251-08>.
- (20) Wu, Y.; Prager, A.; Boos, S.; Resch, M.; Brizic, I.; Mach, M.; Wildner, S.; Scrivano, L.; Adler, B. Human Cytomegalovirus Glycoprotein Complex gH/gL/gO Uses PDGFR- $\alpha$  as a Key for Entry. *PLOS Pathog.* **2017**, *13* (4), e1006281. <https://doi.org/10.1371/journal.ppat.1006281>.
- (21) Martinez-Martin, N.; Marcandalli, J.; Huang, C. S.; Arthur, C. P.; Perotti, M.; Foglierini, M.; Ho, H.; Dosey, A. M.; Shriver, S.; Payandeh, J.; Leitner, A.; Lanzavecchia, A.; Perez, L.; Ciferri, C. An Unbiased Screen for Human Cytomegalovirus Identifies Neuropilin-2 as a Central Viral Receptor. *Cell* **2018**, *174* (5), 1158-1171.e19. <https://doi.org/10.1016/j.cell.2018.06.028>.
- (22) Kalejta, R. F. Functions of Human Cytomegalovirus Tegument Proteins Prior to Immediate Early Gene Expression. In *Human Cytomegalovirus*; Shenk, T. E., Stinski, M. F., Eds.; Compans, R. W., Cooper, M. D., Honjo, T., Koprowski, H., Melchers, F., Oldstone, M. B. A., Olsnes, S., Vogt, P. K., Series Eds.; Current Topics in Microbiology and Immunology; Springer Berlin Heidelberg: Berlin, Heidelberg, 2008; Vol. 325, pp 101–115. [https://doi.org/10.1007/978-3-540-77349-8\\_6](https://doi.org/10.1007/978-3-540-77349-8_6).
- (23) Xuan, B.; Qian, Z.; Torigoi, E.; Yu, D. Human Cytomegalovirus Protein pUL38 Induces ATF4 Expression, Inhibits Persistent JNK Phosphorylation, and Suppresses Endoplasmic Reticulum Stress-Induced Cell Death. *J. Virol.* **2009**, *83* (8), 3463–3474. <https://doi.org/10.1128/JVI.02307-08>.
- (24) Fu, Y.-Z.; Su, S.; Gao, Y.-Q.; Wang, P.-P.; Huang, Z.-F.; Hu, M.-M.; Luo, W.-W.; Li, S.; Luo, M.-H.; Wang, Y.-Y.; Shu, H.-B. Human Cytomegalovirus Tegument Protein UL82 Inhibits STING-Mediated Signaling to Evade Antiviral Immunity. *Cell Host Microbe* **2017**, *21* (2), 231–243. <https://doi.org/10.1016/j.chom.2017.01.001>.
- (25) Bechtel, J. T.; Shenk, T. Human Cytomegalovirus UL47 Tegument Protein Functions after Entry and before Immediate-Early Gene Expression. *J. Virol.* **2002**, *76* (3), 1043–1050. <https://doi.org/10.1128/JVI.76.3.1043-1050.2002>.
- (26) Beck, K.; Meyer-König, U.; Weidmann, M.; Nern, C.; Hufert, F. T. Human Cytomegalovirus Impairs Dendritic Cell Function: A Novel Mechanism of Human Cytomegalovirus Immune Escape. *Eur. J. Immunol.* **2003**, *33* (6), 1528–1538. <https://doi.org/10.1002/eji.200323612>.
- (27) Moorman, N. J.; Sharon-Friling, R.; Shenk, T.; Cristea, I. M. A Targeted Spatial-Temporal Proteomics Approach Implicates Multiple Cellular Trafficking Pathways in Human Cytomegalovirus Virion Maturation. *Mol. Cell. Proteomics* **2010**, *9* (5), 851–860. <https://doi.org/10.1074/mcp.M900485-MCP200>.
- (28) Crough, T.; Khanna, R. Immunobiology of Human Cytomegalovirus: From Bench to Bedside. *Clin. Microbiol. Rev.* **2009**, *22* (1), 76–98. <https://doi.org/10.1128/CMR.00034-08>.
- (29) Jean Beltran, P. M.; Cristea, I. M. The Life Cycle and Pathogenesis of Human Cytomegalovirus Infection: Lessons from Proteomics. *Expert Rev. Proteomics* **2014**, *11* (6), 697–711. <https://doi.org/10.1586/14789450.2014.971116>.

- (30) Gerna, G.; Kabanova, A.; Lilleri, D. Human Cytomegalovirus Cell Tropism and Host Cell Receptors. *Vaccines* **2019**, *7* (3), 70. <https://doi.org/10.3390/vaccines7030070>.
- (31) Kondo, K.; Xu, J.; Mocarski, E. S. Human Cytomegalovirus Latent Gene Expression in Granulocyte-Macrophage Progenitors in Culture and in Seropositive Individuals. *Proc. Natl. Acad. Sci.* **1996**, *93* (20), 11137–11142. <https://doi.org/10.1073/pnas.93.20.11137>.
- (32) Hahn, G.; Jores, R.; Mocarski, E. S. Cytomegalovirus Remains Latent in a Common Precursor of Dendritic and Myeloid Cells. *Proc. Natl. Acad. Sci.* **1998**, *95* (7), 3937–3942. <https://doi.org/10.1073/pnas.95.7.3937>.
- (33) Goodrum, F. The Complex Biology of Human Cytomegalovirus Latency. In *Advances in Virus Research*; Elsevier, 2022; Vol. 112, pp 31–85. <https://doi.org/10.1016/bs.aivir.2022.01.001>.
- (34) Boshart, M.; Weber, F.; Jahn, G.; Dorschler, K.; Fleckenstein, B.; Schaffner, W. A Very Strong Enhancer Is Located Upstream of an Immediate Early Gene of Human Cytomegalovirus. *Cell* **1985**, *41* (2), 521–530. [https://doi.org/10.1016/S0092-8674\(85\)80025-8](https://doi.org/10.1016/S0092-8674(85)80025-8).
- (35) Stinski, M. F.; Isomura, H. Role of the Cytomegalovirus Major Immediate Early Enhancer in Acute Infection and Reactivation from Latency. *Med. Microbiol. Immunol. (Berl.)* **2008**, *197* (2), 223–231. <https://doi.org/10.1007/s00430-007-0069-7>.
- (36) Groves, I. J.; Reeves, M. B.; Sinclair, J. H. Lytic Infection of Permissive Cells with Human Cytomegalovirus Is Regulated by an Intrinsic ‘Pre-Immediate-Early’ Repression of Viral Gene Expression Mediated by Histone Post-Translational Modification. *J. Gen. Virol.* **2009**, *90* (10), 2364–2374. <https://doi.org/10.1099/vir.0.012526-0>.
- (37) Jenkins, C.; Abendroth, A.; Slobedman, B. A Novel Viral Transcript with Homology to Human Interleukin-10 Is Expressed during Latent Human Cytomegalovirus Infection. *J. Virol.* **2004**, *78* (3), 1440–1447. <https://doi.org/10.1128/JVI.78.3.1440-1447.2004>.
- (38) Bego, M.; Maciejewski, J.; Khaiboullina, S.; Pari, G.; St. Jeor, S. Characterization of an Antisense Transcript Spanning the UL81–82 Locus of Human Cytomegalovirus. *J. Virol.* **2005**, *79* (17), 11022–11034. <https://doi.org/10.1128/JVI.79.17.11022-11034.2005>.
- (39) Poole, E.; Walther, A.; Raven, K.; Benedict, C. A.; Mason, G. M.; Sinclair, J. The Myeloid Transcription Factor GATA-2 Regulates the Viral UL144 Gene during Human Cytomegalovirus Latency in an Isolate-Specific Manner. *J. Virol.* **2013**, *87* (8), 4261–4271. <https://doi.org/10.1128/JVI.03497-12>.
- (40) Rossetto, C. C.; Tarrant-Elorza, M.; Pari, G. S. Cis and Trans Acting Factors Involved in Human Cytomegalovirus Experimental and Natural Latent Infection of CD14 (+) Monocytes and CD34 (+) Cells. *PLoS Pathog.* **2013**, *9* (5), e1003366. <https://doi.org/10.1371/journal.ppat.1003366>.
- (41) Humby, M. S.; O’Connor, C. M. Human Cytomegalovirus US28 Is Important for Latent Infection of Hematopoietic Progenitor Cells. *J. Virol.* **2016**, *90* (6), 2959–2970. <https://doi.org/10.1128/JVI.02507-15>.
- (42) Krishna, B. A.; Poole, E. L.; Jackson, S. E.; Smit, M. J.; Wills, M. R.; Sinclair, J. H. Latency-Associated Expression of Human Cytomegalovirus US28 Attenuates Cell Signaling Pathways To Maintain Latent Infection. *mBio* **2017**, *8* (6), e01754-17. <https://doi.org/10.1128/mBio.01754-17>.
- (43) Reeves, M. B.; MacAry, P. A.; Lehner, P. J.; Sissons, J. G. P.; Sinclair, J. H. Latency, Chromatin Remodeling, and Reactivation of Human Cytomegalovirus in the Dendritic Cells of Healthy Carriers. *Proc. Natl. Acad. Sci.* **2005**, *102* (11), 4140–4145. <https://doi.org/10.1073/pnas.0408994102>.
- (44) Reeves, M. B.; Lehner, P. J.; Sissons, J. G. P.; Sinclair, J. H. An in Vitro Model for the Regulation of Human Cytomegalovirus Latency and Reactivation in Dendritic Cells by Chromatin Remodelling. *J. Gen. Virol.* **2005**, *86* (11), 2949–2954. <https://doi.org/10.1099/vir.0.81161-0>.
- (45) Kew, V. G.; Yuan, J.; Meier, J.; Reeves, M. B. Mitogen and Stress Activated Kinases Act Co-Operatively with CREB during the Induction of Human Cytomegalovirus Immediate-Early Gene Expression from Latency. *PLoS Pathog.* **2014**, *10* (6), e1004195. <https://doi.org/10.1371/journal.ppat.1004195>.

- (46) Griffiths, P.; Reeves, M. Pathogenesis of Human Cytomegalovirus in the Immunocompromised Host. *Nat. Rev. Microbiol.* **2021**, *19* (12), 759–773. <https://doi.org/10.1038/s41579-021-00582-z>.
- (47) Adland, E.; Klenerman, P.; Goulder, P.; Matthews, P. C. Ongoing Burden of Disease and Mortality from HIV/CMV Coinfection in Africa in the Antiretroviral Therapy Era. *Front. Microbiol.* **2015**, *6*. <https://doi.org/10.3389/fmicb.2015.01016>.
- (48) Goodrum, F. Human Cytomegalovirus Latency: Approaching the Gordian Knot. *Annu. Rev. Virol.* **2016**, *3* (1), 333–357. <https://doi.org/10.1146/annurev-virology-110615-042422>.
- (49) Cope, A. V.; Sabin, C.; Burroughs, A.; Rolles, K.; Griffiths, P. D.; Emery, V. C. Interrelationships among Quantity of Human Cytomegalovirus (HCMV) DNA in Blood, Donor-Recipient Serostatus, and Administration of Methylprednisolone as Risk Factors for HCMV Disease Following Liver Transplantation. *J. Infect. Dis.* **1997**, *176* (6), 1484–1490. <https://doi.org/10.1086/514145>.
- (50) Fishman, J. A.; Emery, V.; Freeman, R.; Pascual, M.; Rostaing, L.; Schlitt, H. J.; Sgarabotto, D.; Torre-Cisneros, J.; Uknis, M. E. Cytomegalovirus in Transplantation – Challenging the *Status Quo*. *Clin. Transplant.* **2007**, *21* (2), 149–158. <https://doi.org/10.1111/j.1399-0012.2006.00618.x>.
- (51) Humar, A.; Kumar, D.; Boivin, G.; Caliendo, A. M. Cytomegalovirus (CMV) Virus Load Kinetics to Predict Recurrent Disease in Solid-Organ Transplant Patients with CMV Disease. *J. Infect. Dis.* **2002**, *186* (6), 829–833. <https://doi.org/10.1086/342601>.
- (52) Griffiths, P.; Baraniak, I.; Reeves, M. The Pathogenesis of Human Cytomegalovirus. *J. Pathol.* **2015**, *235* (2), 288–297. <https://doi.org/10.1002/path.4437>.
- (53) Rawlinson, W. D.; Boppana, S. B.; Fowler, K. B.; Kimberlin, D. W.; Lazzarotto, T.; Alain, S.; Daly, K.; Doutré, S.; Gibson, L.; Giles, M. L.; Greenlee, J.; Hamilton, S. T.; Harrison, G. J.; Hui, L.; Jones, C. A.; Palasanthiran, P.; Schleiss, M. R.; Shand, A. W.; Van Zuylen, W. J. Congenital Cytomegalovirus Infection in Pregnancy and the Neonate: Consensus Recommendations for Prevention, Diagnosis, and Therapy. *Lancet Infect. Dis.* **2017**, *17* (6), e177–e188. [https://doi.org/10.1016/S1473-3099\(17\)30143-3](https://doi.org/10.1016/S1473-3099(17)30143-3).
- (54) Manicklal, S.; Emery, V. C.; Lazzarotto, T.; Boppana, S. B.; Gupta, R. K. The “Silent” Global Burden of Congenital Cytomegalovirus. *Clin. Microbiol. Rev.* **2013**, *26* (1), 86–102. <https://doi.org/10.1128/CMR.00062-12>.
- (55) Carlson, A.; Norwitz, E. R.; Stiller, R. J. Cytomegalovirus Infection in Pregnancy: Should All Women Be Screened? *Rev. Obstet. Gynecol.* **2010**, *3* (4), 172–179.
- (56) Hodowanec, A. C.; Pikiš, A.; Komatsu, T. E.; Sampson, M. R.; Younis, I. R.; O’Rear, J. J.; Singer, M. E. Treatment and Prevention of CMV Disease in Transplant Recipients: Current Knowledge and Future Perspectives. *J. Clin. Pharmacol.* **2019**, *59* (6), 784–798. <https://doi.org/10.1002/jcph.1363>.
- (57) Scarpini, S.; Morigi, F.; Betti, L.; Dondi, A.; Biagi, C.; Lanari, M. Development of a Vaccine against Human Cytomegalovirus: Advances, Barriers, and Implications for the Clinical Practice. *Vaccines* **2021**, *9* (6), 551. <https://doi.org/10.3390/vaccines9060551>.
- (58) Hage, E.; Wilkie, G. S.; Linnenweber-Held, S.; Dhingra, A.; Suárez, N. M.; Schmidt, J. J.; Kay-Fedorov, P. C.; Mischak-Weissinger, E.; Heim, A.; Schwarz, A.; Schulz, T. F.; Davison, A. J.; Ganzenmueller, T. Characterization of Human Cytomegalovirus Genome Diversity in Immunocompromised Hosts by Whole-Genome Sequencing Directly From Clinical Specimens. *J. Infect. Dis.* **2017**, *215* (11), 1673–1683. <https://doi.org/10.1093/infdis/jix157>.
- (59) Renzette, N.; Pokalyuk, C.; Gibson, L.; Bhattacharjee, B.; Schleiss, M. R.; Hamprecht, K.; Yamamoto, A. Y.; Mussi-Pinhata, M. M.; Britt, W. J.; Jensen, J. D.; Kowalik, T. F. Limits and Patterns of Cytomegalovirus Genomic Diversity in Humans. *Proc. Natl. Acad. Sci.* **2015**, *112* (30). <https://doi.org/10.1073/pnas.1501880112>.
- (60) Arcangeletti, M.-C.; Vasile Simone, R.; Rodighiero, I.; De Conto, F.; Medici, M.-C.; Martorana, D.; Chezzi, C.; Calderaro, A. Combined Genetic Variants of Human Cytomegalovirus Envelope Glycoproteins as Congenital Infection Markers. *Viol. J.* **2015**, *12* (1), 202. <https://doi.org/10.1186/s12985-015-0428-8>.

- (61) Wang, H.-Y.; Valencia, S. M.; Pfeifer, S. P.; Jensen, J. D.; Kowalik, T. F.; Permar, S. R. Common Polymorphisms in the Glycoproteins of Human Cytomegalovirus and Associated Strain-Specific Immunity. *Viruses* **2021**, *13* (6), 1106. <https://doi.org/10.3390/v13061106>.
- (62) Chee, M. S.; Bankier, A. T.; Beck, S.; Bohni, R.; Brown, C. M.; Cerny, R.; Horsnell, T.; Hutchison, C. A.; Kouzarides, T.; Martignetti, J. A.; Preddie, E.; Satchwell, S. C.; Tomlinson, P.; Weston, K. M.; Barrell, B. G. Analysis of the Protein-Coding Content of the Sequence of Human Cytomegalovirus Strain AD169. In *Cytomegaloviruses*; McDougall, J. K., Ed.; Compans, R. W., Cooper, M., Koprowski, H., McConnell, I., Melchers, F., Nussenzweig, V., Oldstone, M., Olsnes, S., Saedler, H., Vogt, P. K., Wagner, H., Wilson, I., Series Eds.; Current Topics in Microbiology and Immunology; Springer Berlin Heidelberg: Berlin, Heidelberg, 1990; Vol. 154, pp 125–169. [https://doi.org/10.1007/978-3-642-74980-3\\_6](https://doi.org/10.1007/978-3-642-74980-3_6).
- (63) Borst, E.-M.; Hahn, G.; Koszinowski, U. H.; Messerle, M. Cloning of the Human Cytomegalovirus (HCMV) Genome as an Infectious Bacterial Artificial Chromosome in *Escherichia Coli*: A New Approach for Construction of HCMV Mutants. *J. Virol.* **1999**, *73* (10), 8320–8329. <https://doi.org/10.1128/JVI.73.10.8320-8329.1999>.
- (64) Yu, D.; Smith, G. A.; Enquist, L. W.; Shenk, T. Construction of a Self-Excisable Bacterial Artificial Chromosome Containing the Human Cytomegalovirus Genome and Mutagenesis of the Diploid TRL/IRL13 Gene. *J. Virol.* **2002**, *76* (5), 2316–2328. <https://doi.org/10.1128/jvi.76.5.2316-2328.2002>.
- (65) Akter, P.; Cunningham, C.; McSharry, B. P.; Dolan, A.; Addison, C.; Dargan, D. J.; Hassan-Walker, A. F.; Emery, V. C.; Griffiths, P. D.; Wilkinson, G. W. G.; Davison, A. J. Two Novel Spliced Genes in Human Cytomegalovirus. *J. Gen. Virol.* **2003**, *84* (5), 1117–1122. <https://doi.org/10.1099/vir.0.18952-0>.
- (66) Stanton, R. J.; Baluchova, K.; Dargan, D. J.; Cunningham, C.; Sheehy, O.; Seirafian, S.; McSharry, B. P.; Neale, M. L.; Davies, J. A.; Tomasec, P.; Davison, A. J.; Wilkinson, G. W. G. Reconstruction of the Complete Human Cytomegalovirus Genome in a BAC Reveals RL13 to Be a Potent Inhibitor of Replication. *J. Clin. Invest.* **2010**, *120* (9), 3191–3208. <https://doi.org/10.1172/JCI42955>.
- (67) Waldman, W. J.; Roberts, W. H.; Davis, D. H.; Williams, M. V.; Sedmak, D. D.; Stephens, R. E. Preservation of Natural Endothelial Cytopathogenicity of Cytomegalovirus by Propagation in Endothelial Cells. *Arch. Virol.* **1991**, *117* (3–4), 143–164. <https://doi.org/10.1007/BF01310761>.
- (68) Grazia Revello, M.; Baldanti, F.; Percivalle, E.; Sarasini, A.; De-Giuli, L.; Genini, E.; Lilleri, D.; Labò, N.; Gerna, G. In Vitro Selection of Human Cytomegalovirus Variants Unable to Transfer Virus and Virus Products from Infected Cells to Polymorphonuclear Leukocytes and to Grow in Endothelial Cells. *J. Gen. Virol.* **2001**, *82* (6), 1429–1438. <https://doi.org/10.1099/0022-1317-82-6-1429>.
- (69) Hahn, G.; Khan, H.; Baldanti, F.; Koszinowski, U. H.; Revello, M. G.; Gerna, G. The Human Cytomegalovirus Ribonucleotide Reductase Homolog UL45 Is Dispensable for Growth in Endothelial Cells, as Determined by a BAC-Cloned Clinical Isolate of Human Cytomegalovirus with Preserved Wild-Type Characteristics. *J. Virol.* **2002**, *76* (18), 9551–9555. <https://doi.org/10.1128/jvi.76.18.9551-9555.2002>.
- (70) Dargan, D. J.; Douglas, E.; Cunningham, C.; Jamieson, F.; Stanton, R. J.; Baluchova, K.; McSharry, B. P.; Tomasec, P.; Emery, V. C.; Percivalle, E.; Sarasini, A.; Gerna, G.; Wilkinson, G. W. G.; Davison, A. J. Sequential Mutations Associated with Adaptation of Human Cytomegalovirus to Growth in Cell Culture. *J. Gen. Virol.* **2010**, *91* (6), 1535–1546. <https://doi.org/10.1099/vir.0.018994-0>.
- (71) Goodrum, F.; Reeves, M.; Sinclair, J.; High, K.; Shenk, T. Human Cytomegalovirus Sequences Expressed in Latently Infected Individuals Promote a Latent Infection in Vitro. *Blood* **2007**, *110* (3), 937–945. <https://doi.org/10.1182/blood-2007-01-070078>.
- (72) Tomasec, P.; Wang, E. C. Y.; Davison, A. J.; Vojtesek, B.; Armstrong, M.; Griffin, C.; McSharry, B. P.; Morris, R. J.; Llewellyn-Lacey, S.; Rickards, C.; Nomoto, A.; Sinzger, C.; Wilkinson, G. W. G. Downregulation of Natural Killer Cell-Activating Ligand CD155

- by Human Cytomegalovirus UL141. *Nat. Immunol.* **2005**, *6* (2), 181–188. <https://doi.org/10.1038/ni1156>.
- (73) Prod'homme, V.; Sugrue, D. M.; Stanton, R. J.; Nomoto, A.; Davies, J.; Rickards, C. R.; Cochrane, D.; Moore, M.; Wilkinson, G. W. G.; Tomasec, P. Human Cytomegalovirus UL141 Promotes Efficient Downregulation of the Natural Killer Cell Activating Ligand CD112. *J. Gen. Virol.* **2010**, *91* (8), 2034–2039. <https://doi.org/10.1099/vir.0.021931-0>.
- (74) Ashiru, O.; Bennett, N. J.; Boyle, L. H.; Thomas, M.; Trowsdale, J.; Wills, M. R. NKG2D Ligand MICA Is Retained in the *Cis* -Golgi Apparatus by Human Cytomegalovirus Protein UL142. *J. Virol.* **2009**, *83* (23), 12345–12354. <https://doi.org/10.1128/JVI.01175-09>.
- (75) Bughio, F.; Umashankar, M.; Wilson, J.; Goodrum, F. Human Cytomegalovirus *UL135* and *UL136* Genes Are Required for Postentry Tropism in Endothelial Cells. *J. Virol.* **2015**, *89* (13), 6536–6550. <https://doi.org/10.1128/JVI.00284-15>.
- (76) Sinzger, C.; Grefte, A.; Plachter, B.; Gouw, A. S. H.; The, T. H.; Jahn, G. Fibroblasts, Epithelial Cells, Endothelial Cells and Smooth Muscle Cells Are Major Targets of Human Cytomegalovirus Infection in Lung and Gastrointestinal Tissues. *J. Gen. Virol.* **1995**, *76* (4), 741–750. <https://doi.org/10.1099/0022-1317-76-4-741>.
- (77) Sinzger, C.; Jahn, G. Human Cytomegalovirus Cell Tropism and Pathogenesis. *Intervirology* **1996**, *39* (5–6), 302–319. <https://doi.org/10.1159/000150502>.
- (78) Sinzger, C.; Knapp, J.; Plachter, B.; Schmidt, K.; Jahn, G. Quantification of Replication of Clinical Cytomegalovirus Isolates in Cultured Endothelial Cells and Fibroblasts by a Focus Expansion Assay. *J. Virol. Methods* **1997**, *63* (1–2), 103–112. [https://doi.org/10.1016/S0166-0934\(97\)02082-X](https://doi.org/10.1016/S0166-0934(97)02082-X).
- (79) Grundy, J. E.; Lawson, K. M.; MacCormac, L. P.; Fletcher, J. M.; Yong, K. L. Cytomegalovirus-Infected Endothelial Cells Recruit Neutrophils by the Secretion of C-X-C Chemokines and Transmit Virus by Direct Neutrophil-Endothelial Cell Contact and during Neutrophil Transendothelial Migration. *J. Infect. Dis.* **1998**, *177* (6), 1465–1474. <https://doi.org/10.1086/515300>.
- (80) Waldman, W. J.; Knight, D. A.; Huang, E. H.; Sedmak, D. D. Bidirectional Transmission of Infectious Cytomegalovirus between Monocytes and Vascular Endothelial Cells: An In Vitro Model. *J. Infect. Dis.* **1995**, *171* (2), 263–272. <https://doi.org/10.1093/infdis/171.2.263>.
- (81) Bentz, G. L.; Jarquin-Pardo, M.; Chan, G.; Smith, M. S.; Sinzger, C.; Yurochko, A. D. Human Cytomegalovirus (HCMV) Infection of Endothelial Cells Promotes Naïve Monocyte Extravasation and Transfer of Productive Virus To Enhance Hematogenous Dissemination of HCMV. *J. Virol.* **2006**, *80* (23), 11539–11555. <https://doi.org/10.1128/JVI.01016-06>.
- (82) Gerna, G.; Baldanti, F.; Revello, M. G. Pathogenesis of Human Cytomegalovirus Infection and Cellular Targets. *Hum. Immunol.* **2004**, *65* (5), 381–386. <https://doi.org/10.1016/j.humimm.2004.02.009>.
- (83) Smith, M. S.; Bentz, G. L.; Alexander, J. S.; Yurochko, A. D. Human Cytomegalovirus Induces Monocyte Differentiation and Migration as a Strategy for Dissemination and Persistence. *J. Virol.* **2004**, *78* (9), 4444–4453. <https://doi.org/10.1128/JVI.78.9.4444-4453.2004>.
- (84) Smith, N. A.; Chan, G. C.; O'Connor, C. M. Modulation of Host Cell Signaling during Cytomegalovirus Latency and Reactivation. *Viol. J.* **2021**, *18* (1), 207. <https://doi.org/10.1186/s12985-021-01674-1>.
- (85) Kurn, H.; Daly, D. T. Histology, Epithelial Cell. In *StatPearls*; StatPearls Publishing: Treasure Island (FL), 2024.
- (86) Heieren, M. H.; Kim, Y.; Balfour, H. H. HUMAN CYTOMEGALOVIRUS INFECTION OF KIDNEY GLOMERULAR VISCERAL EPITHELIAL AND TUBULAR EPITHELIAL CELLS IN CULTURE: *Transplantation* **1988**, *46* (3), 426–432. <https://doi.org/10.1097/00007890-198809000-00019>.

- (87) Bissinger, A. L.; Sinzger, C.; Kaiserling, E.; Jahn, G. Human Cytomegalovirus as a Direct Pathogen: Correlation of Multiorgan Involvement and Cell Distribution with Clinical and Pathological Findings in a Case of Congenital Inclusion Disease. *J. Med. Virol.* **2002**, *67* (2), 200–206. <https://doi.org/10.1002/jmv.2208>.
- (88) Wang, D.; Shenk, T. Human Cytomegalovirus UL131 Open Reading Frame Is Required for Epithelial Cell Tropism. *J. Virol.* **2005**, *79* (16), 10330–10338. <https://doi.org/10.1128/JVI.79.16.10330-10338.2005>.
- (89) Michiels, C. Endothelial Cell Functions. *J. Cell. Physiol.* **2003**, *196* (3), 430–443. <https://doi.org/10.1002/jcp.10333>.
- (90) Myerson, D.; Hackman, R. C.; Nelson, J. A.; Ward, D. C.; McDougall, J. K. Widespread Presence of Histologically Occult Cytomegalovirus. *Hum. Pathol.* **1984**, *15* (5), 430–439. [https://doi.org/10.1016/S0046-8177\(84\)80076-3](https://doi.org/10.1016/S0046-8177(84)80076-3).
- (91) Percivalle, E.; Revello, M. G.; Vago, L.; Morini, F.; Gerna, G. Circulating Endothelial Giant Cells Permissive for Human Cytomegalovirus (HCMV) Are Detected in Disseminated HCMV Infections with Organ Involvement. *J. Clin. Invest.* **1993**, *92* (2), 663–670. <https://doi.org/10.1172/JCI116635>.
- (92) Gerna, G.; Percivalle, E.; Baldanti, F.; Sozzani, S.; Lanzarini, P.; Genini, E.; Lilleri, D.; Revello, M. G. Human Cytomegalovirus Replicates Abortively in Polymorphonuclear Leukocytes after Transfer from Infected Endothelial Cells via Transient Microfusion Events. *J. Virol.* **2000**, *74* (12), 5629–5638. <https://doi.org/10.1128/JVI.74.12.5629-5638.2000>.
- (93) Bentz, G. L.; Yurochko, A. D. Human CMV Infection of Endothelial Cells Induces an Angiogenic Response through Viral Binding to EGF Receptor and  $\beta_1$  and  $\beta_3$  Integrins. *Proc. Natl. Acad. Sci.* **2008**, *105* (14), 5531–5536. <https://doi.org/10.1073/pnas.0800037105>.
- (94) Hahn, G.; Revello, M. G.; Patrone, M.; Percivalle, E.; Campanini, G.; Sarasini, A.; Wagner, M.; Gallina, A.; Milanesi, G.; Koszinowski, U.; Baldanti, F.; Gerna, G. Human Cytomegalovirus UL131-128 Genes Are Indispensable for Virus Growth in Endothelial Cells and Virus Transfer to Leukocytes. *J. Virol.* **2004**, *78* (18), 10023–10033. <https://doi.org/10.1128/JVI.78.18.10023-10033.2004>.
- (95) Ziessman, H. A.; O'Malley, J. P.; Thrall, J. H. Infection and Inflammation. In *Nuclear Medicine*; Elsevier, 2006; pp 384–418. <https://doi.org/10.1016/B978-0-323-02946-9.50017-9>.
- (96) Britt, W. Virus Entry into Host, Establishment of Infection, Spread in Host, Mechanisms of Tissue Damage. In *Human Herpesviruses: Biology, Therapy, and Immunoprophylaxis*; Arvin, A., Campadelli-Fiume, G., Mocarski, E., Moore, P. S., Roizman, B., Whitley, R., Yamanishi, K., Eds.; Cambridge University Press: Cambridge, 2007.
- (97) Maidji, E.; Percivalle, E.; Gerna, G.; Fisher, S.; Pereira, L. Transmission of Human Cytomegalovirus from Infected Uterine Microvascular Endothelial Cells to Differentiating/Invasive Placental Cytotrophoblasts. *Virology* **2002**, *304* (1), 53–69. <https://doi.org/10.1006/viro.2002.1661>.
- (98) Comerford, I.; McColl, S. R. Mini-review Series: Focus on Chemokines. *Immunol. Cell Biol.* **2011**, *89* (2), 183–184. <https://doi.org/10.1038/icb.2010.164>.
- (99) Lurain, N. S.; Fox, A. M.; Lichy, H. M.; Bhorade, S. M.; Ware, C. F.; Huang, D. D.; Kwan, S.-P.; Garrity, E. R.; Chou, S. Analysis of the Human Cytomegalovirus Genomic Region from UL146 through UL147A Reveals Sequence Hypervariability, Genotypic Stability, and Overlapping Transcripts. *Virol. J.* **2006**, *3* (1), 4. <https://doi.org/10.1186/1743-422X-3-4>.
- (100) Heo, J.; Dogra, P.; Masi, T. J.; Pitt, E. A.; De Kruijf, P.; Smit, M. J.; Sparer, T. E. Novel Human Cytomegalovirus Viral Chemokines, vCXCL-1s, Display Functional Selectivity for Neutrophil Signaling and Function. *J. Immunol.* **2015**, *195* (1), 227–236. <https://doi.org/10.4049/jimmunol.1400291>.

- (101) Hassan-Walker, A. F.; Okwuadi, S.; Lee, L.; Griffiths, P. D.; Emery, V. C. Sequence Variability of the A-chemokine UL146 from Clinical Strains of Human Cytomegalovirus. *J. Med. Virol.* **2004**, *74* (4), 573–579. <https://doi.org/10.1002/jmv.20210>.
- (102) Burn, G. L.; Foti, A.; Marsman, G.; Patel, D. F.; Zychlinsky, A. The Neutrophil. *Immunity* **2021**, *54* (7), 1377–1391. <https://doi.org/10.1016/j.immuni.2021.06.006>.
- (103) Gerna, G.; Zipeto, D.; Percivalle, E.; Parea, M.; Revello, M. G.; Maccario, R.; Peri, G.; Milanesi, G. Human Cytomegalovirus Infection of the Major Leukocyte Subpopulations and Evidence for Initial Viral Replication in Polymorphonuclear Leukocytes from Viremic Patients. *J. Infect. Dis.* **1992**, *166* (6), 1236–1244. <https://doi.org/10.1093/infdis/166.6.1236>.
- (104) Saltzman, R. L.; Quirk, M. R.; Jordan, M. C. Disseminated Cytomegalovirus Infection. Molecular Analysis of Virus and Leukocyte Interactions in Viremia. *J. Clin. Invest.* **1988**, *81* (1), 75–81. <https://doi.org/10.1172/JCI113313>.
- (105) Turtinen, L. W.; Saltzman, R.; Jordan, M. C.; Haase, A. T. Interactions of Human Cytomegalovirus with Leukocytes in Vivo: Analysis by in Situ Hybridization. *Microb. Pathog.* **1987**, *3* (4), 287–297. [https://doi.org/10.1016/0882-4010\(87\)90062-3](https://doi.org/10.1016/0882-4010(87)90062-3).
- (106) Gerna, G.; Zipeto, D.; Parea, M.; Percivalle, E.; Zavattoni, M.; Gaballo, A.; Milanesi, G. Early Virus Isolation, Early Structural Antigen Detection and DNA Amplification by the Polymerase Chain Reaction in Polymorphonuclear Leukocytes from AIDS Patients with Human Cytomegalovirus Viraemia. *Mol. Cell. Probes* **1991**, *5* (5), 365–374. [https://doi.org/10.1016/S0890-8508\(06\)80008-3](https://doi.org/10.1016/S0890-8508(06)80008-3).
- (107) Pocock, J. M.; Storisteanu, D. M. L.; Reeves, M. B.; Juss, J. K.; Wills, M. R.; Cowburn, A. S.; Chilvers, E. R. Human Cytomegalovirus Delays Neutrophil Apoptosis and Stimulates the Release of a Prosurvival Secretome. *Front. Immunol.* **2017**, *8* (SEP). <https://doi.org/10.3389/fimmu.2017.01185>.
- (108) Parihar, A.; Eubank, T. D.; Doseff, A. I. Monocytes and Macrophages Regulate Immunity through Dynamic Networks of Survival and Cell Death. *J. Innate Immun.* **2010**, *2* (3), 204–215. <https://doi.org/10.1159/000296507>.
- (109) Wang, S.; Liu, R.; Yu, Q.; Dong, L.; Bi, Y.; Liu, G. Metabolic Reprogramming of Macrophages during Infections and Cancer. *Cancer Lett.* **2019**, *452*, 14–22. <https://doi.org/10.1016/j.canlet.2019.03.015>.
- (110) Laura C Miller, Y. S. Macrophage Polarization in Virus-Host Interactions. *J. Clin. Cell. Immunol.* **2015**, *06* (02). <https://doi.org/10.4172/2155-9899.1000311>.
- (111) Nogalski, M. T.; Chan, G.; Stevenson, E. V.; Gray, S.; Yurochko, A. D. Human Cytomegalovirus-Regulated Paxillin in Monocytes Links Cellular Pathogenic Motility to the Process of Viral Entry. *J. Virol.* **2011**, *85* (3), 1360–1369. <https://doi.org/10.1128/JVI.02090-10>.
- (112) Kim, J. H.; Collins-McMillen, D.; Caposio, P.; Yurochko, A. D. Viral Binding-Induced Signaling Drives a Unique and Extended Intracellular Trafficking Pattern during Infection of Primary Monocytes. *Proc. Natl. Acad. Sci.* **2016**, *113* (31), 8819–8824. <https://doi.org/10.1073/pnas.1604317113>.
- (113) Kim, J. H.; Collins-McMillen, D.; Buehler, J. C.; Goodrum, F. D.; Yurochko, A. D. Human Cytomegalovirus Requires Epidermal Growth Factor Receptor Signaling To Enter and Initiate the Early Steps in the Establishment of Latency in CD34<sup>+</sup> Human Progenitor Cells. *J. Virol.* **2017**, *91* (5), e01206-16. <https://doi.org/10.1128/JVI.01206-16>.
- (114) Stevenson, E.; Collins-McMillen, D.; Kim, J.; Cieply, S.; Bentz, G.; Yurochko, A. HCMV Reprogramming of Infected Monocyte Survival and Differentiation: A Goldilocks Phenomenon. *Viruses* **2014**, *6* (2), 782–807. <https://doi.org/10.3390/v6020782>.
- (115) Compton, T.; Nowlin, D. M.; Cooper, N. R. Initiation of Human Cytomegalovirus Infection Requires Initial Interaction with Cell Surface Heparan Sulfate. *Virology* **1993**, *193* (2), 834–841. <https://doi.org/10.1006/viro.1993.1192>.
- (116) Connolly, S. A.; Jardetzky, T. S.; Longnecker, R. The Structural Basis of Herpesvirus Entry. *Nat. Rev. Microbiol.* **2021**, *19* (2), 110–121. <https://doi.org/10.1038/s41579-020-00448-w>.



- (117) Lee, B.-J.; Min, C.-K.; Hancock, M.; Streblow, D. N.; Caposio, P.; Goodrum, F. D.; Yurochko, A. D. Human Cytomegalovirus Host Interactions: EGFR and Host Cell Signaling Is a Point of Convergence Between Viral Infection and Functional Changes in Infected Cells. *Front. Microbiol.* **2021**, *12*, 660901. <https://doi.org/10.3389/fmicb.2021.660901>.
- (118) Kabanova, A.; Marcandalli, J.; Zhou, T.; Bianchi, S.; Baxa, U.; Tsybovsky, Y.; Lilleri, D.; Silacci-Fregni, C.; Foglierini, M.; Fernandez-Rodriguez, B. M.; Druz, A.; Zhang, B.; Geiger, R.; Pagani, M.; Sallusto, F.; Kwong, P. D.; Corti, D.; Lanzavecchia, A.; Perez, L. Platelet-Derived Growth Factor- $\alpha$  Receptor Is the Cellular Receptor for Human Cytomegalovirus gHgLgO Trimer. *Nat. Microbiol.* **2016**, *1* (8), 16082. <https://doi.org/10.1038/nmicrobiol.2016.82>.
- (119) Compton, T. Receptors and Immune Sensors: The Complex Entry Path of Human Cytomegalovirus. *Trends Cell Biol.* **2004**, *14* (1), 5–8. <https://doi.org/10.1016/j.tcb.2003.10.009>.
- (120) E, X.; Meraner, P.; Lu, P.; Ferreira, J. M.; Aker, A. M.; McDougall, W. M.; Zhuge, R.; Chan, G. C.; Gerstein, R. M.; Caposio, P.; Yurochko, A. D.; Brass, A. L.; Kowalik, T. F. OR1411 Is a Receptor for the Human Cytomegalovirus Pentameric Complex and Defines Viral Epithelial Cell Tropism. *Proc. Natl. Acad. Sci.* **2019**, *116* (14), 7043–7052. <https://doi.org/10.1073/pnas.1814850116>.
- (121) Vanarsdall, A. L.; Chin, A. L.; Liu, J.; Jardetzky, T. S.; Mudd, J. O.; Orloff, S. L.; Streblow, D.; Mussi-Pinhata, M. M.; Yamamoto, A. Y.; Duarte, G.; Britt, W. J.; Johnson, D. C. HCMV Trimer- and Pentamer-Specific Antibodies Synergize for Virus Neutralization but Do Not Correlate with Congenital Transmission. *Proc. Natl. Acad. Sci.* **2019**, *116* (9), 3728–3733. <https://doi.org/10.1073/pnas.1814835116>.
- (122) Haspot, F.; Lavault, A.; Sinzger, C.; Laib Sampaio, K.; Stierhof, Y.-D.; Pilet, P.; Bressolette-Bodin, C.; Halary, F. Human Cytomegalovirus Entry into Dendritic Cells Occurs via a Macropinocytosis-Like Pathway in a pH-Independent and Cholesterol-Dependent Manner. *PLoS ONE* **2012**, *7* (4), e34795. <https://doi.org/10.1371/journal.pone.0034795>.
- (123) Ryckman, B. J.; Jarvis, M. A.; Drummond, D. D.; Nelson, J. A.; Johnson, D. C. Human Cytomegalovirus Entry into Epithelial and Endothelial Cells Depends on Genes UL128 to UL150 and Occurs by Endocytosis and Low-pH Fusion. *J. Virol.* **2006**, *80* (2), 710–722. <https://doi.org/10.1128/JVI.80.2.710-722.2006>.
- (124) Gerna, G.; Percivalle, E.; Perez, L.; Lanzavecchia, A.; Lilleri, D. Monoclonal Antibodies to Different Components of the Human Cytomegalovirus (HCMV) Pentamer gH/gL/pUL128L and Trimer gH/gL/gO as Well as Antibodies Elicited during Primary HCMV Infection Prevent Epithelial Cell Syncytium Formation. *J. Virol.* **2016**, *90* (14), 6216–6223. <https://doi.org/10.1128/JVI.00121-16>.
- (125) Foglierini, M.; Marcandalli, J.; Perez, L. HCMV Envelope Glycoprotein Diversity Demystified. *Front. Microbiol.* **2019**, *10*, 1005. <https://doi.org/10.3389/fmicb.2019.01005>.
- (126) Pötzsch, S.; Spindler, N.; Wieggers, A.-K.; Fisch, T.; Rücker, P.; Sticht, H.; Grieb, N.; Baroti, T.; Weisel, F.; Stamminger, T.; Martin-Parras, L.; Mach, M.; Winkler, T. H. B Cell Repertoire Analysis Identifies New Antigenic Domains on Glycoprotein B of Human Cytomegalovirus Which Are Target of Neutralizing Antibodies. *PLoS Pathog.* **2011**, *7* (8), e1002172. <https://doi.org/10.1371/journal.ppat.1002172>.
- (127) Fornara, O.; Odeberg, J.; Khan, Z.; Stragliotto, G.; Peredo, I.; Butler, L.; Söderberg-Nauclér, C. Human Cytomegalovirus Particles Directly Suppress CD4 T-Lymphocyte Activation and Proliferation. *Immunobiology* **2013**, *218* (8), 1034–1040. <https://doi.org/10.1016/j.imbio.2013.01.002>.
- (128) Kschonsak, M.; Johnson, M. C.; Schelling, R.; Green, E. M.; Rougé, L.; Ho, H.; Patel, N.; Kilic, C.; Kraft, E.; Arthur, C. P.; Rohou, A. L.; Comps-Agrar, L.; Martinez-Martin, N.; Perez, L.; Payandeh, J.; Ciferri, C. Structural Basis for HCMV Pentamer Receptor Recognition and Antibody Neutralization. *Sci. Adv.* **2022**, *8* (10), eabm2536. <https://doi.org/10.1126/sciadv.abm2536>.

- (129) Parsons, A. J.; Ophir, S. I.; Duty, J. A.; Kraus, T. A.; Stein, K. R.; Moran, T. M.; Tortorella, D. Development of Broadly Neutralizing Antibodies Targeting the Cytomegalovirus Subdominant Antigen gH. *Commun. Biol.* **2022**, *5* (1), 387. <https://doi.org/10.1038/s42003-022-03294-z>.
- (130) Sun, G.; Chiappesi, F.; Chen, X.; Wang, C.; Tian, E.; Nguyen, J.; Kha, M.; Trinh, D.; Zhang, H.; Marchetto, M. C.; Song, H.; Ming, G.-L.; Gage, F. H.; Diamond, D. J.; Wussow, F.; Shi, Y. Modeling Human Cytomegalovirus-Induced Microcephaly in Human iPSC-Derived Brain Organoids. *Cell Rep. Med.* **2020**, *1* (1), 100002. <https://doi.org/10.1016/j.xcrm.2020.100002>.
- (131) Fornara, C.; Zavaglio, F.; Furione, M.; Sarasini, A.; d'Angelo, P.; Arossa, A.; Spinillo, A.; Lilleri, D.; Baldanti, F. Human Cytomegalovirus (HCMV) Long-Term Shedding and HCMV-Specific Immune Response in Pregnant Women with Primary HCMV Infection. *Med. Microbiol. Immunol. (Berl.)* **2022**, *211* (5–6), 249–260. <https://doi.org/10.1007/s00430-022-00747-4>.
- (132) Macagno, A.; Bernasconi, N. L.; Vanzetta, F.; Dander, E.; Sarasini, A.; Revello, M. G.; Gerna, G.; Sallusto, F.; Lanzavecchia, A. Isolation of Human Monoclonal Antibodies That Potently Neutralize Human Cytomegalovirus Infection by Targeting Different Epitopes on the gH/gL/UL128-131A Complex. *J. Virol.* **2010**, *84* (2), 1005–1013. <https://doi.org/10.1128/JVI.01809-09>.
- (133) Baldanti, F.; Paolucci, S.; Campanini, G.; Sarasini, A.; Percivalle, E.; Revello, M. G.; Gerna, G. Human Cytomegalovirus UL131A, UL130 and UL128 Genes Are Highly Conserved among Field Isolates. *Arch. Virol.* **2006**, *151* (6), 1225–1233. <https://doi.org/10.1007/s00705-005-0696-5>.
- (134) Patel, H. D.; Nikitin, P.; Gesner, T.; Lin, J. J.; Barkan, D. T.; Ciferri, C.; Carfi, A.; Akbarnejad Yazdi, T.; Skewes-Cox, P.; Wiedmann, B.; Jarousse, N.; Zhong, W.; Feire, A.; Hebner, C. M. *In Vitro* Characterization of Human Cytomegalovirus-Targeting Therapeutic Monoclonal Antibodies LJP538 and LJP539. *Antimicrob. Agents Chemother.* **2016**, *60* (8), 4961–4971. <https://doi.org/10.1128/AAC.00382-16>.
- (135) Dole, K.; Segal, F. P.; Feire, A.; Magnusson, B.; Rondon, J. C.; Vemula, J.; Yu, J.; Pang, Y.; Pertel, P. A First-in-Human Study To Assess the Safety and Pharmacokinetics of Monoclonal Antibodies against Human Cytomegalovirus in Healthy Volunteers. *Antimicrob. Agents Chemother.* **2016**, *60* (5), 2881–2887. <https://doi.org/10.1128/AAC.02698-15>.
- (136) Maertens, J.; Logan, A. C.; Jang, J.; Long, G.; Tang, J.-L.; Hwang, W. Y. K.; Koh, L. P.; Chemaly, R.; Gerbitz, A.; Winkler, J.; Yeh, S.-P.; Hiemenz, J.; Christoph, S.; Lee, D.-G.; Wang, P.-N.; Holler, E.; Mielke, S.; Akard, L.; Yeo, A.; Ramachandra, S.; Smith, K.; Pertel, P.; Segal, F. Phase 2 Study of Anti-Human Cytomegalovirus Monoclonal Antibodies for Prophylaxis in Hematopoietic Cell Transplantation. *Antimicrob. Agents Chemother.* **2020**, *64* (4), e02467-19. <https://doi.org/10.1128/AAC.02467-19>.
- (137) Hernández, J. M.; Podbilewicz, B. The Hallmarks of Cell-Cell Fusion. *Development* **2017**, *144* (24), 4481–4495. <https://doi.org/10.1242/dev.155523>.
- (138) Brukman, N. G.; Uygur, B.; Podbilewicz, B.; Chernomordik, L. V. How Cells Fuse. *J. Cell Biol.* **2019**, *218* (5), 1436–1451. <https://doi.org/10.1083/jcb.201901017>.
- (139) Stockton, J. L.; Torres, A. G. Multinucleated Giant Cell Formation as a Portal to Chronic Bacterial Infections. *Microorganisms* **2020**, *8* (11), 1637. <https://doi.org/10.3390/microorganisms8111637>.
- (140) Ku, J. W. K.; Chen, Y.; Lim, B. J. W.; Gasser, S.; Crasta, K. C.; Gan, Y.-H. Bacterial-Induced Cell Fusion Is a Danger Signal Triggering cGAS–STING Pathway via Micronuclei Formation. *Proc. Natl. Acad. Sci.* **2020**, *117* (27), 15923–15934. <https://doi.org/10.1073/pnas.2006908117>.
- (141) Leroy, H.; Han, M.; Woottum, M.; Bracq, L.; Bouchet, J.; Xie, M.; Benichou, S. Virus-Mediated Cell-Cell Fusion. *Int. J. Mol. Sci.* **2020**, *21* (24), 9644. <https://doi.org/10.3390/ijms21249644>.
- (142) Bracq, L.; Xie, M.; Benichou, S.; Bouchet, J. Mechanisms for Cell-to-Cell Transmission of HIV-1. *Front. Immunol.* **2018**, *9*, 260. <https://doi.org/10.3389/fimmu.2018.00260>.

- (143) Ciechonska, M.; Duncan, R. Reovirus FAST Proteins: Virus-Encoded Cellular Fusogens. *Trends Microbiol.* **2014**, *22* (12), 715–724. <https://doi.org/10.1016/j.tim.2014.08.005>.
- (144) Cifuentes-Muñoz, N.; Dutch, R. E.; Cattaneo, R. Direct Cell-to-Cell Transmission of Respiratory Viruses: The Fast Lanes. *PLOS Pathog.* **2018**, *14* (6), e1007015. <https://doi.org/10.1371/journal.ppat.1007015>.
- (145) Spijkerman, I.; De Wolf, F.; Langendam, M.; Schuitemaker, H.; Coutinho, R. Emergence of Syncytium-Inducing Human Immunodeficiency Virus Type 1 Variants Coincides with a Transient Increase in Viral RNA Level and Is an Independent Predictor for Progression to AIDS. *J. Infect. Dis.* **1998**, *178* (2), 397–403. <https://doi.org/10.1086/515627>.
- (146) Cole, N. L.; Grose, C. Membrane Fusion Mediated by Herpesvirus Glycoproteins: The Paradigm of Varicella-zoster Virus. *Rev. Med. Virol.* **2003**, *13* (4), 207–222. <https://doi.org/10.1002/rmv.377>.
- (147) Muggeridge, M. I.; Grantham, M. L.; Johnson, F. B. Identification of Syncytial Mutations in a Clinical Isolate of Herpes Simplex Virus 2. *Virology* **2004**, *328* (2), 244–253. <https://doi.org/10.1016/j.virol.2004.07.027>.
- (148) Gerna, G.; Sarasini, A.; Patrone, M.; Percivalle, E.; Fiorina, L.; Campanini, G.; Gallina, A.; Baldanti, F.; Revello, M. G. Human Cytomegalovirus Serum Neutralizing Antibodies Block Virus Infection of Endothelial/Epithelial Cells, but Not Fibroblasts, Early during Primary Infection. *J. Gen. Virol.* **2008**, *89* (4), 853–865. <https://doi.org/10.1099/vir.0.83523-0>.
- (149) Galitska, G.; Biolatti, M.; De Andrea, M.; Leone, A.; Coscia, A.; Bertolotti, L.; Ala, U.; Bertino, E.; Dell'Oste, V.; Landolfo, S. Biological Relevance of Cytomegalovirus Genetic Variability in Congenitally and Postnatally Infected Children. *J. Clin. Virol.* **2018**, *108*, 132–140. <https://doi.org/10.1016/j.jcv.2018.09.019>.
- (150) Vo, M.; Aguiar, A.; McVoy, M. A.; Hertel, L. Cytomegalovirus Strain TB40/E Restrictions and Adaptations to Growth in ARPE-19 Epithelial Cells. *Microorganisms* **2020**, *8* (4), 615. <https://doi.org/10.3390/microorganisms8040615>.
- (151) Paradowska, E.; Jabłońska, A.; Studzińska, M.; Kasztelewicz, B.; Wiśniewska-Ligier, M.; Dzierżanowska-Fangrat, K.; Woźniakowska-Gęsicka, T.; Czech-Kowalska, J. Distribution of the CMV Glycoprotein gH/gL/gO and gH/gL/pUL128/pUL130/pUL131A Complex Variants and Associated Clinical Manifestations in Infants Infected Congenitally or Postnatally. *Sci. Rep.* **2019**, *9* (1), 16352. <https://doi.org/10.1038/s41598-019-52906-y>.
- (152) Cifuentes-Munoz, N.; El Najjar, F.; Dutch, R. E. Viral Cell-to-Cell Spread: Conventional and Non-Conventional Ways. In *Advances in Virus Research*; Elsevier, 2020; Vol. 108, pp 85–125. <https://doi.org/10.1016/bs.aivir.2020.09.002>.
- (153) Tang, J.; Frascaroli, G.; Zhou, X.; Knickmann, J.; Brune, W. Cell Fusion and Syncytium Formation in Betaherpesvirus Infection. *Viruses* **2021**, *13* (10). <https://doi.org/10.3390/v13101973>.
- (154) Tang, J.; Frascaroli, G.; Lebbink, R. J.; Ostermann, E.; Brune, W. Human Cytomegalovirus Glycoprotein B Variants Affect Viral Entry, Cell Fusion, and Genome Stability. *Proc. Natl. Acad. Sci.* **2019**, *116* (36), 18021–18030. <https://doi.org/10.1073/pnas.1907447116>.
- (155) Zhou, X.; Cimato, G.; Zhou, Y.; Frascaroli, G.; Brune, W. A Virus Genetic System to Analyze the Fusogenicity of Human Cytomegalovirus Glycoprotein B Variants. *Viruses* **2023**, *15* (4), 979. <https://doi.org/10.3390/v15040979>.
- (156) Gerna, G.; Percivalle, E.; Perez, L.; Lanzavecchia, A.; Lilleri, D. Monoclonal Antibodies to Different Components of the Human Cytomegalovirus (HCMV) Pentamer gH/gL/pUL128L and Trimer gH/gL/gO as Well as Antibodies Elicited during Primary HCMV Infection Prevent Epithelial Cell Syncytium Formation. *J. Virol.* **2016**, *90* (14), 6216–6223. <https://doi.org/10.1128/jvi.00121-16>.
- (157) Stropes, M. P.; Schneider, O. D.; Zagorski, W. A.; Miller, J. L. C.; Miller, W. E. The Carboxy-Terminal Tail of Human Cytomegalovirus (HCMV) US28 Regulates Both

- Chemokine-Independent and Chemokine-Dependent Signaling in HCMV-Infected Cells. *J. Virol.* **2009**, *83* (19), 10016–10027. <https://doi.org/10.1128/JVI.00354-09>.
- (158) Kinzler, E. R.; Theiler, R. N.; Compton, T. Expression and Reconstitution of the gH/gL/gO Complex of Human Cytomegalovirus. *J. Clin. Virol.* **2002**, *25*, 87–95. [https://doi.org/10.1016/S1386-6532\(02\)00098-7](https://doi.org/10.1016/S1386-6532(02)00098-7).
- (159) Compton, T.; Nepomuceno, R. R.; Nowlin, D. M. Human Cytomegalovirus Penetrates Host Cells by PH-Independent Fusion at the Cell Surface. *Virology* **1992**, *191* (1), 387–395. [https://doi.org/10.1016/0042-6822\(92\)90200-9](https://doi.org/10.1016/0042-6822(92)90200-9).
- (160) Hetzenecker, S.; Helenius, A.; Krzyzaniak, M. A. HCMV Induces Macropinocytosis for Host Cell Entry in Fibroblasts. *Traffic* **2016**, *17* (4), 351–368. <https://doi.org/10.1111/tra.12355>.
- (161) Adler, B.; Scrivano, L.; Ruzsics, Z.; Rupp, B.; Sinzger, C.; Koszinowski, U. Role of Human Cytomegalovirus UL131A in Cell Type-Specific Virus Entry and Release. *J. Gen. Virol.* **2006**, *87* (9), 2451–2460. <https://doi.org/10.1099/vir.0.81921-0>.
- (162) Vanarsdall, A. L.; Pritchard, S. R.; Wisner, T. W.; Liu, J.; Jardetzky, T. S.; Johnson, D. C. CD147 Promotes Entry of Pentamer-Expressing Human Cytomegalovirus into Epithelial and Endothelial Cells. *mBio* **2018**, *9* (3), e00781-18. <https://doi.org/10.1128/mBio.00781-18>.
- (163) Zhou, M.; Lanchy, J.-M.; Ryckman, B. J. Human Cytomegalovirus gH/gL/gO Promotes the Fusion Step of Entry into All Cell Types, Whereas gH/gL/UL128-131 Broadens Virus Tropism through a Distinct Mechanism. *J. Virol.* **2015**, *89* (17), 8999–9009. <https://doi.org/10.1128/JVI.01325-15>.
- (164) Murrell, I.; Tomasec, P.; Wilkie, G. S.; Dargan, D. J.; Davison, A. J.; Stanton, R. J. Impact of Sequence Variation in the UL128 Locus on Production of Human Cytomegalovirus in Fibroblast and Epithelial Cells. *J. Virol.* **2013**, *87* (19), 10489–10500. <https://doi.org/10.1128/JVI.01546-13>.
- (165) Turtinen, L. W.; Seufzer, B. J. Selective Permissiveness of TPA Differentiated THP-1 Myelomonocytic Cells for Human Cytomegalovirus Strains AD169 and Towne. *Microb. Pathog.* **1994**, *16* (5), 373–378. <https://doi.org/10.1006/mpat.1994.1037>.
- (166) McCormick, A. L.; Roback, L.; Livingston-Rosanoff, D.; St. Clair, C. The Human Cytomegalovirus UL36 Gene Controls Caspase-Dependent and -Independent Cell Death Programs Activated by Infection of Monocytes Differentiating to Macrophages. *J. Virol.* **2010**, *84* (10), 5108–5123. <https://doi.org/10.1128/JVI.01345-09>.
- (167) Sanchez, V.; Dong, J. J.; Battley, J.; Jackson, K. N.; Dykes, B. C. Human Cytomegalovirus Infection of THP-1 Derived Macrophages Reveals Strain-Specific Regulation of Actin Dynamics. *Virology* **2012**, *433* (1), 64–72. <https://doi.org/10.1016/j.virol.2012.07.015>.
- (168) Rozman, B.; Nachshon, A.; Levi Samia, R.; Lavi, M.; Schwartz, M.; Stern-Ginossar, N. Temporal Dynamics of HCMV Gene Expression in Lytic and Latent Infections. *Cell Rep.* **2022**, *39* (2), 110653. <https://doi.org/10.1016/j.celrep.2022.110653>.
- (169) Braun, B.; Sinzger, C. Transmission of Cell-Associated Human Cytomegalovirus Isolates between Various Cell Types Using Polymorphonuclear Leukocytes as a Vehicle. *Med. Microbiol. Immunol. (Berl.)* **2021**, *210* (4), 197–209. <https://doi.org/10.1007/s00430-021-00713-6>.
- (170) Flomm, F. J.; Soh, T. K.; Schneider, C.; Wedemann, L.; Britt, H. M.; Thalassinou, K.; Pfitzner, S.; Reimer, R.; Grunewald, K.; Bosse, J. B. Intermittent Bulk Release of Human Cytomegalovirus. *PLOS Pathog.* **2022**, *18* (8), e1010575. <https://doi.org/10.1371/journal.ppat.1010575>.
- (171) De Boer, P.; Hoogenboom, J. P.; Giepmans, B. N. G. Correlated Light and Electron Microscopy: Ultrastructure Lights Up! *Nat. Methods* **2015**, *12* (6), 503–513. <https://doi.org/10.1038/nmeth.3400>.
- (172) Bradley, A. J.; Lurain, N. S.; Ghazal, P.; Trivedi, U.; Cunningham, C.; Baluchova, K.; Gatherer, D.; Wilkinson, G. W. G.; Dargan, D. J.; Davison, A. J. High-Throughput Sequence Analysis of Variants of Human Cytomegalovirus Strains Towne and AD169. *J. Gen. Virol.* **2009**, *90* (10), 2375–2380. <https://doi.org/10.1099/vir.0.013250-0>.

- (173) Fornara, C.; Schultz, E.; Lilleri, D.; Baldanti, F.; Ryckman, B.; Gerna, G. Fibroblast, Epithelial and Endothelial Cell-Derived Human Cytomegalovirus Strains Display Distinct Neutralizing Antibody Responses and Varying Levels of gH/gL Complexes. *Int. J. Mol. Sci.* **2023**, *24* (5), 4417. <https://doi.org/10.3390/ijms24054417>.
- (174) Scrivano, L.; Sinzger, C.; Nitschko, H.; Koszinowski, U. H.; Adler, B. HCMV Spread and Cell Tropism Are Determined by Distinct Virus Populations. *PLoS Pathog.* **2011**, *7* (1), e1001256. <https://doi.org/10.1371/journal.ppat.1001256>.
- (175) Chowdary, T. K.; Cairns, T. M.; Atanasiu, D.; Cohen, G. H.; Eisenberg, R. J.; Heldwein, E. E. Crystal Structure of the Conserved Herpesvirus Fusion Regulator Complex gH–gL. *Nat. Struct. Mol. Biol.* **2010**, *17* (7), 882–888. <https://doi.org/10.1038/nsmb.1837>.
- (176) Patterson, J. W.; Broecker, A. H.; Kornstein, M. J.; Mills, A. S. Cutaneous Cytomegalovirus Infection in a Liver Transplant Patient: Diagnosis by In Situ DNA Hybridization. *Am. J. Dermatopathol.* **1988**, *10* (6), 524–530. <https://doi.org/10.1097/00000372-198812000-00009>.
- (177) Galitska, G.; Coscia, A.; Forni, D.; Steinbrueck, L.; De Meo, S.; Biolatti, M.; De Andrea, M.; Cagliani, R.; Leone, A.; Bertino, E.; Schulz, T.; Santoni, A.; Landolfo, S.; Sironi, M.; Cerboni, C.; Dell'Oste, V. Genetic Variability of Human Cytomegalovirus Clinical Isolates Correlates With Altered Expression of Natural Killer Cell-Activating Ligands and IFN- $\gamma$ . *Front. Immunol.* **2021**, *12*, 532484. <https://doi.org/10.3389/fimmu.2021.532484>.
- (178) Ciferri, C.; Chandramouli, S.; Donnarumma, D.; Nikitin, P. A.; Cianfrocco, M. A.; Gerrein, R.; Feire, A. L.; Barnett, S. W.; Lilja, A. E.; Rappuoli, R.; Norais, N.; Settembre, E. C.; Carfi, A. Structural and Biochemical Studies of HCMV gH/gL/gO and Pentamer Reveal Mutually Exclusive Cell Entry Complexes. *Proc. Natl. Acad. Sci.* **2015**, *112* (6), 1767–1772. <https://doi.org/10.1073/pnas.1424818112>.
- (179) Murrell, I.; Bedford, C.; Ladell, K.; Miners, K. L.; Price, D. A.; Tomasec, P.; Wilkinson, G. W. G.; Stanton, R. J. The Pentameric Complex Drives Immunologically Covert Cell–Cell Transmission of Wild-Type Human Cytomegalovirus. *Proc. Natl. Acad. Sci.* **2017**, *114* (23), 6104–6109. <https://doi.org/10.1073/pnas.1704809114>.
- (180) Sinclair, J.; Reeves, M. The Intimate Relationship between Human Cytomegalovirus and the Dendritic Cell Lineage. *Front. Microbiol.* **2014**, *5*. <https://doi.org/10.3389/fmicb.2014.00389>.
- (181) Collins-McMillen, D.; Buehler, J.; Peppenelli, M.; Goodrum, F. Molecular Determinants and the Regulation of Human Cytomegalovirus Latency and Reactivation. *Viruses* **2018**, *10* (8), 444. <https://doi.org/10.3390/v10080444>.
- (182) Poole, E.; Juss, J. K.; Krishna, B.; Herre, J.; Chilvers, E. R.; Sinclair, J. Alveolar Macrophages Isolated Directly From Human Cytomegalovirus (HCMV)–Seropositive Individuals Are Sites of HCMV Reactivation In Vivo. *J. Infect. Dis.* **2015**, *211* (12), 1936–1942. <https://doi.org/10.1093/infdis/jiu837>.
- (183) Taylor-Wiedeman, J.; Sissons, P.; Sinclair, J. Induction of Endogenous Human Cytomegalovirus Gene Expression after Differentiation of Monocytes from Healthy Carriers. *J. Virol.* **1994**, *68* (3), 1597–1604. <https://doi.org/10.1128/jvi.68.3.1597-1604.1994>.
- (184) Dupont, L.; Reeves, M. B. Cytomegalovirus Latency and Reactivation: Recent Insights into an Age Old Problem. *Rev. Med. Virol.* **2016**, *26* (2), 75–89. <https://doi.org/10.1002/rmv.1862>.
- (185) Chan, G.; Bivins-Smith, E. R.; Smith, M. S.; Smith, P. M.; Yurochko, A. D. Transcriptome Analysis Reveals Human Cytomegalovirus Reprograms Monocyte Differentiation toward an M1 Macrophage. *J. Immunol.* **2008**, *181* (1), 698–711. <https://doi.org/10.4049/jimmunol.181.1.698>.
- (186) Chan, G.; Bivins-Smith, E. R.; Smith, M. S.; Yurochko, A. D. NF- $\kappa$ B and Phosphatidylinositol 3-Kinase Activity Mediates the HCMV-Induced Atypical M1/M2 Polarization of Monocytes. *Virus Res.* **2009**, *144* (1–2), 329–333. <https://doi.org/10.1016/j.virusres.2009.04.026>.
- (187) Chan, G.; Nogalski, M. T.; Stevenson, E. V.; Yurochko, A. D. Human Cytomegalovirus Induction of a Unique Signalsome during Viral Entry into Monocytes Mediates Distinct

- Functional Changes: A Strategy for Viral Dissemination. *J. Leukoc. Biol.* **2012**, *92* (4), 743–752. <https://doi.org/10.1189/jlb.0112040>.
- (188) Nogalski, M. T.; Chan, G. C. T.; Stevenson, E. V.; Collins-McMillen, D. K.; Yurochko, A. D. The HCMV gH/gL/UL128-131 Complex Triggers the Specific Cellular Activation Required for Efficient Viral Internalization into Target Monocytes. *PLoS Pathog.* **2013**, *9* (7), e1003463. <https://doi.org/10.1371/journal.ppat.1003463>.
- (189) Frank, T.; Niemann, I.; Reichel, A.; Stamminger, T. Emerging Roles of Cytomegalovirus-Encoded G Protein-Coupled Receptors during Lytic and Latent Infection. *Med. Microbiol. Immunol. (Berl.)* **2019**, *208* (3–4), 447–456. <https://doi.org/10.1007/s00430-019-00595-9>.
- (190) Elder, E. G.; Krishna, B. A.; Williamson, J.; Lim, E. Y.; Poole, E.; Sedikides, G. X.; Wills, M.; O'Connor, C. M.; Lehner, P. J.; Sinclair, J. Interferon-Responsive Genes Are Targeted during the Establishment of Human Cytomegalovirus Latency. *mBio* **2019**, *10* (6), e02574-19. <https://doi.org/10.1128/mBio.02574-19>.
- (191) Crawford, L. B.; Caposio, P.; Kreklywich, C.; Pham, A. H.; Hancock, M. H.; Jones, T. A.; Smith, P. P.; Yurochko, A. D.; Nelson, J. A.; Streblow, D. N. Human Cytomegalovirus US28 Ligand Binding Activity Is Required for Latency in CD34 + Hematopoietic Progenitor Cells and Humanized NSG Mice. *mBio* **2019**, *10* (4), e01889-19. <https://doi.org/10.1128/mBio.01889-19>.
- (192) Vomazke, J.; Melnychuk, R. M.; Smith, P. P.; Powell, J.; Hall, L.; DeFilippis, V.; Früh, K.; Smit, M.; Schlaepfer, D. D.; Nelson, J. A.; Streblow, D. N. Differential Ligand Binding to a Human Cytomegalovirus Chemokine Receptor Determines Cell Type-Specific Motility. *PLoS Pathog.* **2009**, *5* (2), e1000304. <https://doi.org/10.1371/journal.ppat.1000304>.
- (193) Adler, B.; Sinzger, C. Endothelial Cells in Human Cytomegalovirus Infection: One Host Cell out of Many or a Crucial Target for Virus Spread? *Thromb. Haemost.* **2009**, *102* (12), 1057–1063. <https://doi.org/10.1160/TH09-04-0213>.
- (194) Braun, B.; Laib Sampaio, K.; Kuderna, A. K.; Widmann, M.; Sinzger, C. Viral and Cellular Factors Contributing to the Hematogenous Dissemination of Human Cytomegalovirus via Polymorphonuclear Leukocytes. *Viruses* **2022**, *14* (7). <https://doi.org/10.3390/v14071561>.
- (195) Ryckman, B. J.; Rainish, B. L.; Chase, M. C.; Borton, J. A.; Nelson, J. A.; Jarvis, M. A.; Johnson, D. C. Characterization of the Human Cytomegalovirus gH/gL/UL128-131 Complex That Mediates Entry into Epithelial and Endothelial Cells. *J. Virol.* **2008**, *82* (1), 60–70. <https://doi.org/10.1128/JVI.01910-07>.
- (196) Skarman, P. J.; Rahbar, A.; Xie, X.; Söderberg-Nauclér, C. Induction of Polymorphonuclear Leukocyte Response by Human Cytomegalovirus. *Microbes Infect.* **2006**, *8* (6), 1592–1601. <https://doi.org/10.1016/j.micinf.2006.01.017>.
- (197) Saez-Lopez, C.; Ngambe-Tourere, E.; Rosenzweig, M.; Petit, J.-C.; Nicolas, J.-C.; Gozlan, J. Immediate-Early Antigen Expression and Modulation of Apoptosis after in Vitro Infection of Polymorphonuclear Leukocytes by Human Cytomegalovirus. *Microbes Infect.* **2005**, *7* (9–10), 1139–1149. <https://doi.org/10.1016/j.micinf.2005.03.021>.
- (198) Clayton, A. R.; Prue, R. L.; Harper, L.; Drayson, M. T.; Savage, C. O. S. Dendritic Cell Uptake of Human Apoptotic and Necrotic Neutrophils Inhibits CD40, CD80, and CD86 Expression and Reduces Allogeneic T Cell Responses: Relevance to Systemic Vasculitis. *Arthritis Rheum.* **2003**, *48* (8), 2362–2374. <https://doi.org/10.1002/art.11130>.
- (199) Serhan, C. N.; Savill, J. Resolution of Inflammation: The Beginning Programs the End. *Nat. Immunol.* **2005**, *6* (12), 1191–1197. <https://doi.org/10.1038/ni1276>.
- (200) Riegler, S.; Hebart, H.; Einsele, H.; Brossart, P.; Jahn, G.; Sinzger, C. Monocyte-Derived Dendritic Cells Are Permissive to the Complete Replicative Cycle of Human Cytomegalovirus. *Microbiology* **2000**, *81* (2), 393–399. <https://doi.org/10.1099/0022-1317-81-2-393>.
- (201) Straschewski, S.; Warmer, M.; Frascaroli, G.; Hohenberg, H.; Mertens, T.; Winkler, M. Human Cytomegaloviruses Expressing Yellow Fluorescent Fusion Proteins -

- Characterization and Use in Antiviral Screening. *PLoS ONE* **2010**, *5* (2), e9174. <https://doi.org/10.1371/journal.pone.0009174>.
- (202) Tischer, B. K.; Smith, G. A.; Osterrieder, N. En Passant Mutagenesis: A Two Step Markerless Red Recombination System. In *In Vitro Mutagenesis Protocols*; Braman, J., Ed.; Methods in Molecular Biology; Humana Press: Totowa, NJ, 2010; Vol. 634, pp 421–430. [https://doi.org/10.1007/978-1-60761-652-8\\_30](https://doi.org/10.1007/978-1-60761-652-8_30).
- (203) Kalejta, R. F.; Bechtel, J. T.; Shenk, T. Human Cytomegalovirus Pp71 Stimulates Cell Cycle Progression by Inducing the Proteasome-Dependent Degradation of the Retinoblastoma Family of Tumor Suppressors. *Mol. Cell. Biol.* **2003**, *23* (6), 1885–1895. <https://doi.org/10.1128/MCB.23.6.1885-1895.2003>.
- (204) Frascaroli, G.; Lecher, C.; Varani, S.; Setz, C.; van der Merwe, J.; Brune, W.; Mertens, T. Human Macrophages Escape Inhibition of Major Histocompatibility Complex-Dependent Antigen Presentation by Cytomegalovirus and Drive Proliferation and Activation of Memory CD4+ and CD8+ T Cells. *Front. Immunol.* **2018**, *9*. <https://doi.org/10.3389/fimmu.2018.01129>.
- (205) Van Zandbergen, G.; Hermann, N.; Laufs, H.; Solbach, W.; Laskay, T. *Leishmania* Promastigotes Release a Granulocyte Chemotactic Factor and Induce Interleukin-8 Release but Inhibit Gamma Interferon-Inducible Protein 10 Production by Neutrophil Granulocytes. *Infect. Immun.* **2002**, *70* (8), 4177–4184. <https://doi.org/10.1128/IAI.70.8.4177-4184.2002>.





## 10 Appendix

### 10.1 Curriculum vitae

#### Personal Information

Giorgia Cimato, born on 7<sup>th</sup> February 1995 in Bologna, Italy (IT).

#### Education

##### PhD candidate

since October 2020

Department of Virus-Host Interaction, Leibniz Institute of Virology (LIV), Hamburg, Germany  
Department of Chemistry, University of Hamburg, Hamburg, Germany

Supervisors: Prof. Dr. Wolfram Brune, PD Dr. Giada Frascaroli, Dr. Tobias Dallenga.

PhD project: Human cytomegalovirus genetic determinants of viral tropism in epithelial cells and human leukocytes.

##### Master Degree

October 2017 – December 2019

M.Sc. in Health Biology at the University of Bologna, Bologna, Italy (IT), with a grade of 110/110 cum laude.

Supervisors: Prof. Dr. Stefania Varani, Dr. Margherita Ortalli.

Master thesis project: Identification of natural-like compounds as potential anti-*Leishmania* drugs and study of their mechanisms of action.

##### Bachelor Degree

September 2014 – October 2017

B.Sc. in Biological Sciences at the University of Bologna, Bologna, Italy (IT), with a grade of 109/110.

Supervisors: Prof. Dr. Fulvia Farabegoli, Dr. Paola Selva.











Bachelor thesis project: Comparative evaluation of instruments for the determination of glycosylated and pathological haemoglobins.















##### High school











September 2009 – July 2014

High school diploma at the “Liceo Classico Marco Minghetti”, Bologna, Italy (IT), with a grade of 98/100.

## 10.2 List of hazardous substances

Substance	GHS symbol	Hazard statements	Precautionary statements
2-mercaptoethanol		H301+H331-H310- H315-H317-H318- H373-H410	P273-P280- P302+P352- P304+P340- P305+P351+P338+P310
Acetone		H225-H319-H336	P210-P305+P351+P338- P312-P370+P378- P403+P233+P235-P501
Acetic acid		H226-H314	P210-P280- P301+P330+P331- P305+P361+P353- P305+P351+P338-P310
Acrylamide		H302-H315-H317- H319-H340-H350- H361F-H372	P260-P280-P302+P352- P305+P351+P338- P308+P313-P314-P333- P337-P501
Ammonium bicarbonate		H302	P301+P312+P330
Ammonium persulfate		H272-H302+H312- H315-H317-H319- H334-H335-H412	P220-P261-P280- P305+P351+P338- P342+P311
Ampicillin		H315-H317-H319- H334-H335	P261-P280- P305+P351+P338- P342+P311
Bis-acrylamide		H302+H332	
Boric acid		H360FD	P201-P308+P313
Bromophenol blue		H332-H302-H319	P261-P264-P280- P304+P340- P312-P301+P312-P330- P305+3P51+P338- P337+P313

Chloramphenicol		H318-H351- H361FD	P202-P280- P305+P351+P338- P308+P313
DTT (1,4-Dithiothreitol)		H302-H315-319- H335-H412	P260-P280- P305+P351+P338- P337+P313
Dimethyl sulfoxide		H227	P210-P280-P370+P378- P403+P235-P501
EDTA		H319	P305+P351+P338
Ethanol		H225-H319	P210-P280- P305+P351+P338- P337+P313-P403+P235
Ethidium bromide		H302-H330-H341	P260-P281-P284-P310
Glycerin		H315-H319-H335	P280-P302+P352-P304 +P340-P305+P351+P338
Hydrochloric acid		H290-H314-H335	P261-P280- P305+P351+P338-P310
Isopropanol		H225-H319-H336	P210-P261- P305+P351+P338
Kanamycin		H360D	P260-P308+P313
Liquid nitrogen		H281	P202-P271+P403-P282
Methanol		H225- H301+H311+H331- H370	P210-P260-P280- P301+P310-P311
Nonidet-P40		H315-H319-H302	P264-P280- P305+P351+P338- P332+P313-P337+P313- P362+P364
Paraformaldehyde		H228-H302+H332- H315-H317-H318- H335-H341-H350	P202-P210-P270-P280- P305+P351+P338- P308+P313

Penicillin		H317-H334	P261-P280-P342+P311
Phorbol 12-myristate 13-acetate		H300-H330-H310- H314-H318-H334- H317-H351	P202-P260-P280- P303+P361+P353- P304+P340+P310- P305+P351+P338
Ponceau S		H315-H319-H335	P260-P280-P302+P352- P305+P351+P338
Puromycin		H373	
Sodium dodecyl sulfate		H315-H318-H335	P280-P304+P340+P312- P305+P351+P338+P310
Sodium hydroxide		H290-H314	P280-P305+P351+P338- P310
Streptomycin		H302-H361	P281
TEMED		H225-H302-H314- H332	P210-P280- P305+P351+P338-P310
Triton X-100		H302-H319-H411	P273-P280- P301+P312+P330- P337+P313-P391-P501
Zeocin		H302-341	P264-P301+P312

## 11 Acknowledgements

I would firstly like to thank my supervisor Prof. Dr. Wolfram Brune for giving me the opportunity to do a doctoral thesis in his laboratory and providing me with a challenging and interesting project. I would also like to thank my first co-supervisor PD Dr. Giada Frascaroli for the expertise, teachings, and support she provided me at the beginning of this journey. Under their guidance, I had the opportunity to work in freedom and develop my own ideas. Furthermore, I would like to thank my second co-supervisor Dr. Tobias Dallenga for his helpful advice and constructive discussions during my doctoral studies.

I would like to thank Prof. Dr. Nicole Fischer for agreeing to be an evaluator of my dissertation and Prof. Dr. Michael Kolbe and Prof. Dr. Jens Bosse who agreed to be the examiners of my disputation.

Special thanks go to Irke Waßmann for helping me with the German translation. I would like to thank Dr. Felix Flomm and Carola Schneider for their collaboration and help to perform experiments that otherwise I would have not been able to perform alone. I would like to express my gratitude to Xuan Zhou, whose valuable insights, constant suggestions, and both technical and mental support have greatly contributed to the development of this thesis. I thank also Jan Knickmann for his patience and help in the analysis of next generation sequencing data.

Thanks to all present and former lab members of the LIV research group Virus-Host Interaction: Laura, Irke, Laura-Marie, Jan, Eleonore, Maria, Michaela, Dongdong, Enrico, Luis, Ina, it was nice working with you. Particularly, I am tremendously grateful to Xuan, Ana, Andrea, and Maria Pia for all sarcastic comments, complaints, laughter, and delicious food they shared with me inside and outside the lab.

I wish to express my deepest gratitude to my parents, Manuela and Brenno, and my whole family for their constant support and love. Special thanks go to my person Federica for being with me every day even 1300 km away. I would never have survived all this without Riccardo, I will always be grateful to him for completely changing his life because of me.



## 12 Declaration on oath

I hereby declare and affirm that this doctoral dissertation is my own work and that I have not used any aids and sources other than those indicated. If electronic resources based on generative artificial intelligence (gAI) were used in the course of writing this dissertation, I confirm that my own work was the main and value adding contribution and that complete documentation of all resources used is available in accordance with good scientific practice. I am responsible for any erroneous or distorted content, incorrect references, violations of data protection and copyright law or plagiarism that may have been generated by the gAI. The submitted written version corresponds to the version on the electronic storage medium. I hereby declare that I have not previously applied or pursued for a doctorate (Ph.D. studies).

Hamburg, July 2024



Giorgia Cimato